CORA Cork Open Research Archive
Cartlann Taighde Oscailte Chorcaí

Title	The crystal landscape and cocrystallization of primary aromatic sulfonamides
Authors	Downey, John D.
Publication date	2020-07
Original Citation	Downey, J. D. 2020. The crystal landscape and cocrystallization of primary aromatic sulfonamides. MRes Thesis, University College Cork.
Type of publication	Masters thesis (Research)
Rights	© 2020, John D. Downey. - https://creativecommons.org/licenses/by-nc-nd/4.0/
Download date	2026-11-15 08:14:36
Item downloaded from	https://hdl.handle.net/10468/10471

UCC
University College Cork, Ireland
Coláiste na hOllscoile Corcaigh

The Crystal Landscape and Cocrystallization of Primary Aromatic Sulfonamides



John D. Downey, B.Sc.

A Thesis Presented for the Degree of

Master of Science

To

THE NATIONAL UNIVERSITY OF IRELAND

School of Chemistry

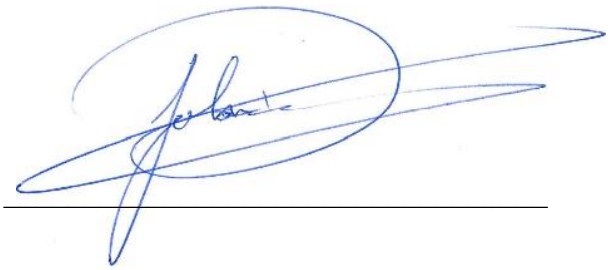
University College Cork

Supervisor: Dr Simon E. Lawrence

July 2020

Declaration of Authorship

This is to certify that the work I am submitting is my own and has not been submitted for another degree, either at University College Cork or elsewhere. All external references and sources are clearly acknowledged and identified within the contents. I have read and understood the regulations of University College Cork concerning plagiarism.



John D. Downey B.Sc.

Acknowledgements

I would like to thank Dr Simon Lawrence for his help and guidance on this project throughout the year. I am especially grateful for all the support he has provided me with, both academic and personal. I would also like to acknowledge Lab 4.27, Shan, Will and Mark, who were always willing to give me help and advice when needed and made the lab an enjoyable place to work. I would also like to thank Jack for all the work he has done throughout his FYP. A special thanks to Hazel who listened to me at every point of my research, and to my family who have always supported me and helped me to strive for success.

Abstract

This thesis is focused on primary benzenesulfonamides. They have been structurally characterised and analysed for common structural motifs present in the solid state. A systematic investigation of their cocrystallization with a range of neutral, zwitterionic and ionic coformers has been carried, with a strong focus on coformers that have the potential for sulfonamide drug development.

Chapter One discusses and illustrates the literature for the solid-state and supramolecular chemistry of benzenesulfonamides; topics covered include non-covalent interactions, synthons, crystal engineering, cocrystallization, eutectic compositions, solvates, biochemistry of sulfa drugs and crystal polymorphism.

Chapter Two delves into the crystal landscape of the sulfonamide functional group. In this chapter we critically assess several simple primary aromatic sulfonamides identifying the different motifs present in their crystalline structures.

Chapter Three focuses on the design and cocrystallization of sulfonamides with a range of neutral, zwitterion and ionic coformers. Initial screening was complemented by the solid-state characterization of the products obtained.

Chapter Four outlines the future work that could be implemented to advance the library of supramolecular synthons for the sulfonamide functional group, in addition to furthering the improvement of sulfonamide drug development whether by using cocrystallization, solvate formation or by eutectic compositions.

List of Abbreviations

Abbreviation	Interpretation
4-ABSA	4-Aminobenzenesulfonamide
ALA	Alanine
ATR-FTIR	Attenuated Total Reflectance Fourier Transform Infrared Spectroscopy
BSA	Benzenesulfonamide
2-BrBSA	2-Bromobenzenesulfonamide
3-BrBSA	3-Bromobenzensulfonamide
4-BrBSA	4-Bromobenzenesulfonamide
CCDC	Cambridge Crystallographic Data Centre
2-ClBSA	2-Chlorobenzenesulfonamide
3-ClBSA	3-Chlorobenzenesulfonamide
4-ClBSA	4-Chlorobenzenesulfonamide
CPR	Caprolactam
CSD	Cambridge Structural Database
CSD Refcodes	Cambridge Structural Database CSD Refcodes have the general format AAAAAA and are used to refer to crystal structures found in the CSD, suffixes of 01/02 etc. relate to polymorphs of these materials
CuAc	Copper (II) Acetate Monohydrate
DSC	Differential Scanning Calorimetry
EtOAc	Ethyl Acetate
EtOH	Ethanol
2-FBSA	2-Fluorobenzenesulfonamide

3-FBSA	3-Fluorobenzenesulfonamide
4-FBSA	4-Fluorobenzenesulfonamide
FTIR	Fourier Transform Infrared Spectroscopy
GLY	Glycine
Hz	Hertz
2IM	2-Imidazolidone
INA	Isonicotinic Acid
IR	Infrared Spectroscopy
IUPAC	International Union of Pure and Applied Chemistry
2-MeBSA	2-Methylbenzenesulfonamide
4-MeBSA	4-Methylbenzenesulfonamide
MeOH	Methanol
m.p.	Melting Point
NA	Nicotinic Acid
2-NBSA	2-Nitrobenzeensulfonamide
3-NBSA	3-Nitrobenzenesulfonamide
4-NBSA	4-Nitrobenzenesulfonamide
NMR	Nuclear Magnetic Resonance Spectroscopy
3-OMeBSA	3-Methoxybenzenesulfonamide
4-OMeBSA	4-Meothxybenzenesulfonamide
OXA	Oxalic Acid
PAM	Picolinamide
4PNO	4-Picoline-*N*-Oxide
PRO	Proline
PXRD	Powder X-ray Diffraction

RT	Room Temperature
SA	Salicylic Acid
SCXRD	Single Crystal X-ray Diffraction
SER	Serine
SMBA	Sulfamoylbenzoic Acid
SDM	Sulfadimethazine
SNA	Sulfanilamide
SNI	Succinimide
Sulfa	Sulfonamide
TTA	Tartaric Acid
VLM	Valerolactam

Table of Contents

Declaration of Authorship Page 1

Acknowledgements Page 2

Abstract Page 3

Abbreviations Page 4

Chapter One – Introduction

1. Introduction Page 10
   - 1.1 Supramolecular Synthons Page 12
   - 1.2 Polymorphism Page 14
   - 1.3 Crystal Engineering and Cocrystals Page 19
     - 1.3.1 Etter's Rules Page 20
     - 1.3.2 Etter's Graph Set Analysis Page 20
     - 1.3.3 Hunter's Table Page 21
     - 1.3.4 ΔpKa Page 22
     - 1.3.5 Molecular and Pharmaceutical Cocrystals Page 23
     - 1.3.6 Ionic Cocrystals Page 27
     - 1.3.7 Eutectic Composition Page 28
       - 1.3.7.1 Relationship between Eutectics and Cocrystals Page 30
     - 1.3.8 Solvates Page 32
   - 1.4 Cocrystallization Involving Sulfonamides Page 34
     - 1.4.1 Amide Coformers Page 42
     - 1.4.2 Carboxylic Acid Coformers Page 46
     - 1.4.3 Pyridine Coformers Page 49
     - 1.4.4 Drug-Drug Cocrystals Page 51
   - 1.5 Conclusion Page 53
   - 1.6 Objectives Page 53

References Page 55

Chapter Two – Crystal Landscape of Primary Aromatic Sulfonamides

2. Crystal Landscape of Primary Aromatic Sulfonamides Page 63
   2.1 Abstract Page 63
   2.2 Introduction Page 63
   2.3 Experimental Page 66
   2.4 Results & Discussion Page 68
      2.4.1 Crystal Structure Analysis Page 68
   2.5 Conclusion Page 75

   References Page 76

   Supporting Information Page 81

Chapter Three – Cocrystallization of Primary Aromatic Sulfonamides

3. Cocrystallization of Primary Aromatic Sulfonamides Page 119
   3.1 Abstract Page 119
   3.2 Introduction Page 119
   3.3 Experimental Page 123
   3.4 Results Page 125
   3.5 Discussion Page 128
   3.6 Conclusion Page 130

   References Page 131

   Supporting Information Page 133

Chapter Four – Future Work

4. Future Work Page 143

Chapter One – Introduction

1. *Introduction*

There are a variety of non-covalent interactions which include hydrogen bonding, halogen bonding, π-π stacking and van der Waals forces. The non-covalent interaction of interest for this thesis is hydrogen bonding. A hydrogen bond is primarily an electrostatic force of attraction between a hydrogen atom which is covalently bound to a more electronegative atom and another electronegative atom which bears a lone pair of electrons.[1] The groups present in this non-covalent bond are the hydrogen bond donor and the hydrogen bond acceptor. Such a system is denoted as D-H···A; where D is the 'donor' of the hydrogen bond and A is the 'acceptor' for the hydrogen bond. IUPAC as of 2011 have provided a more defined definition for the hydrogen bond as: "*The hydrogen bond is an attractive interaction between a hydrogen atom from a molecule or a molecular fragment X-H in which X is more electronegative than H, and an atom or a group of atoms in the same or a different molecule, in which there is evidence of bond formation*."[1]

Hydrogen bonds can be either intermolecular or intramolecular depending on the donor and acceptor atoms which constitute the bond, their geometry, environment and the energy of the bond which can vary between strong (15-40 kcal mol^{-1}), moderate (4-15 kcal mol^{-1}) and weak (1-4 kcal mol^{-1}), **Figure 1.1**.[2] There are clear defined regions for hydrogen bond interactions but at the weak range of hydrogen bonding there is little distinction between a weak hydrogen bond and van der Waals forces.[2] Due to this, hydrogen bonds can be considered stronger than a van der Waal interaction but weaker than electrostatic interactions.[2]

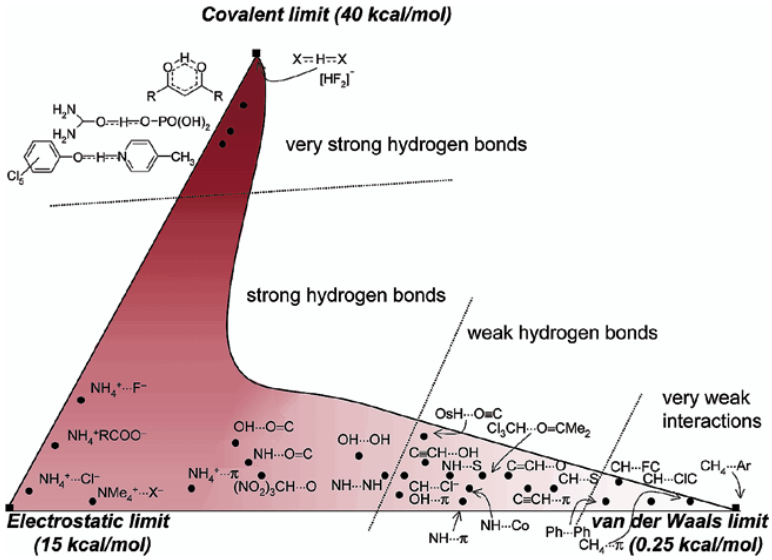


Figure 1.1: The 'Hydrogen Bridge' which is a diagrammatic representation of the different types of hydrogen bonds.[2]

While hydrogen bonds are known not to form covalent bonds, they are known to contain some features of covalency in that the hydrogen bond can be strong and multi-directional.[3] They can occur over interatomic distances with a long range meaning, that the donor hydrogen atom can interact with more than one acceptor as indicated by **Figure 1.2**.[3] If the two hydrogen bond distances are different the longer bond becomes known as the 'minor' component whereas the shorter bond becomes known as the 'major' component. However, these types of valency are only substantial when the acceptor binds the hydrogen from a more electronegative donor.[3]

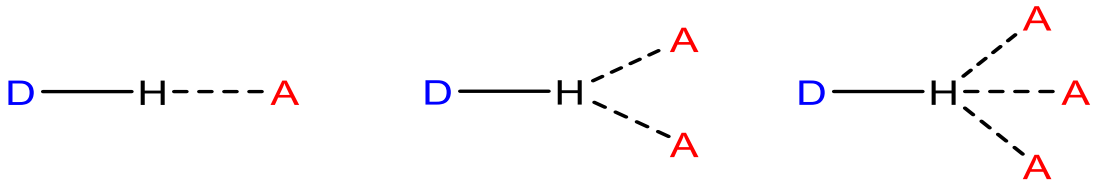


Figure 1.2: Various hydrogen bond modes **1)** with a single acceptor, **2)** two acceptors and **3)** three acceptors, adapted from reference 3.

It becomes quite clear from the literature that the hydrogen bond plays an essential role for non-covalent intermolecular interactions, which is exemplified in **Table 1.1**.[4] Drug molecules and active pharmaceutical ingredients (APIs) consist of hydrogen-bonding functional groups such as carboxylic acids, amides, alcohols, amines, and sulfonamides, and are generally flexible which promote crystallization directed by supramolecular synthons.[5] The amide-carbonyl hydrogen bond is reported to be the best with sulfonamides.[6] From this, it can be said that the hydrogen bond is an important tool in the field of crystal engineering and that understanding its role in terms of cocrystallization allows for the construction of novel cocrystals, which are finding increasing use in the pharmaceutical sector due to their ability to manipulate the physicochemical properties of solid-state materials.

Table 1.1: Guidelines for hydrogen bond classification.[4]

Interaction Type	*Strong (Strongly Covalent)*	*Moderate (Mostly Electrostatic)*	*Weak (Electrostatic/ Dispersion)*
Bond Length (Å) H···A	1.2 - 1.5	1.5 - 2.2	> 2.2
Lengthening of X-H (Å)	0.08 - 0.25	0.02 - 0.08	< 0.02
X···A (Å)	2.2 - 2.5	2.5 - 3.2	> 3.2
Directionality	Strong	Moderate	Weak
Bond Angles (°)	170 - 180	> 130	> 90
Bond Energy (kcal mol^{-1})	15 - 40	4 - 15	< 4
Relative IR Shift (cm^{-1})	25 %	10 – 25 %	< 10 %
^{1}H Downfield Shift (ppm)	14 - 22	< 14	-

1.1 *Supramolecular Synthons*

Functional groups have the ability to interact with other functional groups, and the molecular interactions between similar and different functional groups seen in a wide variety of crystal structures have been coined ‘supramolecular’ synthons.[7] A synthon is a structural unit within

a molecule which is related to a possible synthetic operation. In other words, when molecular building blocks interact with one another via non-covalent interactions it can lead to the formation of solid-state materials.[7] Synthons were described by Desiraju in 1995 and are currently defined as: "*Supramolecular synthons are structural units within supermolecules that can be formed and/or assembled by known or conceivable synthetic operations involving intermolecular interactions".*[7] Synthons are central to the development of novel solid-state materials and are critical in pharmaceutical development due to the various types of solid-state materials that can be formed through the intermolecular interactions of various functional groups.[7]

Synthons have been classified into two distinct groups; homosynthons and heterosynthons as outlined by **Figure 1.3**.[8] Homosynthons form self-complementary moieties through non-covalent interactions between similar functional groups and heterosynthons form contrasting moieties through non-covalent interactions between different functional groups.[9] In terms of non-covalent interactions the hydrogen bond plays an important role in the formation of larger molecules and cocrystals.[10] The reason for this is due to the distance and directionality of hydrogen bonds which allows for the design of novel supramolecular and solid-state materials.

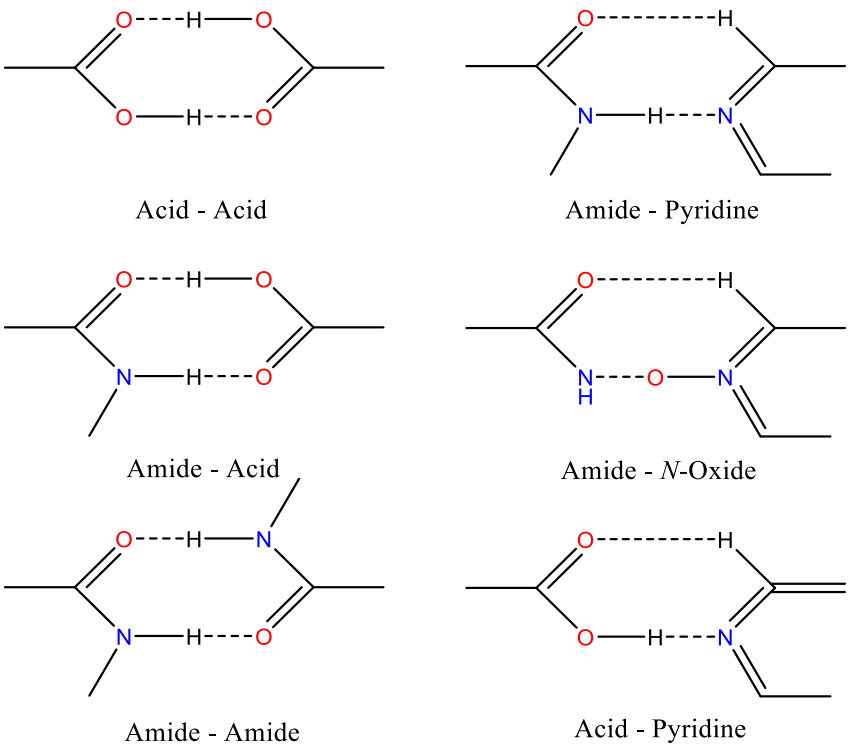


Figure 1.3: Some examples of homosynthons and heterosynthons where the dashed lines denote the hydrogen bond and the blue/red atoms are the hydrogen bonds donor/acceptor, adapted from reference 11.

1.2 *Polymorphism*

Polymorphism is the phenomenon whereby the same chemical compound can exist in different crystal formations and displays varying physicochemical properties.[12] Polymorphs have been defined as: "*Different crystalline forms of the same substance. This may include solvation or hydration products (also known as pseudopolymorphs) and amorphous forms.*"[12] Polymorphism arises due to the competition between kinetic and thermodynamic factors during the crystallization process.[13] While long-range strong intermolecular interactions dictate the formation of kinetic crystals, the close packing of molecules generally drives the thermodynamic outcome. Polymorphs have different stabilities and may spontaneously convert

from a metastable form to the stable form at a particular temperature.[14] The polymorphism phenomenon was first described in 1832 when Friedrich Wöhler and Justus von Liebig were studying the organic compound benzamide.[15]

In organic molecules, three types of polymorphism are mainly observed and are illustrated in **Figure 1.4**.[16] Packing polymorphism arises when molecules pack in different ways to give different structures. Conformational polymorphism, on the other hand is mostly seen in flexible molecules where molecules have multiple conformational possibilities within a small energy window. As a result, multiple crystal structures can be obtained with the same molecule but in different conformations. The rarest form of polymorphism arises from the differences in the primary synthon and this type of polymorphism is called synthon polymorphism.[16] With the recent and continuous growth in research into cocrystallization, it has been observed that cocrystals can also be polymorphic.[16] Most polymorphs of organic molecules only differ by a few kJ mol^{-1} in lattice energy. They may also exhibit different melting points, solubilities and X-ray crystal and diffraction patterns.

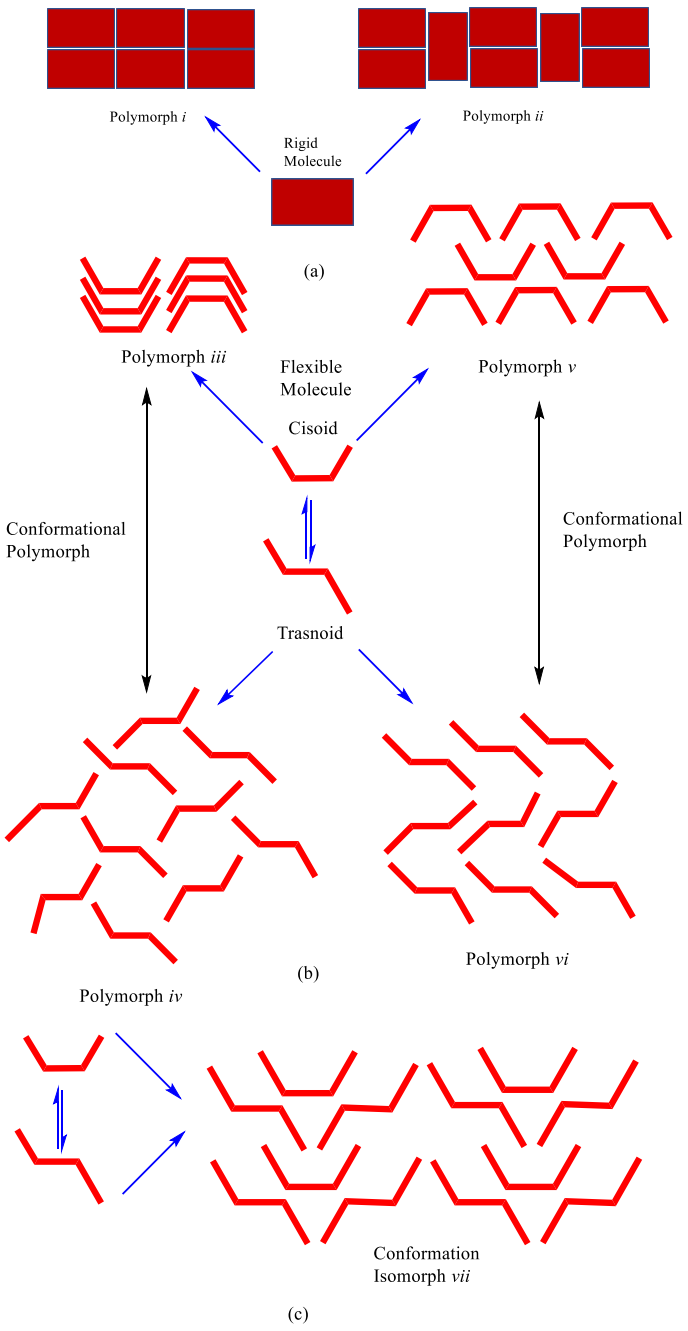


Figure 1.4: Schematic diagram of **a)** conformational polymorphism, **b)** synthon polymorphism and **c)** packing polymorphism, adapted from reference 16.

The thermodynamically stable polymorph is most likely to form when dealing with a close packing of the hydrogen bond and the kinetically stable polymorph when the nucleus is stabilised by hydrogen bonding.[16] Since polymorphs only differ by a few kJ mol^{-1} it is possible or both to crystallize simultaneously which is known as a concomitant polymorphism. Various

different conditions in the crystallisation process are often the main reasons responsible for the formation of different polymorphic forms.[17]

These conditions include:

- Solvent effects as the packing of crystal may be different in polar and nonpolar solvents.
- Certain impurities inhibiting growth pattern and favour the growth of metastable polymorphs.
- The level of supersaturation from which the material is crystallized.
- Temperature at which crystallisation is carried out.
- Change in stirring conditions.

Ostwald's rule or Ostwald's step rule, conceived by Wilhelm Ostwald, states that in general it is not the most stable but the least stable polymorph that crystallizes first for crystallization from solution or the melt. This converts to the next lower metastable form until it reaches the lowest energy thermodynamically stable form crystallizes, as seen on **Figure 1.5**.[18]

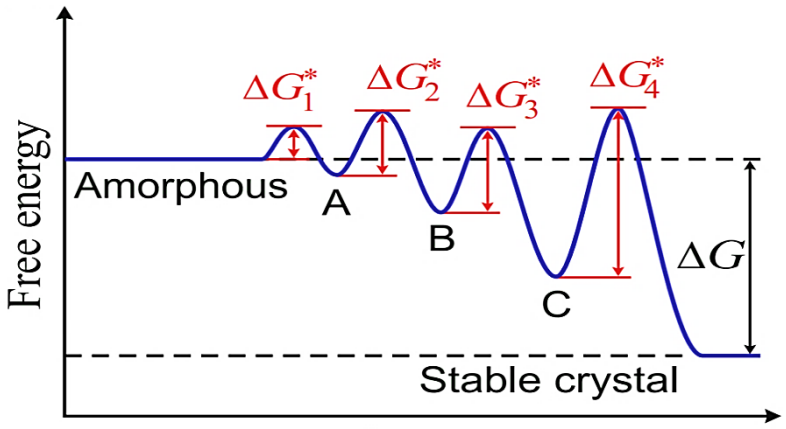


Figure 1.5: Diagrammatic representation of Ostwald's rule.[18]

From a thermodynamic viewpoint polymorphism can be divided into two types: 1) monotropic and 2) enantiotropic, illustrated in **Figure 1.6**. Monotropic is where one polymorph

is the most stable at and the other forms convert to this form. Enantiotropic is where one polymorph is stable at one temperature and another is stable at a different temperature.[19]

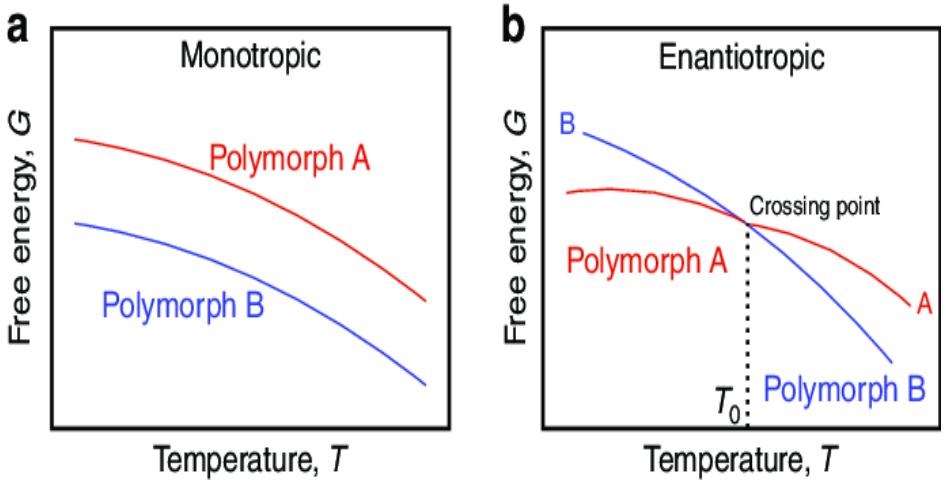


Figure 1.6: Outline of monotropic and enantiotropic systems.[20]

Polymorphism is an important factor in terms of the development of pharmaceutical ingredients.[21] The reason for this is that only selected solid forms are suitable for the development of final dosage forms. Polymorphism in drugs have direct medical implications as dissolution rates depend on the exact crystal form of a polymorph.[22] For example, the drug sulfathiazole is an organosulfur compound which was used to treat common oral and topical antimicrobial infections. It exists in five polymorphic forms with the imine tautomer being the most dominant due to its stability in the solid-state, outlined in **Figure 1.7**.[23] One key factor to note about tautomeric polymorphism is desmotropism.[24] Desmotropism is a form of tautomerism in organic compounds in which two molecules may have atoms of the same number, kind, and valence, and arranged in the same position, but with the shifting double bond permitting the independent existence of two types of the compound.[24] This is important to know as in the case of sulfathiazole it is strongly recommended to use desmotropism to describe this compounds. Knowing exactly how to describe a drug as well as the many polymorphic forms a potential drug has and understanding which one will be the most stable in the solid-state at

production and storage conditions is why it's important for pharmaceutical companies to fully explore all crystal structures of potential drugs.

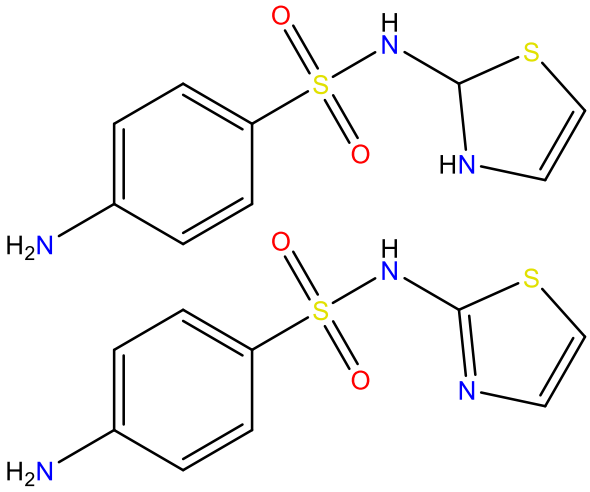


Figure 1.7: Two tautomers of sulfathiazole: top is the imino tautomer and bottom is the amino tautomer, adapted from reference 23.

1.3 *Crystal Engineering and Cocrystals*

Crystal Engineering is considered to be the design and growth of crystalline supramolecular structures with the objective of influencing physicochemical properties, where the majority of the self-directed intermolecular interactions in the solid-state are held together by the hydrogen bond.[25] Crystal engineering has been defined as: "*The understanding of intermolecular interactions in the context of crystal packing and the utilization of such understanding in the design of new solids with desired physical and chemical properties.*"[26] Crystal engineering has made many advances in the field of chemistry in the last number of years and because of this, the necessity to understand the role of the hydrogen bond in both supramolecular and solid-state chemistry has increased.[27] By understanding hydrogen bonding in supramolecular

synthons the rational design and growth of crystalline molecules with the desired physicochemical properties can be attained by utilisation of crystal engineering principals.[27]

1.3.1 *Etter's Rules*

In 1990 Margaret Etter designed and established hydrogen bonding principals which states that the best proton donor will always form a hydrogen bond with the best proton acceptor.[28] The analysis of hydrogen bond patterns has allowed for the determination of functional groups which have the potential to hydrogen bond.[28] The three hydrogen bond rules put forth by Margaret Etter reflect this knowledge and sheds light on useful information about preferential connectivity patterns, hydrogen bond selectivity and stereoelectronic properties of hydrogen bonds.[28] The first rule is that: *all acidic hydrogens available in a molecule will be used in hydrogen bonding in the crystal structure of that compound,* the second is: *all good acceptors will be used in hydrogen bonding when there are available hydrogen bond donors* and lastly: *the best hydrogen bond donor will preferentially form hydrogen bonds with the best hydrogen bond acceptor*.[28] These rules are reflective of the energetically favourable intermolecular interactions and are also observed in crystal packing patterns. Hydrogen bonds will not always form due to the presence of multiple competitive hydrogen bond sites, steric hinderance or competing dipolar and ionic forces.[28]

1.3.2 *Etter's Graph set analysis*

Graph set analysis is a method of defining the motifs observed in hydrogen bonded systems.[29] Etter's originally proposed the use of $pG_d^a(r)$, where p refers to the total number of donors and

acceptors in the molecules, a and d are the participating donors and acceptors, and r represents the dimensions of the ring if present. G can be changed for one of three specified hydrogen bonding modes, I (intramolecular), C (chain) or R (rings).[29] However, it has since been revised suggesting the use of C, R, S and D to describe chains, rings, intramolecular bonds and finite bonds in place of G.[30] The final graph set established by Bernstein has $G_d^a(n)$, where n is the number of atoms participating in the motif. This system allowed for accurate characterization of simple unitary graph sets, where only one type of hydrogen bonding is involved, as well as more complex systems.[30]

1.3.3 *Hunter's Table*

Hunter's table was a key piece of literature added to the field of crystal engineering in 2004.[31] It was a publication of quantified intermolecular interactions in which, the numerical evaluation of the hydrogen bond donor/acceptor abilities of different functional groups was outlined. He detailed this based on the hydrogen bond donor/acceptor constants and molecular electrostatic potential calculations.[31]The hydrogen bond acceptor constants were based on literature values providing an expression of the energy of a hydrogen bond interaction as the product of the positive charge on the hydrogen bond donor (α_2^H) and the negative charge on the hydrogen bond acceptor (β_2^H).[31]

This table allowed for the general assessment of potential non-covalent interactions between suitable hydrogen bond donors and hydrogen bond acceptors in the design of supramolecular constructs, cocrystals in particular. For this project I generated a small table of select functional groups I think will cocrystallize with primary benzenesulfonamides as outlined in **Table 1.2**.

Table 1.2: Hydrogen bond parameters for functional groups pertinent to this work, derived from reference 31.

H-Bond Donor	*α*	*H-Bond Acceptor*	*β*
Pyridine	1.4[b]	*Carboxylic Acid*	5.3[a]
Carbamate	2.8[a]	*Imine*	5.8[a]
Amide	2.9[a]	*Sulfonamide*	5.8[a]
Sulfonamide	3.2[b]	*Pyridine*	7.0[a]
Carboxylic Acid	3.6[a]	*Carbamate*	7.3[a]
Imidazole	3.7[a]	*Amide*	8.3[a]

α – Literature values (α_2^H) and (β_2^H). B – Molecular electrostatic potential surface.

1.3.4 ΔpK_a

Cocrystal formation can be predicted by proton transfer between acids and bases. The formation of cocrystals can be predicted by considering the ΔpKa= [pKa (base)-pKa(acid)].[32] It is generally accepted that proton transfer will occur from acid to base if the difference in the pKa values is greater than 2 or 3. A smaller ΔpKa value, less than 0 indicates the likely formation of cocrystals whereas higher value more than 2 or 3 indicates high likelihood of the formation of salts. ΔpKa rule was validated and quantified by studying 6465 cocrystals from CSD which explained a linear relationship between ΔpKa value and the possibility of proton transfer between the acid-base pair.[32] pKa is important as acidity effects hydrogen bonding and, ultimately, whether it will be a salt or cocrystal.[32] This parameter is not accurate to predict the formation of cocrystals in solids between the ΔpKa values 0 and 3, however, the possibility of salt formation will increase when the ΔpKa increases.[32]

1.3.5 *Molecular and Pharmaceutical Cocrystals*

One of the major developments over the last thirty years in the field of crystal engineering was the advancement of multi-component crystals. One of the clearest definitions of a cocrystal arose from the Indo-US bilateral meeting: "*Cocrystals are solids that are crystalline single phase materials composed of two or more different molecular and/or ionic compounds generally in a stoichiometric ratio which are neither solvates nor simple salts*."[33] However, recently it was stressed that cocrystals should be classified as either 'molecular' or 'ionic' cocrystals depending on the nature of the coformers.[33]

For the pharmaceutical industry cocrystals require an API and a neutral coformer or dual - drug coformers. Coformers can also be chosen based on a list provided by the Food and Drug Administration (FDA), European Food Safety Authority (EFSA) and Priority based Assessment of Food Additives (PAFA) of generally recognised as safe (GRAS) compounds.[34] However, ΔpK_a and Etter's three rules play a more pivotal role in predicting potential coformers.

The first cocrystal reported was in 1844 by Friedrich Wöhler who cocrystallized quinone and hydroquinone in a 1:1 equimolar ratio.[35] Cocrystals can be categorised based on the number of components that are observed in the crystal lattice i.e. binary, ternary, quaternary and even quintenary which has only been recently reported.[36,37] Cocrystallization is a technique that is used to modify the intrinsic properties of a drug by altering its physicochemical properties at the molecular level, illustrated in **Figure 1.8**. Cocrystallization allows for the optimization of many physicochemical properties of various drugs.[38] This process has been known to improve the properties of APIs including the melting point, tabletability, solubility, stability and bioavailability dissolution, hydration, flowability, permeability and certain pharmacokinetic properties.[38]

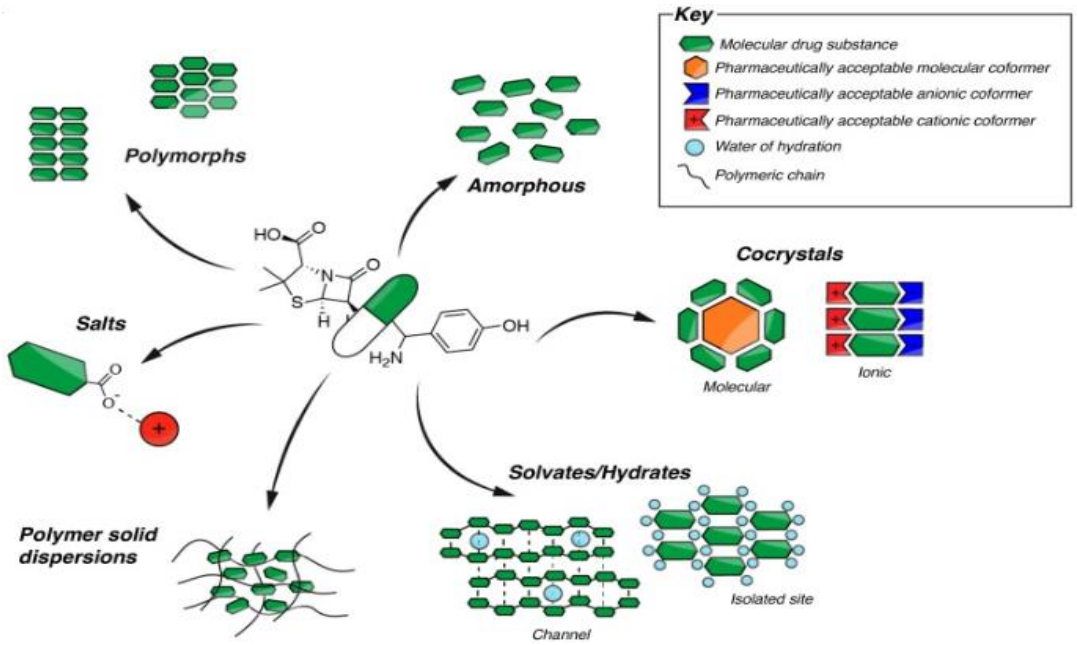


Figure 1.8: Profile of various pharmaceutical crystalline solid-state materials.[39]

To produce a cocrystal there are various techniques but the most interesting is called liquid assisted grinding (LAG). LAG involves the addition of a solvent to the grinding of two components.[40] However, while LAG may be the choice of technique for cocrystal formation for this thesis due to its ability to increase the likelihood of cocrystal formation during ball and mill grinding, there are other notable techniques outlined in **Table 1.3**.[40] To generate a crystal for analysis, the best approach would be to place some ground product in minimal solution and leave to slowly evaporate until single crystals form. Utilising various solvents can alter the supramolecular interactions of the two compounds and can lead to the formation of polymorphs.[40] Cocrystals are typically characterised using powder X-Ray diffraction (PXRD), single-crystal X-Ray diffraction (SCXRD), Infrared spectroscopy (IR) and Differential Scanning Calorimetry (DSC) as outlined in **Table 1.4**.[40]

Table 1.3: Methods to Produce Cocrystals.[40]

Technique	*Method*	*Advantages*	*Disadvantages*
Solution Based	Solvent Evaporation	Highly crystalline product formed	Both components must be soluble in solvent
	CryoCrystallization	Cocrystal formation can be predicted by phase diagram	Phase diagrams are time intensive to generate
	Reaction Crystallization	Less likely to form single component crystals	Large volumes of solvent required
	Spray Drying	Can generate pure cocrystals form saturated solutions	Poor flowability
	Freeze Drying	Can generate pure cocrystals form saturated solutions	Batch process
Solid-state Based	Hot Melt Extrusion	Final product will have negligible quantities of oxygen and water	Unsuitable for thermally unstable APIs and coformers
	Dry Grinding	Useful for cocrystal screening	Poor kinetics of cocrystal formation

Table 1.4: Methods to Characterize Cocrystals.[40]

Spectroscopy	X-ray Diffraction	Thermal	Other
FTIR	Powder XRD	Differential Scanning Calorimetry (incl. modulated and hyper DSC)	Dynamic Vapour Sorption
ATR-FTIR	Single Crystal XRD	Thermogravimetric Analysis	Hirshfeld Surface Analysis
Raman		Hot Stage Microscopy	Density Functional Theory Calculations
Solid State Nuclear Magnetic Resonance			
X-ray Photoelectron Spectroscopy			

Molecular cocrystals are known to contain two or more different neutral coformers in a stoichiometric ratio and are typically sustained by non-covalent interactions. Subclassified under molecular cocrystals is 'pharmaceutical' cocrystals as most reported pharmaceutical cocrystals have a tendency to have neutral coformers which are solid at room temperature.[40] Pharmaceutical cocrystals contain an API which has biological activity that can be used in the diagnosis, treatment or cure of a disease.[41] Cocrystals have received elevated levels of attention from the pharmaceutical sector due to their aforementioned ability to modify the physicochemical properties of pharmaceutical compounds to improve their use as effective mechanisms of disease treatment, cure or prevention.[41]

Currently, orally delivered pharmaceutical compounds have been classified into four main categories based on their individual levels of solubility and permeability, as indicated by **Table 1.5**.

Table 1.5: Biopharmaceutics Classification System (BCS) for Orally Administered Pharmaceutical Compounds.[42]

BCS Classification	*Solubility*	*Permeability*
Class I	High	High
Class II	Low	High
Class III	High	Low
Class IV	Low	Low

Pharmaceutical compounds should have a certain level of bioavailability and therefore require suitable solubility so that they can be absorbed by the body in the gastrointestinal tract and be transported in the bloodstream to the relevant cellular organelles and compartments.[42] One particular class of compounds of interest to the pharmaceutical sector are sulfonamides due to their use as antimicrobial agents and low production cost. The sulfonamide is a functional group that is the basis of several groups of pharmaceutical drugs which are widely recognised as sulfa drugs.[43]

1.3.6 *Ionic Cocrystals*

Ionic cocrystals bear resemblance to molecular cocrystals however their structure is comprised of an ionic compound and a neutral coformer. They can be defined as "*Multi-component materials formed from a salt and a molecular or ionic compound* ".[44] Numerous studies have been reported in the literature to date which shows improved physicochemical properties of

ionic cocrystals and more recently, this research has expanded into primary benzenesulfonamides (BSAs). There are limited publications on ionic cocrystal structures of BSA however the current ionic cocrystal structures are composed of *N*-Oxides and metal ions exclusively, some of which are detailed in section *1.4.3*. Classified under ionic cocrystals are zwitterionic cocrystals. Zwitterionic cocrystals have been relatively unexplored to date, however, they are starting to share the research spotlight with molecular cocrystals.[44] The most intriguing zwitterions are the twenty proteogenic amino acids with alanine, glycine and proline being of high interest due to their uncharacteristic properties. Amino acids suffer from extremely poor solubility with the vast majority being soluble in water only. Proline and a select few amino acids do not suffer from this issue and are soluble in organic solvent-water mixtures. In terms of BSA, zwitterions have yet to be explored and could provide and exciting avenue for research and development of novel sulfonamide drugs.

1.3.7 *Eutectic Composition*

Eutectics are a class of multi-component solid forms with wide applicability in daily life.[45] Eutectics are known to have low melting points as compared to the individual components. There are multiple examples of eutectic mixtures in the literature inclusive of marketed pharmaceutical eutectic compositions, such as prilocaine and lidocaine, which are local anaesthetics. For these compounds, lidocaine has a m.p. of 68 °C and prilocaine has a m.p. of 38°C both of which are higher than body temperature resulting in low permeability and slow pharmacological action. The eutectic composition of these two compounds is an oil with a m.p. of 22 °C which gives it faster skin permeability and rapid pharmacological action.[45] For a long time, it was believed that crystal engineering principles could not be applied to eutectic

compositions however, in the last decade, *Nangia* & *Cherukuvada* designed and explained eutectics based on well-established crystal engineering principle, **Figure 1.9**.

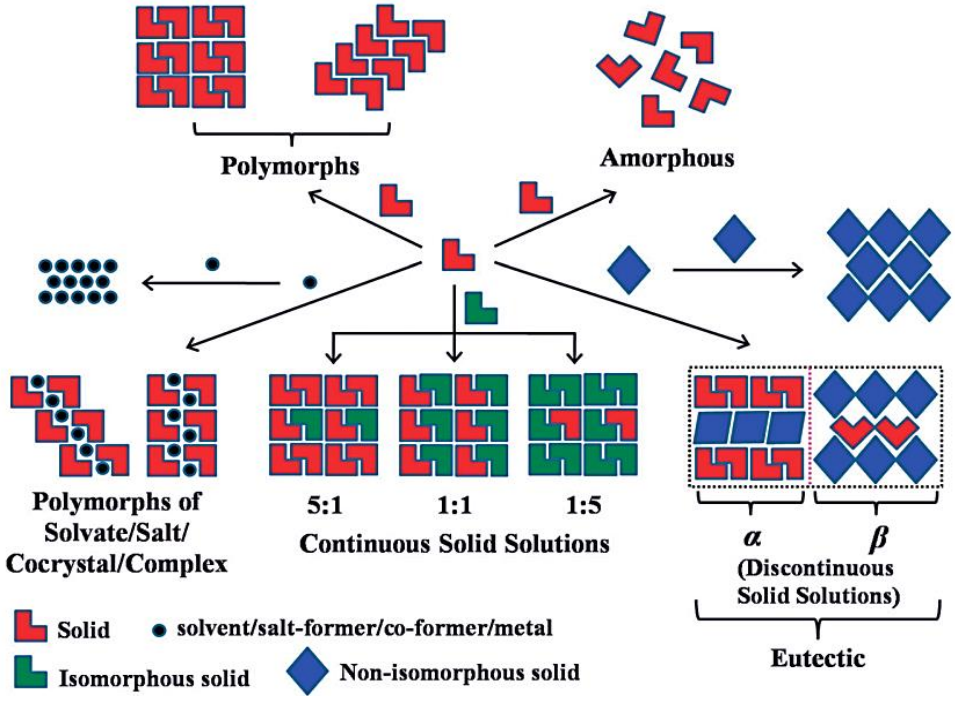


Figure 1.9: Diagram proposing eutectics can be classified under crystal engineering principles.[45]

In eutectics, the heteromolecular interactions are relatively weak and as a result characterization of eutectics is challenging. X-ray Diffraction (XRD) and IR alone are not sensitive enough to detect such weak van der Waals interactions between the two components therefore, thermal methods are required for analysis.[45] However, *Nangia* has reported that the use of Nuclear Magnetic Resonance Spectroscopy (NMR), solid-state NMR (ss-NMR), in addition to XRD, IR and thermal analysis, are sufficient techniques in determining the composition as a eutectic. It has also been observed that eutectics can be the unintended product of failed cocrystallization experiments. It has been proposed that eutectics are the intermediary step in specific cocrystals, and it has been noted that solution eutectic constants are critical for cocrystal formation and stabilisation in solution. Hence, it can be stipulated cocrystals,

eutectics and solid solutions are intimately related but not the same.[45] What links eutectics to benzenesulfonamide cocrystals is the drug sulfathiazole. Sulfathiazole is a prominent sulfa drug which was reported to form a eutectic with Urea in the early 1960s, **Figure 1.10**. This compound was investigated and determined to have a higher drug absorption rate than the pure drug.[45]

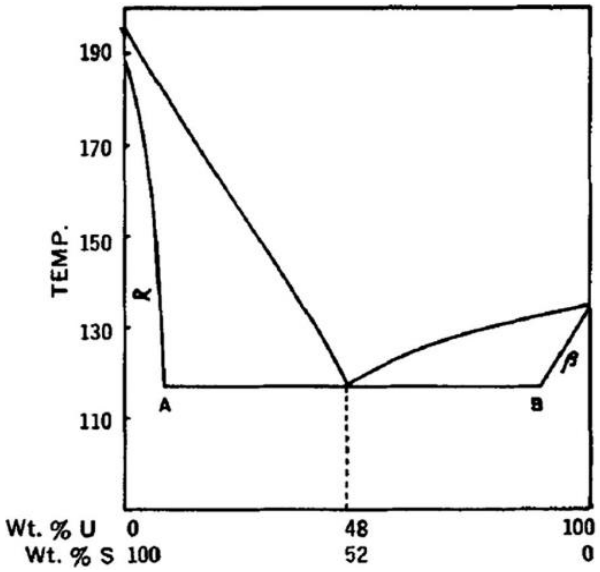


Figure 1.10: Phase diagram of sulfathiazole-urea eutectic composition.[45]

Cocrystallization is a prominent technique used to improve physicochemical properties however, cocrystal formation is performed on a trial and error basis. The use of eutectics provides another promising avenue to investigate if common cocrystal techniques fail to produce a cocrystal.

1.3.7.1 Relationship Between Eutectics and Cocrystals

In the past the boundary between cocrystals, eutectics and solid solutions was not well defined due to the three systems being strongly interlinked. However, with phase diagrams, which can

be obtained with the aid of DSC measurements, it is for most cases possible to differentiate between eutectics, cocrystals and solid solutions. For eutectics the idealised phase diagram is the eutectic point, which is the point on a phase diagram where the maximum number of allowable phases are in equilibrium. When this point is reached, the temperature must remain constant until one of the phases disappears. For cocrystals the idealised phase diagram is the point on a phase diagram where the solvent, API and coformer reaches equilibrium according to the composition of a mixture of the three components at constant temperature and pressure.

There is one specific example that highlights the connection present between eutectics, solid solutions and cocrystals which is benzoic acid and its analogues. Benzoic acid can combine with 4-fluorobenzoic acid, pentafluorobenzoic acid, and benzamide to form a solid solution, a cocrystal and a eutectic respectively.[45] The 4-fluorobenzoate and benzoate are isomorphic, which is the property that is responsible for the formation of the solid solution. The benzoate-pentafluorobenzoate cocrystal is formed due to the crucial stabilization from auxiliary C-H···F interactions. The line is blurred for the benzoate-benzamide system as in 2008, *Singh et al* reported the formation of a binary eutectic system however, in 2009, *Brittain* reported a cocrystal for the same system based on differences in spectroscopic and diffraction patterns.[45] In 2011, *Seaton et al,* concluded that the absence of secondary-auxiliary interactions rendered the compound as a eutectic rather than a cocrystal. The line between eutectic, solid solution and cocrystal is fine however, with the knowledge and grading system from this paper as well as the phase diagrams it appears that the weak adhesive interactions are the key in determining the classification of the system. This example is one of two well documented examples with the other being curcumin-resorcinol (cocrystal) and curcumin-hydroquinone (eutectic).[45]

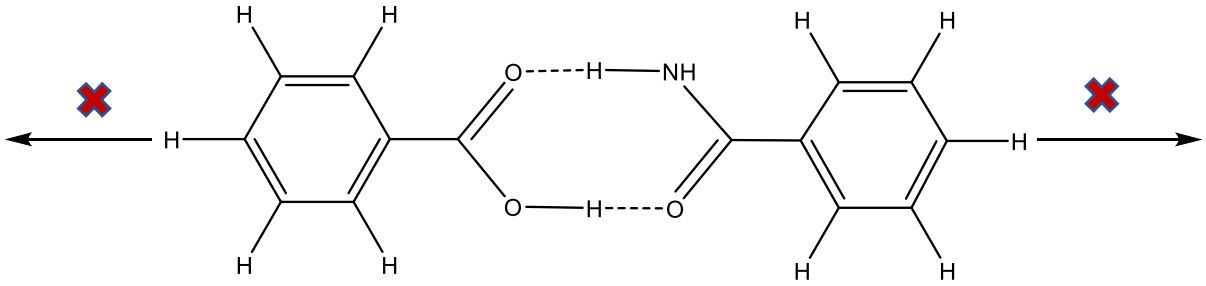


Figure 1.11: The absence of secondary-auxiliary interactions in benzoate-benzamide system means a eutectic product will form instead of a cocrystal, adapted from reference 45.

1.3.8 *Solvates*

IUPAC provided the definition for solvates as: "*Solvation is an interaction of a solute with the solvent, which leads to stabilization of the solute species in the solution*".[46] Solvates basically are multicomponent crystalline solid molecular adducts containing both the target molecule and a solvent incorporated into the crystal lattice structure. Solvates consist of hydrogen bonds, van der Waals forces and coordinate covalent bonds in a crystal lattice between APIs and excipients.[46] Most small molecular weight APIs and excipients form solvates readily due to their small molecular size. Solvents can lead to problems in organic compounds by inducing disorder in the crystal structure however, solvent molecules in the crystal lattice can create strong non-covalent interactions to form flexible clusters which can improve solubility and metastability of solid forms.[46] As such, cocrystal solvates have been recognised for their pharmaceutical relevance in the last number of years.

Cocrystal solvates belong to a separate class of crystalline solid forms than cocrystals but are often discovered during the cocrystal screening process (ethanol liquid assisted grinding or ethanol slow evaporations) and have significant pharmaceutical relevance.[46] In terms of the pharmaceutical industry, cocrystal solvates are recognised as suitable solid form once the

solvent used in the crystal lattice is ethanol. The reason for the use of pharmaceutical ethanol is due to its ability to improve drug solubility, bactericidal activity, endogeneity in human intestinal organs and its preservative properties.[46]

However, the probability of two component crystals being formed depends on the varied and multiple hydrogen bonding motifs and different functional groups. The combination of these structure-related factors and process-related factors gives rise to diverse possibilities for supramolecular transformations. These possibilities make determining the outcome of cocrystal/solvate experiments very difficult as different polymorphic forms or solvates may form, see **Figure 1.12**.[46]

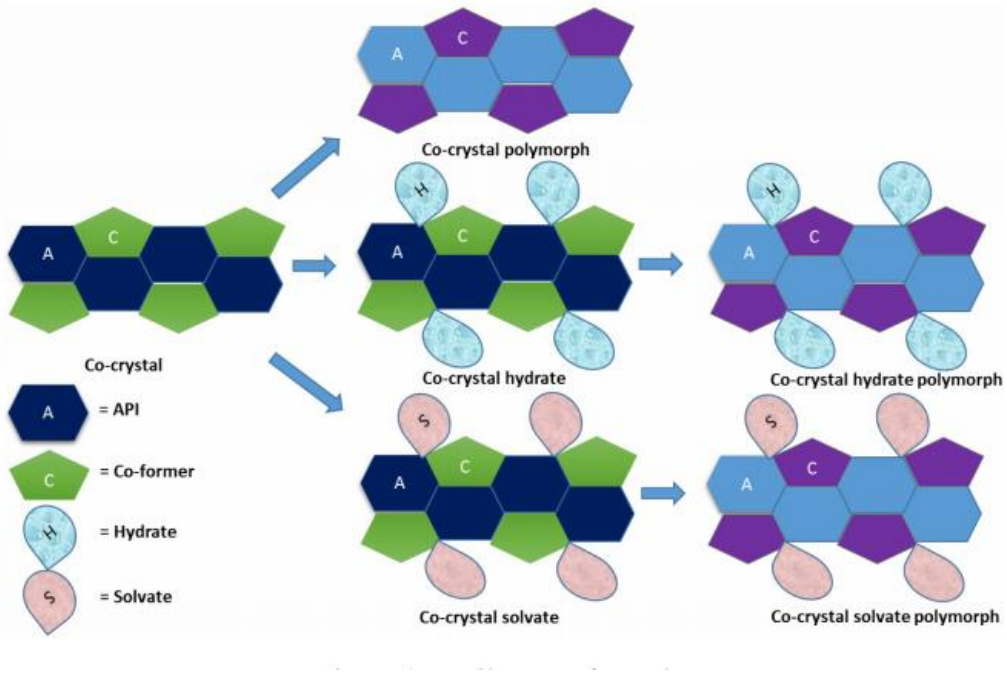


Figure 1.12: Various possible outcomes of cocrystals.[46]

Sulfonamide-coformer cocrystal solvates have been explored for the last decade with some success.[47] One example (**Figure 1.13**) is the chlorothiazide-pyridine (1:3) cocrystal solvate.[47] The reason sulfa-drugs are investigated for solvate formation is because APIs such

as chlorothiazide are well known to crystallize in a solvated form.[47] The crystal structure is stabilized by strong intermolecular N-H···N hydrogen bonds.[47]

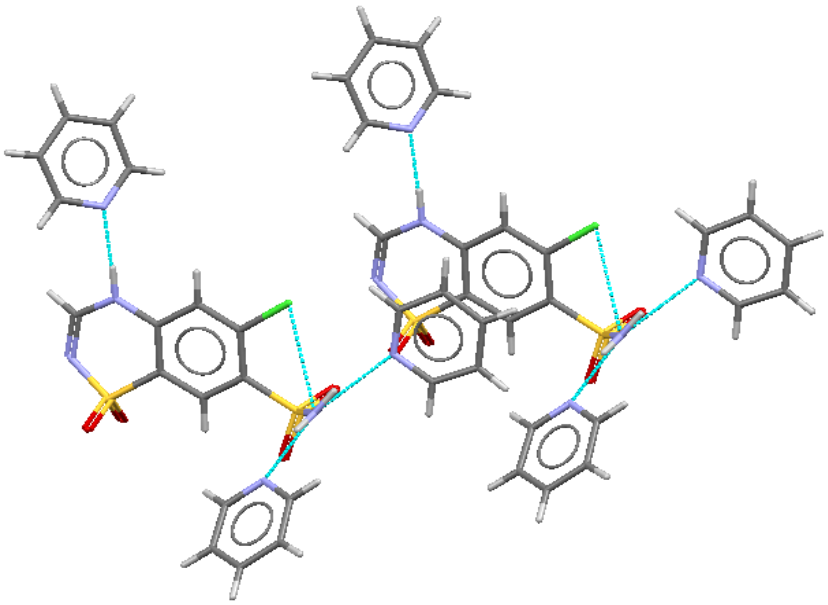


Figure 1.13: The crystal packing in chlorothiazide-pyridine (1/3) solvate.[47]

1.4 *Cocrystallization Involving Sulfonamides*

Sulfonamide drugs were the first antibacterials to be used systemically, and paved the way for the antibiotic revolution where newer antibacterial and antimicrobial drugs, mainly penicillin's, supplanted many sulfonamide drugs due to their superior mechanism of action.[48] Sulfonamides are classified into oral and topical sulfonamides with short, intermediate and long acting half-lives. In terms of biochemical activity, the free NH_2 group in the para position is essential for sulfonamide activity. Substitution of the phenyl ring in either the ortho (*o*-) or para (*p*-) position has negative consequences for sulfonamide activity. The sulfonamide functional group must be attached to the phenyl ring for antimicrobial activity.[49]

The first sulfonamide drug was called Prontosil which was a prodrug.[50] A prodrug is a medication or compound that, once administered, undergoes phase I metabolism primarily via Cytochromes P-450 enzymes into a pharmacologically active drug however, metabolism of a prodrug can occur through alternate routes in the body, illustrated in **Figure 1.14.**

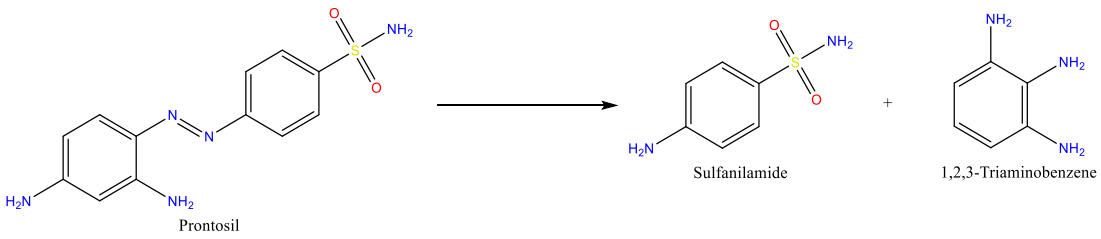


Figure 1.14: Sulfonamide drugs common core structure (sulfanilamide) by-product of prontosil metabolism adapted from reference 50.

The antibacterial properties of prontosil was first described by *Gerhard Domagk* in the 1930's.[50] He and a Bayer scientist named *Josef Klarer* recognised that azo-dyes exhibited preferential binding to bacteria and some parasites *in vivo*. This breakthrough discovery was not published until 1935 and shortly after in 1936 the metabolic pathway of prontosil was discovered by *Ernest Fourneau* and his team.[50] Once prontosil was administered they observed that it was metabolised to sulfanilamide which is the primary metabolite and antibacterial agent of the sulfonamide drug. This triggered the explosion into the development of sulfonamide drugs throughout the 1930's and 1940's, as seen in **Figure 1.15**, as well developing ideas about bioactivation, which is now a well-defined concept in the area of toxicology.[50]

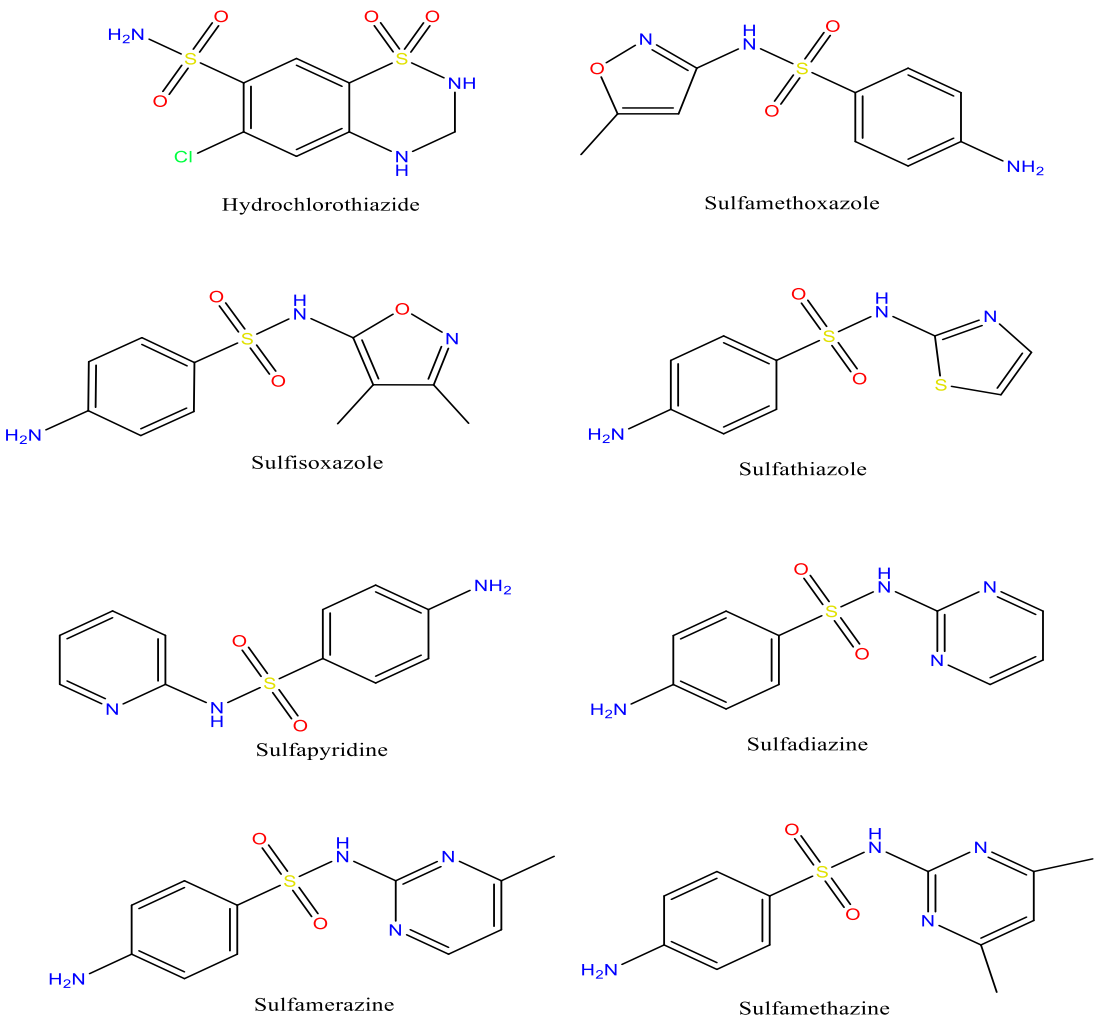


Figure 1.15: Structures of common sulfa drugs, adapted from reference 50.

Sulfonamides are competitive antagonists of *p*-amino-benzoic acid (PABA) which is essential for folate synthesis and thus bacterial growth and reproduction. The core structure of sulfonamide drugs is known as a benzenesulfonamide, **Figure 1.16**. BSA consists of a phenyl ring covalently bonded to the sulfonamide group. Sulfonamides reversibly block folate synthesis therefore having bacteriostatic effect.[50] The basis for this inhibitory effect is due to the likeness of *p*-amino-benzoic acid and sulfanilamide.

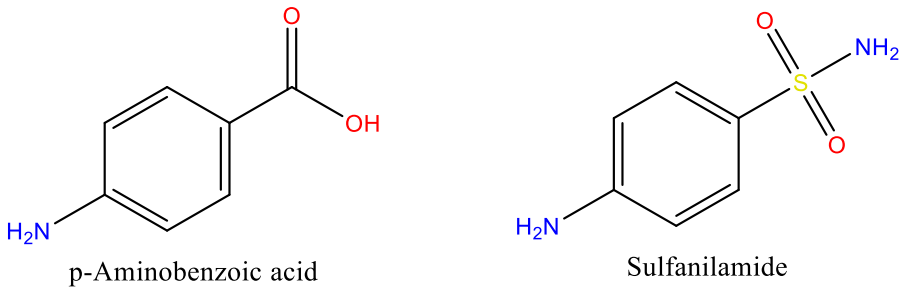


Figure 1.16: Structural similarities between *p*-amino-benzoic acid and sulfanilamide adapted from reference 50.

The first step of folate synthesis is the reaction of PABA and pteridine in the presence of dihydropteroate synthase resulting in dihydro pteroic acid. This intermediate reacts with glutamic acid producing dihydrofolic acid via enzyme dihydrofolate synthase. This intermediate is reduced by dihydrofolate reductase which is used by bacteria to synthesise methionine, purine, and pyrimidine bases.[50] The sulfanilamide moiety binds to dihydropteroate synthase to prevent folic acid and DNA synthesis, outlined in **Figure 1.17**.

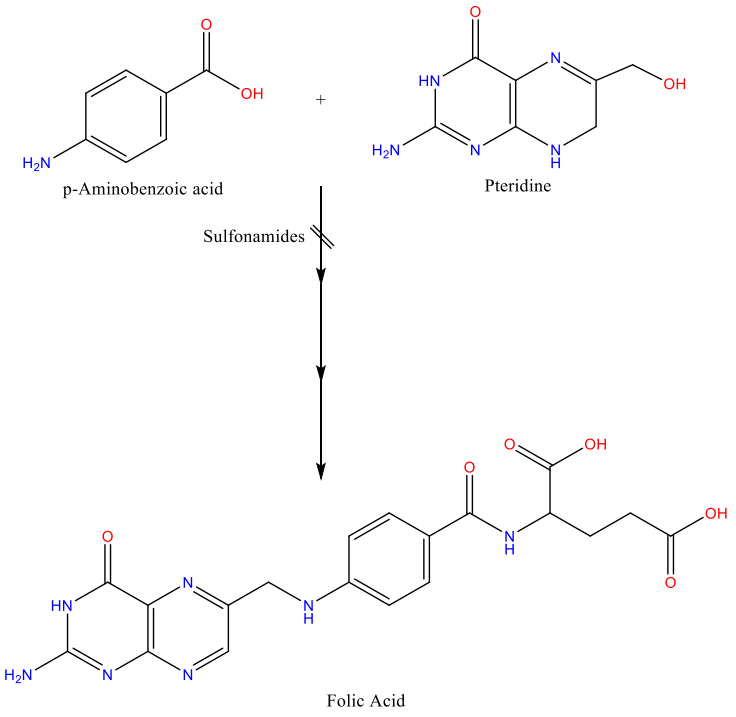


Figure 1.17: Sulfonamide mechanism of action, adapted from reference 50.

Metabolism of sulfonamides in humans occurs in the liver by acetylation of the amino group. The *N*-acetyl metabolites are inactive and can be excreted in urine with unchanged sulfonamides. *N*-oxidation is another possible avenue. Once formed, hydroxylamino metabolites can undergo auto-oxidation to the corresponding nitrozo intermediates.[50] Nitrozo metabolites are unstable in body fluids and can be reduced using glutathione and excreted. However, when the capacity for conjugation with glutathione is exceeded, the reactive metabolites show a direct cytotoxic activity or can be bound to proteins and participate in the immune reactions.[50]

Sulfonamide drugs are not limited by their antibacterial and antimicrobial properties. Sulfonamides also displayed anti-malarial and anti-fungal properties and are often present in other medications:[51]

1) Anti-Hyperglycaemic Agents; Sulfonylurea was commonly used to treat type two diabetes. It was discovered that the sulfa drug had the ability to stimulate the beta cells of the pancreas via action upon the ATP ion channels which resulted in the release of insulin. However, its use is short lived due to its adverse effect on bone marrow.
2) Diuretics; In general diuretics such as carbonic anhydrase, thiazides and loop diuretics are sulfonamide compounds. Loop diuretics are considered safer and high ceiling diuretics and find frequent use in the treatment of hypertension.
3) Serotonin Antagonists; Sumatriptan for example is a 5-HT3 receptor antagonist as such, they are used as anti-depressants.
4) Anti-Inflammatory; Celecoxib is a well-established sulfonamide drug with anti-inflammatory properties. It operates by selectively inhibiting COX-2 enzymes. This prevents prostaglandins and inflammatory substrate production.

There are many other types of pharmacological sulfonamides in the literature that are reported to treat several other well-known diseases which include HIV, Epilepsy, Migraines and Arthritis, for example.[51]

Sulfonamides, like any other pharmaceutical compound have the potential to cause a variety of adverse reactions such as urinary tract disorders, porphyria, and hypersensitivity. When used in large doses they can result in a strong allergic reaction.[51] The most serious cases are classified as severe cutaneous adverse reactions and the most prominent members of these cases is Stevens-Johnson, toxic epidermal necrolysis and Drug reaction with eosinophilia and systemic symptoms.[51] Approximately 3% of the general population have adverse allergic reactions to sulfa drugs. This hypersensitivity is less common in the nonantibiotic forms. There are two specific features of allergic response: 1) the N1 heterocyclic ring and 2) the N4 amino nitrogen which can form reactive metabolites.[51]

The major issue with sulfonamide drugs outside of the adverse hypersensitivity is that sulfonamide compounds are more active in the protonated form.[51] Sulfonamides like many potential pharmaceutical compounds suffer from very poor aqueous solubility which is one of the primary problems with pharmaceutical compounds resulting in sulfonamides being classified into either BCS class II or, most often, the BCS class IV drugs, see **Table 1.5**. Poor aqueous solubility results in sulfa drugs being eliminated through phase II and phase III conjugation reactions before they can exhibit their therapeutic effects. To overcome this issue patients who take sulfa drugs must drink copious amounts of water to prevent the crystallisation of sulfonamides in the kidneys. Now, through crystal engineering, manipulation of the supramolecular and solid-state chemistry has allowed for the controlled drug development of sulfa drugs primarily through cocrystallisation of sulfonamides with both neutral, ionic and GRAS coformers, salt formation and polymorphisms.[51]

Cocrystallisation of monosubstituted phenyl sulfonamides allows for an in-depth study of the supramolecular and solid-state chemistries of sulfa-drugs. More importantly, it allows for a review into the sulfonamide functional group and as such in the past three decades amide-amide, acid-amide and amide-pyridine synthons have been utilised to elucidate information about the sulfonamide functional group. Sulfonamides have two acidic protons and three electronegative atoms, all of which can potentially form a hydrogen bond making them excellent targets for cocrystal studies, examples of which are illustrated in **Figure 1.18**.

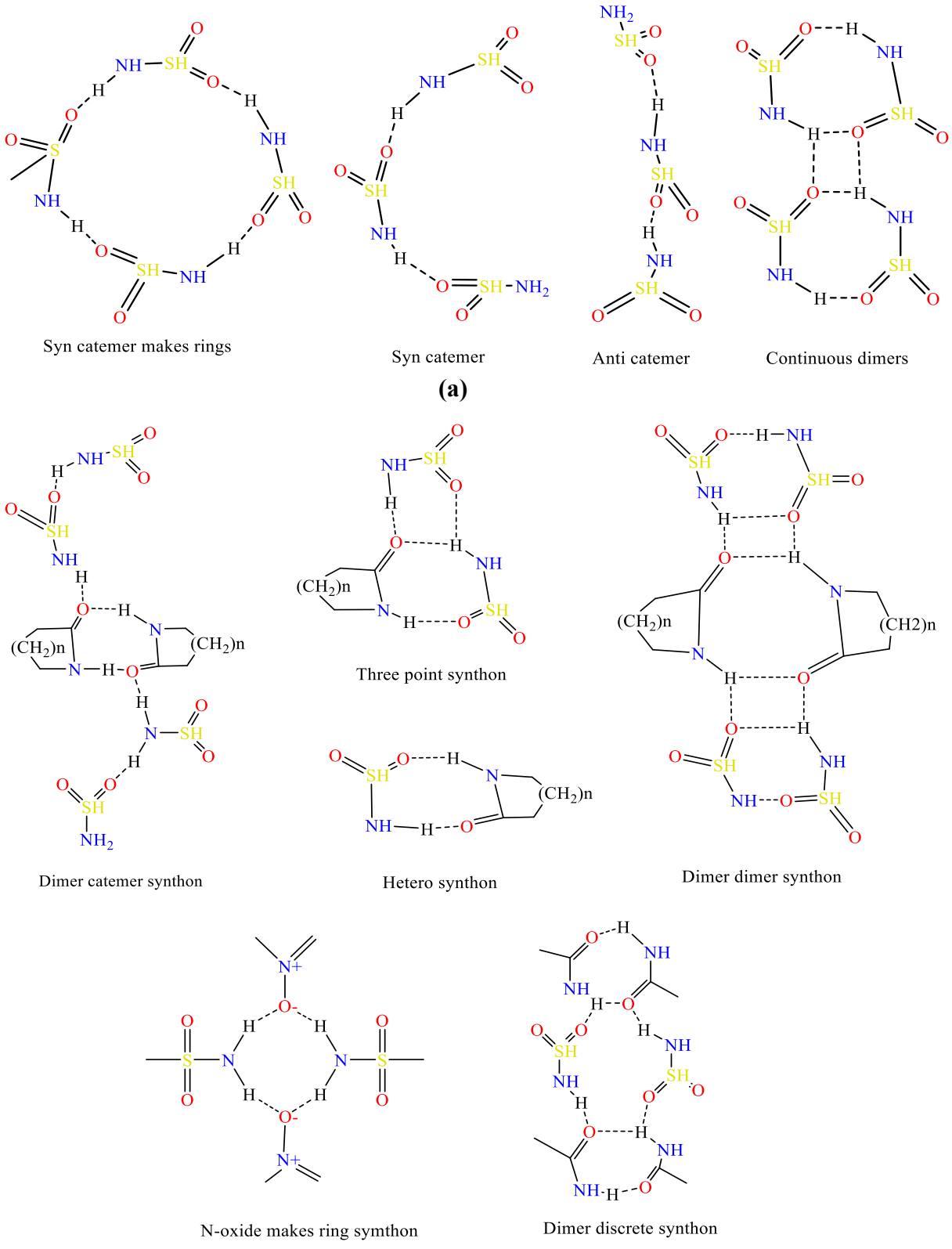


Figure 1.18: Homosynthons present in primary sulfonamides, **(a)**, and synthons present in sulfonamide cocrystals, **(b)**, adapted from reference 52.

1.4.1 *Amide Coformers*

A CSD search for primary benzenesulfonamides yielded 664 hits which showed that several sulfa drugs such as celecoxib, hydrochlorothiazide, and furosemide as well as monosubstituted benzenesulfonamides were used in cocrystallization studies with amide coformers. Primary amides are well represented in the literature with the dominant supramolecular homosynthon being the centrosymmetric dimer.[52] This homosynthon has complimentary hydrogen bond donors and acceptors and can self-organise into tapes and sheets.[52]

Sulfonamide-Amide cocrystals have been widely reported with papers dedicated to research on both homosynthon and heterosynthon generation.[52] Sulfonamide-Amide cocrystals can be categorised by the structure of the amide coformer. For example, sulfonamides tend to form either dimer or catemer synthons whereas carboxamides, a class of cyclic amides, form dimer synthons.[52] Cyclic amides have received more attention than primary amides.[52] The use of lactams for sulfonamide cocrystals has gained a lot of attention due to the complementary functional groups of the two components. Sulfonamides have two hydrogen bond acceptor and two donor atoms which makes their pairing with lactams, which only have one of each, suitable for cocrystal development.[52] Some of the major lactams used in sulfonamide research are caprolactam, 2-pyrrolidone, 1-aza-2-cyclooctanone (AZL) and valerolactam as they are considered GRAS compounds. *Bolla* and *Nangia* reported that the cocrystallization of benzenesulfonamides with lactams resulted in 13 sulfonamide-syn-2carboxamide catemers, 2 dimer-cyclic synthons and 4 dimer-catemer synthons.[52] The three types of synthons were observed:

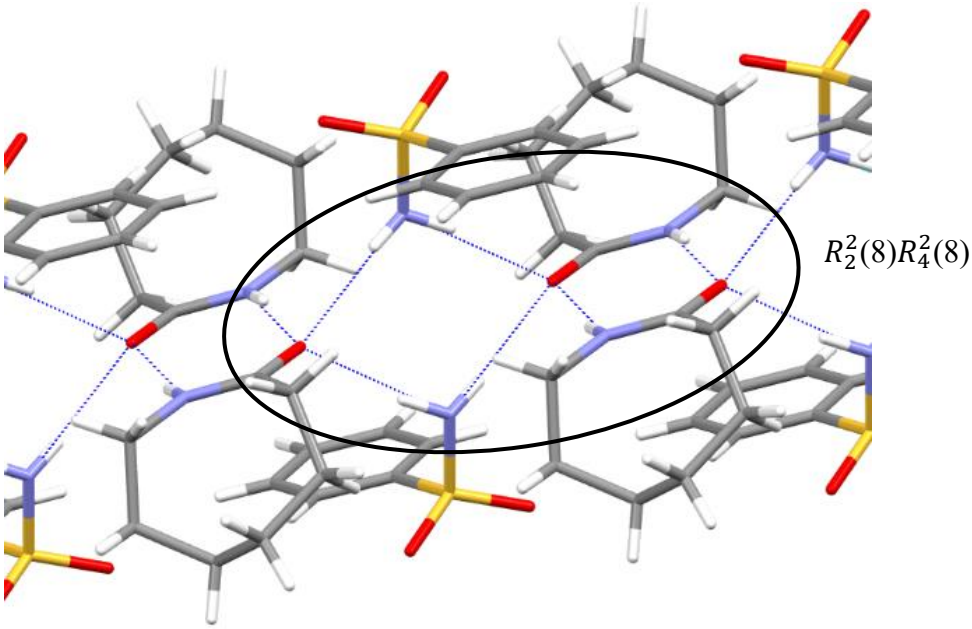
1) the catemer motif of graph-set $C_2^1(4)$,

2) dimer-cyclic synthon motif of $R_2^2(8)$ $R_2^4(8)$,

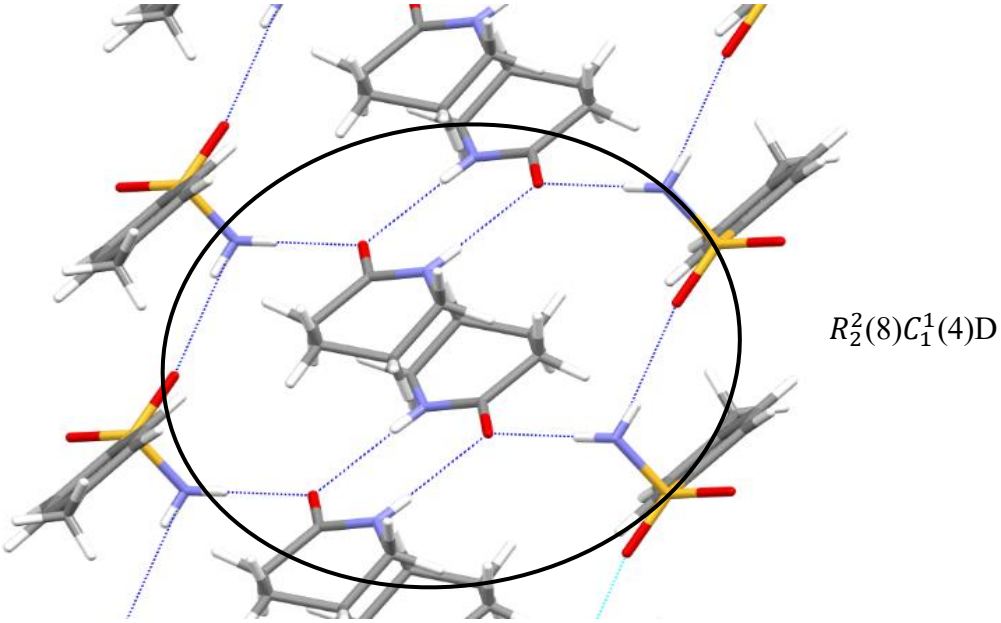
and 3) dimer-catemer motifs $R_2^2(8)$ $C_1^1(4)$.[52]

In this paper the sulfonamides NH_2 donates an N-H···O hydrogen bond to both sides of the carbonyl group of the lactam acceptor in all three synthons with the BSA-AZL cocrystal having an additional C-H···O=S interaction. This interaction is rare and is only found with certain sulfonamides as outlined in **Chapter 2**.

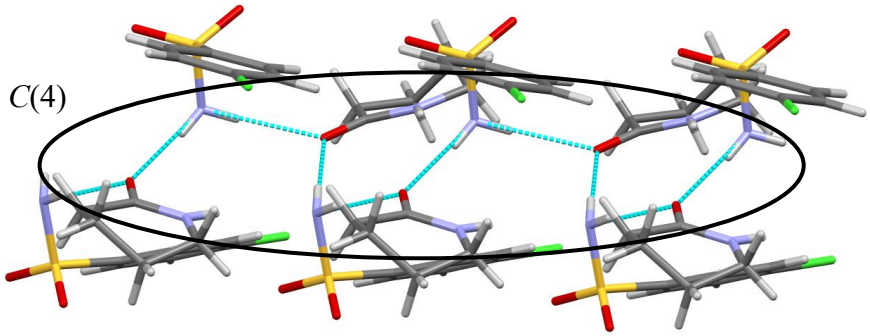
To date, most of the research and information available about sulfonamide-amide cocrystals has been reported by *Nangia* and *Bolla*. They are pioneering the investigation into sulfonamide cocrystallization with a strong focus on coformers that have the potential for sulfa drug development.



(a)



(b)



(c)

Figure 1.19: dimer-cyclic synthon **(a)**, dimer-catemer synthon **(b)** and catemer synthon **(c)** as reported by *Nangia* and *Bolla.*[52]

Pyridine Carboxamides; picolinamide, nicotinamide and isonicotinamde were also utilised by *Nangia* for a study of heterosynthons in binary systems with 4-sulfamoylbenzenesulfonamide.

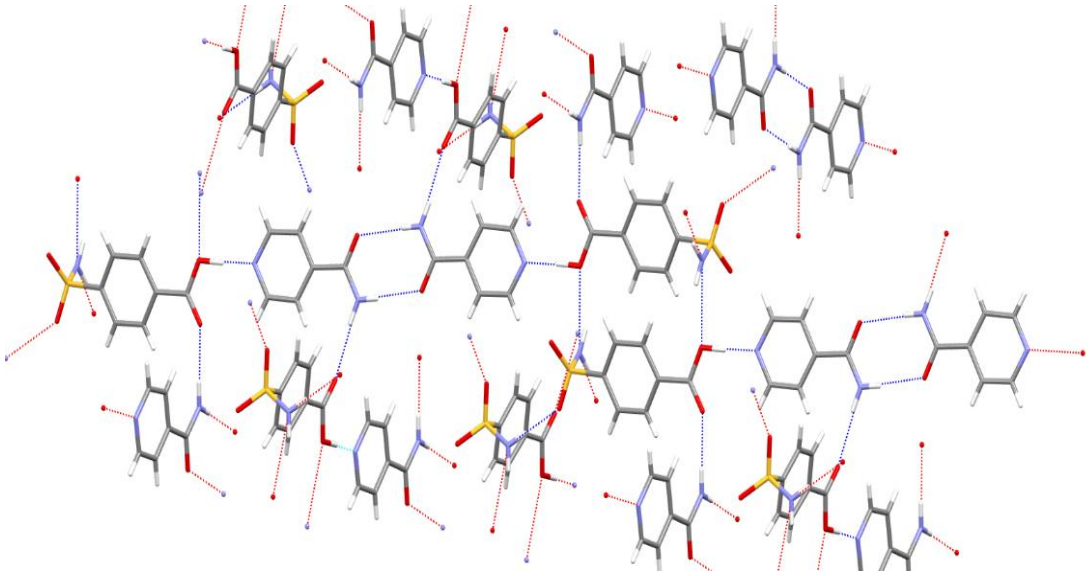


Figure 1.20: Crystal structure of 4-sulfamoylbenzenesulfonamide (3SMBA)-Isonicotinamide (INA) was solved in the monoclinic *C*2/*c* crystals system.[53]

In this paper, homodimers of INA form acid-amide heterosynthon with anti N-H amide and C=O of the acid groups. The O-H of carboxylic acid forms acid-pyridine heterosynthon with INA pyridine N atom. The SMBA molecules form dimers via sulfonamide and carboxylic acid groups (N-H···O), and furthermore the sulfonamides extended through catemer chains (H-N···S=O) along the 21-screw axis.[53]

One particular sulfonamide drug cocrystal, Sulfadimethoxine (SDM)-Isonicotinamide (INA) contains one molecule of SDM and one molecule of INA. SDM chains grow along the a-axis through N-$H_{terminal}$ amine···$O_{sulfone}$ hydrogen bonds, with the SDM molecules oriented in a head-to-tail fashion. These chains, based on the $C_1^1(8)$ motif, are bridged by two antiparallel INA chains through N-$H_{sulfonamide}$···O_{ISO} and N-H_{ISO}···$N_{terminal}$ amine hydrogen bonds, in which the connection between INA molecules is established via N-H_{amine}···$N_{pyridine}$ ring interactions.[54]

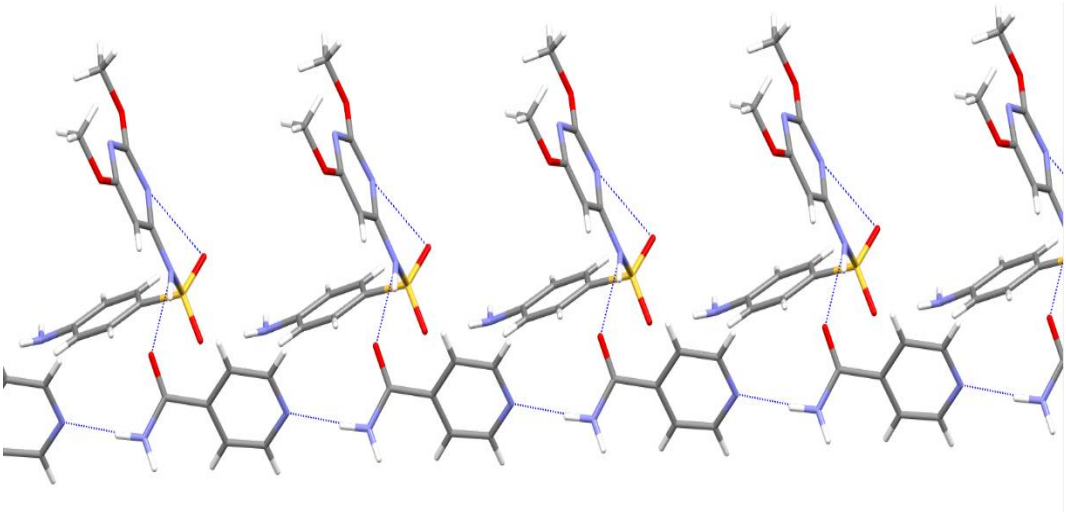


Figure 1.21: Sulfadimethoxine-Isonicotinamde cocrystal displaying N-$H_{sulfonamide}$ (SDM)···O(INA) (blue), and N-H_{amide} (INA)···$N_{terminal}$ amine (SDM) interactions.[54]

1.4.2 *Carboxylic Acid Coformer*

Carboxylic acids moieties are the longest and best studied functional group in terms of understanding hydrogen bonding in solution and solid-state. They exhibit a wide range of diversity in their supramolecular chemistry which has allowed for the study of polymorphism. Carboxylic acids self-organize in the form of supramolecular homosynthons, the dimer and catemer synthons.[55] They tend to favour the formation of Carboxylic Acid-Amide heterosynthons.

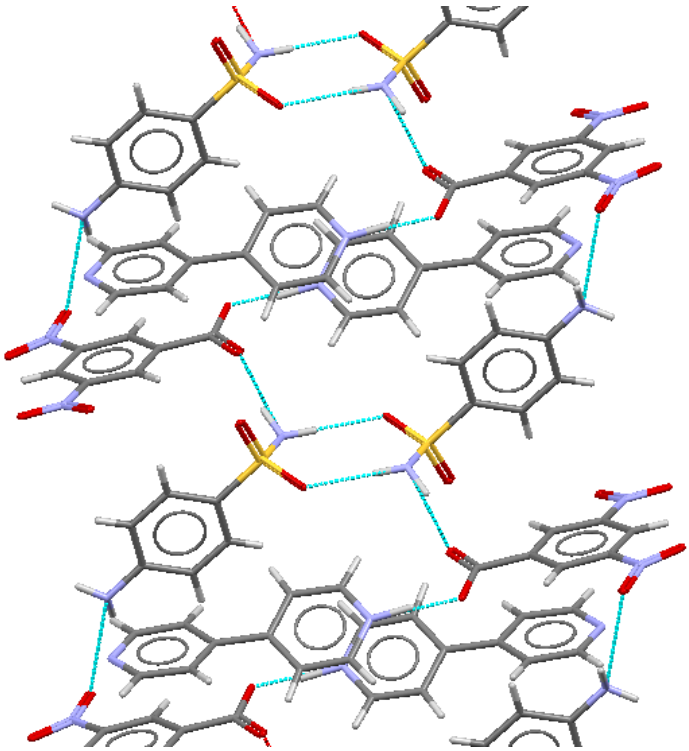


Figure 1.22: Ternary crystalline molecular complex with 3,5-dinitrobenzoic acid (DNBA), bipyridine and sulfanilamide. The ternary complex has a 1:1:1 composition, in which 3,5-dnba binds to bipyridine through a discrete $CO_2H\cdots N_{pyridine}$ hydrogen bond and the sulfanilamide molecules form a homodimer by a $R_2^2(8)$ $NH_2\cdots O{=}S$ interaction.[55]

Carboxylic acids are regularly cocrystallized with drug molecules to improve their solubility and permeability. The hydrogen bonds between these functional groups are classified as strong O-H···O/N-H···O bonds. Sulfonamide-Carboxylic Acid cocrystals however, have not been widely explored with a CSD search reporting minimal Sulfonamide-Carboxylic Acid cocrystals.

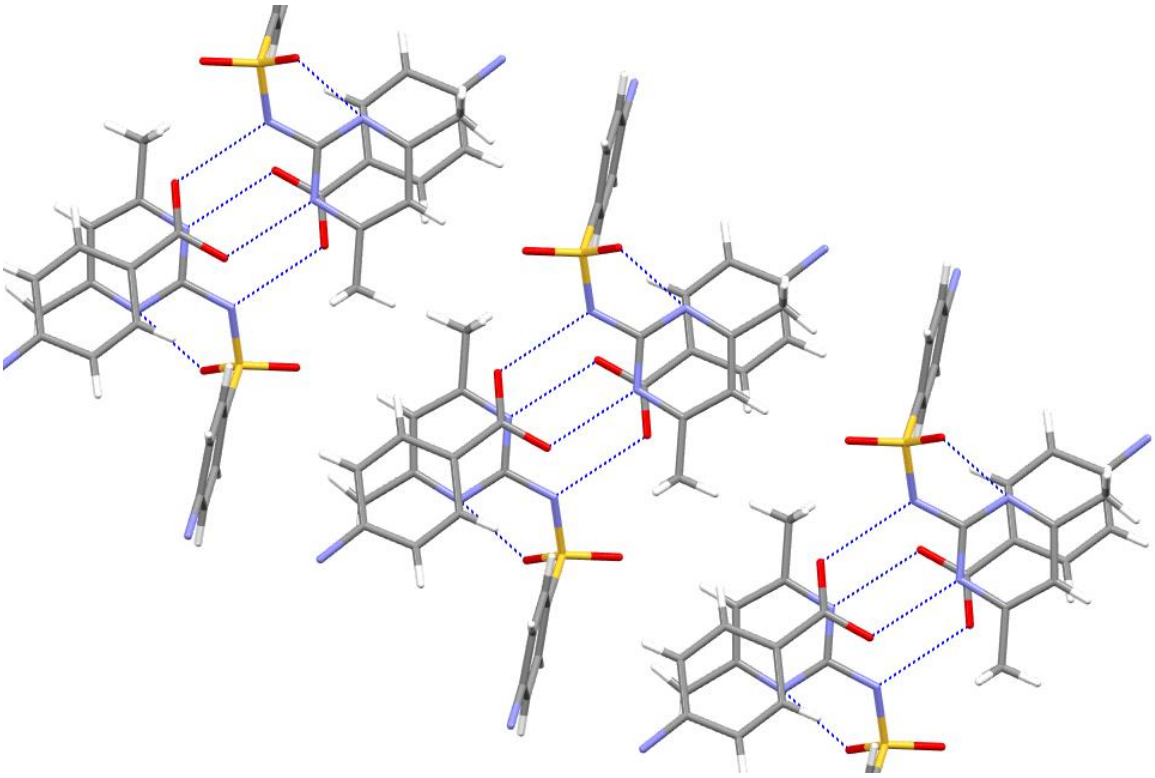


Figure 1.23: The asymmetric unit consists of one molecule of Sulfamethazine (STH) and PABA interacting with each other via intermolecular hydrogen bonds to form a supramolecular oligomer.[56]

Pan et al reported the STH-PABA cocrystal crystallizes in triclinic space group $P\bar{1}$. More specifically, the carbonyl (C=O) and hydroxyl (C-OH) groups in PABA are involved in hydrogen bonding interactions with N atoms of the amide and pyrimidine groups in STH, respectively. The distances of $N_{pyrimidine}\cdots H\text{-}O_{hydroxyl}$ and $N_{amide}\text{-}H\cdots O_{carbonyl}$ are classified as ordinary H-bonds although the former is slightly shorter and thus are considered as neutral hydrogen bonds required for cocrystal formation. Packing of the oligomers resulted in the extended structure of STH-PABA cocrystal via extensive π···π and C-H···π interactions between phenyl rings of PABA and/or STH.[56]

Sulfa drugs are known for their antimicrobial and anti-infective properties and as such are desirable coformers with other medications. Acids such as *p*-aminobenzoic acid have been

cocrystallized with sulfa drugs like sulfamethazine and furosemide to improve its BCS classification.[57] The Furosemide-PABA cocrystal was reported by *Harriss et al* to form synthon 1 dimers as well as reporting halogen bonding between the chlorine atom of furosemide and the oxygen of the carboxylic acid. The paper also reported a modest increase in the solubility of furosemide.[57] Sulfa drugs have been known to cocrystallize with pain relief medication like aspirin and tramadol. Bumetanide-Carboxylic acids have been recorded to from ternary cocrystals which are of significant interest in the pharmaceutical sector due to their potential application as multi-drug complexes. *Nangia* investigated the solid-liquid phase transitions of the cocrystal Sulfamethazine - Salicylic acid, in which they formed binary cocrystals.[58]

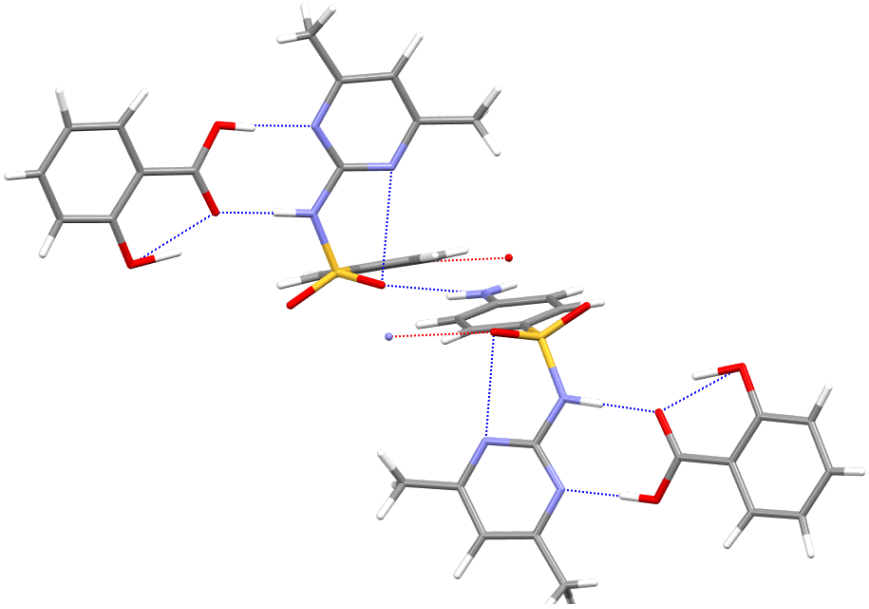


Figure 1.24: Sulfamethazine-Salicylic Acid cocrystal.[58]

1.4.3 *Pyridine Coformers*

Widely reported is the structural stability of Sulfonamide-Pyridine-*N*-Oxide cocrystals.[59] However, *N*-Oxide compounds are not classified as GRAS compounds and are not used with

APIs despite their complimentary functional groups.[59] Different geometries were found for pyridine coformers, ranging from discrete (D) assemblies to chains I and rings I. The most common synthon is the $C_1^1(8)$ chain which competes with the occurrence of the $R_2^1(8)$ synthon.[59] A 2-Chlorobenzenesulfonamide-Bipy-*N*-Oxide (BPNO) cocrystal was reported by *Nangia* where N-H···O_{Noxide} bonding was observed. One of the sulfonamides oxygens is involved in intramolecular C-C···O halogen bonding.[60] The same results were observed for 2-Bromobenzenesulfonamide and 4-Methoxybenzenesulfonamide with Bipyridine-*N*-oxide cocrystals.[60]

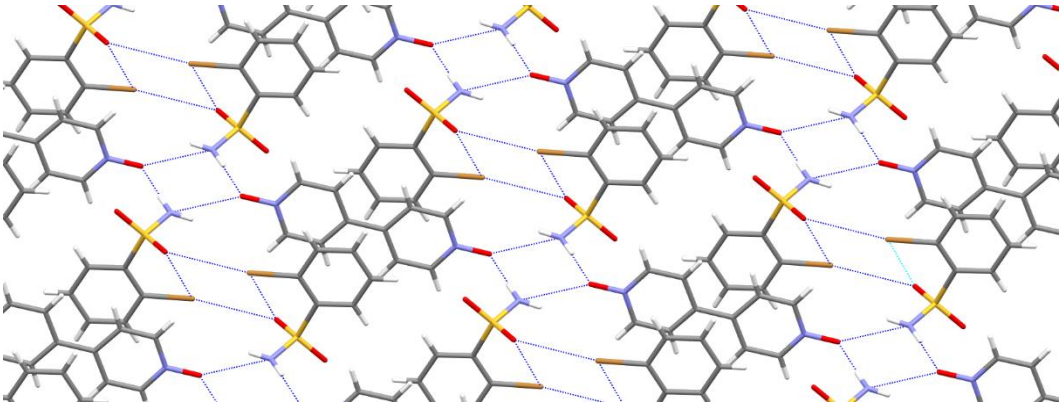


Figure 1.25: 2BrBSA-4,4-Bipyridine-*N*-oxide cocrystal as reported by *Nangia.*[60] 2BrBSA and BPNO molecules form a two-dimensional array of tetrameric ring motif $R_2^4(8)$ of N-H and O-N_{oxide} hydrogen bonds.

The crystal structure of cocrystal celecoxib (CEL)-bipyridine (BPY) was solved and refined in a triclinic system with the $P^{-}1$ space group. One celecoxib and one 4,4′-bipyridine molecules are included in the asymmetric unit. The CEL and BPY molecules are connected by a set of intermolecular H-bonding interactions between a sulfonamide group and aromatic nitrogen N_{arom} via hydrogen bonding synthon II N3–H···N1, (2.21 Å) and N3–H···N2′, (2.07 Å) to form a one-dimensional chain. These one-dimensional chains are further aligned in parallel and ranged along the b and c axes to generate a 2D structure.[61]

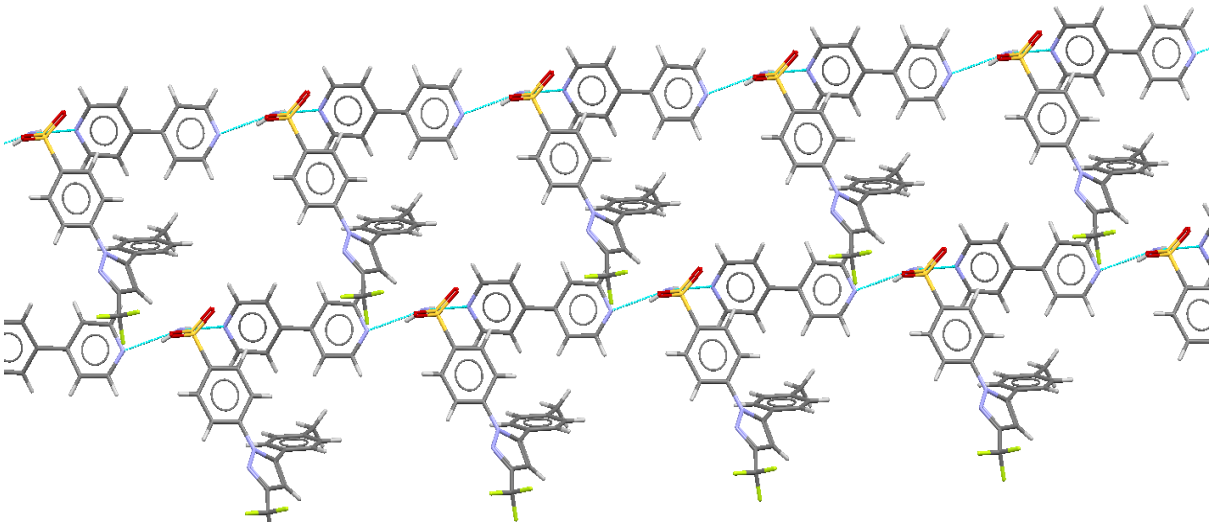


Figure 1.26: Binary cocrystal of celecoxib and bipyridine.[61]

1.4.4 *Drug – Drug Cocrystal*

A drug-drug cocrystal is a subclass of pharmaceutical compounds where the coformer is another API with its own biological activities. They are an essential tool in the sector for fighting multi-drug resistance by improving the pharmacological effects of both individual drugs. The dual-drug combination has been an approach to offer a synergistic therapy in recent years. It shows potential advantages of reducing drug dosage, toxicity, and resistance, and enhancing the efficacy of therapy.[62]

Hydrochlorothiazide (HCT) is a sulfa drug used to treat hypertension and oedemas. Pyrazinamide is one of the most important medicines for the treatment of tuberculosis and was discovered to be a suitable coformer with HCT. The HCT-Pyrazinamide cocrystal is a cornerstone of sulfonamide drug-drug pharmaceutical cocrystals.[62] As a structural analogue to dapsone, sulfanilamide contains both sulfonamide and aromatic amino functionalities.

Hydrogen bonding in the crystal structure of Dapsone (DAP)-SNA is very complex. There are multiple potential H-bonding donors/acceptors in both DAP and SNA molecules. Each of these groups can participate in the formation of at least two hydrogen bonds.[63] Major H-bonding interactions can be identified in the complementary sulfonamide-sulfonamide interactions of SNA to form a one-dimensional chain structure. SNA was connected with the other two SNA molecules by intermolecular N5-H27⋯ O3, (2.23 Å), and N5-H28⋯O4, (2.49 Å), hydrogen bonds to give a one-dimensional chain structure along the a axis.[62] The amino group of DAP was also found to form a H-bonding interaction with the sulfonamide oxygen from SNA via synthon I N6-H15⋯O1, (2.54 Å).[63] The sulfonyl group of DAP, on the other hand, formed a H-bonding interaction with the aromatic amino group of SNA also via synthon I N1-H4B⋯O4, (2.20 Å). The multiple H-bonding interactions between DAP and SNA result in the 3D packing pattern.[63]

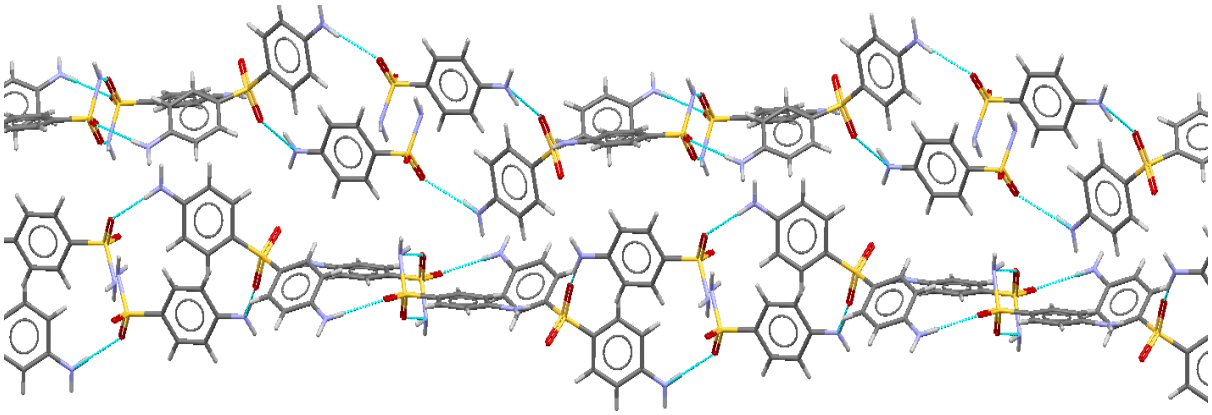


Figure 1.27: DAP and SUL were crystallized in 1:2 stoichiometry, and the single-crystal structure was solved and refined in the monoclinic system with the C2/c space group and one DAP and two SNA molecules in the asymmetric unit.[63]

Sulfathiazole and sulfanilamide are two model sulfa drugs which have also been reported to cocrystallize in drug-drug cocrystals.[64] Five polymorphs of the sulfathiazole-

sulfanilamide cocrystal were obtained and all displayed improved solubility. The mechanism of action exhibited for all these drug-drug cocrystal was pH independent.[64]

One interesting result was a drug-drug cocrystal between Chlorothiazide-Carbamazepine. This cocrystal was reported to present as dimers with the typical $R_2^2(8)$ amide homosynthon. The dimers are linked by two chlorothiazide molecules via $NH_{thiadiazine}\cdots O_{amide}$ and $NH_{amide}\cdots O{=}S$ interactions into an infinite chain.[65]

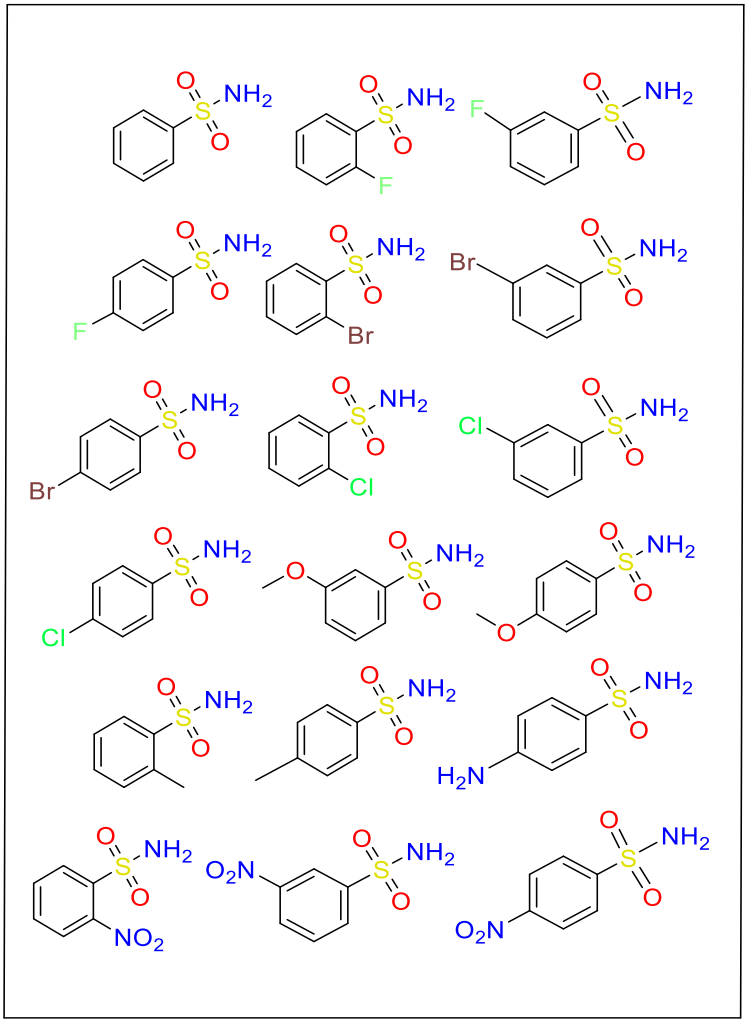
1.5 *Conclusion*

The understanding of intermolecular interactions is a prerequisite for successful cocrystal design. The systems of cocrystals cited in this review were chosen to support the view that drugs such as sulfonamides, have potential for pharmaceutical development.[66] Pharmaceuticals suffer greatly from poor aqueous solubility and low bioavailability and amongst the various techniques for improvement cocrystallisation has high potential to improve the physiochemical properties of sulfa drugs.[66]

1.6 *Objectives*

The main objective of this research M.Sc. is to utilise a range of BSA to investigate the interactions between the primary benzenesulfonamide and commonly used pharmaceutical coformers and APIs. This will help develop an understanding of the sulfonamide-coformer crystal structure as well add knowledge to the literature which focuses on supramolecular synthons for the sulfonamide functional group.[66] This will be achieved by employing a crystal engineering strategy. Sulfonamide cocrystallization has been largely overlooked to date but

there is a rising interest due to their applications in sulfa-drug development. A major component of this work will be on the use of LAG, PXRD and SCXRD for the generation and elucidation of the crystal structures of any crystalline material formed.



References

1. Arunan, E.; Desiraju, G.; Klein, R.; Sadlej, J.; Scheiner, S.; Alkorta, I.; Clary, D.; Crabtree, R.; Dannenberg, J.; Hobza, P.; Kjaergaard, H.; Legon, A.; Mennucci, B.; Nesbitt, D. Definition Of The Hydrogen Bond (IUPAC Recommendations 2011). *Pure App. Chem.* **2011**, *83*, 1637-1641.
2. Desiraju, G. ChemInform Abstract: Hydrogen Bridges in Crystal Engineering: Interactions Without Borders. *ChemInform*. **2010**, *33*, 565-573.
3. Steiner, T. The Hydrogen Bond in The Solid State. *Angew. Chem. Int. Ed.* **2002**, *41*, 48-76.
4. Dannenberg, J. An Introduction to Hydrogen Bonding by George A. Jeffrey. *J. Am. Chem. Soc.* **1998**, *120*, 5604-5604.
5. Wood, P.; Feeder, N.; Furlow, M.; Galek, P.; Groom, C.; Pidcock, E. Knowledge-Based Approaches to Co-Crystal Design. *Cryst. Eng. Comm.* **2014**, *16*, 5839-5848.
6. Adsmond, D.; Grant, D. Hydrogen Bonding In Sulfonamides. *J. Pharm. Sci.* **2001**, *90*, 2058-2077.
7. Desiraju, G. Supramolecular Synthons in Crystal Engineering-A New Organic Synthesis. *Angew. Chem. Int. Ed.* **1995**, *34*, 2311-2327.
8. Almarsson, O.; Zaworotko, M. Crystal Engineering of The Composition of Pharmaceutical Phases. Do Pharmaceutical Co-Crystals Represent A New Path to Improved Medicines? *ChemInform*. **2004**, *35*, 1889-1896.
9. Allu, S.; Suresh, K.; Bolla, G.; Mannava, M.; Nangia, A. Role of Hydrogen Bonding in Cocrystal and Coamorphous Solids: Indapamide As A Case Study. *Cryst. Eng. Comm.* **2019**, *21*, 2043-2048.
10. Bolla, G.; Nangia, A. Supramolecular Synthon Hierarchy in Sulfonamide Cocrystals With Syn-Amides And N-Oxides. *IUCrJ* **2019**, *6*, 751-760.

11. Lawrence, S.; McAuliffe, M.; Moynihan, H. Mimics Of A R22(8) Hydrogen-Bond Dimer Motif: Synthesis And Influence On The Crystallisation Of Sulfathiazole And Sulfapyridine. *Eur. J* **2010**, *6*, 1134-1141.
12. Athira, A.; Anu, S.; Seeja, S.; Thaifa, M. A Review On Pharmaceutical Cocrystals. *Int. J. Pharm. Res. Scholars* **2018**, *7*, 1-17.
13. Lohani, S.; Grant, D. Thermodynamics of Polymorphs. *ChemInform*. **2007**, 38, 21-42.
14. Cruz-Cabeza, A.; Reutzel-Edens, S.; Bernstein, J. Facts and Fictions About Polymorphism. *Chem. Soc. Rev.* **2015**, *44*, 8619-8635.
15. Thun, J.; Seyfarth, L.; Butterhof, C.; Senker, J.; Dinnebier, R.; Breu, J. Wöhler And Liebig Revisited: 176 Years of Polymorphism in Benzamide – And the Story Still Continues! *Cryst. Growth Des.* **2009**, *9*, 2435-2441.
16. Nangia, A. Conformational Polymorphism in Organic Crystals. *Acc. Chem. Res.* **2008**, *41*, 595-604.
17. Nyman, J.; Day, G. Static and Lattice Vibrational Energy Differences Between Polymorphs. *Cryst. Eng. Comm.* **2015**, *17*, 5154-5165.
18. Threlfall, T. Structural and Thermodynamic Explanations of Ostwald's Rule. *Org. Process Res. Dev.* **2003**, *7*, 1017-1027.
19. Chung, S.; Kim, Y.; Kim, J.; Kim, Y. Multiphase Transformation and Ostwald's Rule of Stages During Crystallization of a Metal Phosphate. *Nat. Phys.* **2008**, *5*, 68-73.
20. Lee, E. A Practical Guide to Pharmaceutical Polymorph Screening & Selection. *J. Pharm. Sci.* **2014**, *9*, 163-175.
21. Li, L.; Salamończyk, M.; Shadpour, S.; Zhu, C.; Jákli, A.; Hegmann, T. An Unusual Type of Polymorphism in A Liquid Crystal. *Nat. Comm.* **2018**, *9*, 714, 1-8.
22. Grossjohann, C.; Serrano, D.; Paluch, K.; O'Connell, P.; Vella-Zarb, L.; Manesiotis, P.; McCabe, T.; Tajber, L.; Corrigan, O.; Healy, A. Polymorphism in Sulfadimidine/4-

Aminosalicylic Acid Cocrystals: Solid-State Characterization and Physicochemical Properties. *J. Pharm. Sci.* **2015**, *104*, 1385-1398.

23. Munroe, Á.; Rasmuson, Å.; Hodnett, B.; Croker, D. Relative Stabilities of The Five Polymorphs of Sulfathiazole. *Cryst. Growth Des.* **2012**, *12*, 2825-2835.
24. Elguero, J. Polymorphism And Desmotropy In Heterocyclic Crystal Structures. Crystal Growth & Design **2011**, *11*, 4731-4738.
25. Peterson, M.; Hickey, M.; Zaworotko, M.; Almarsson, Ö. Expanding the Scope of Crystal Form Evaluation in Pharmaceutical Science. *J. Pharm. Sci.* **2006**, *9*, 317-326.
26. Nangia, A.; Desiraju, G. Crystal Engineering: An Outlook for The Future. *Angew. Chem. Int. Ed.* **2019**, *58*, 4100-4107.
27. Desiraju, G. The crystal as a supramolecular entity; John Wiley & Sons: Chichester, *Angew. Chem.* **1997**, *109*, 1056-1056.
28. Etter, M. Cheminform Abstract: Encoding and Decoding Hydrogen-Bond Patterns of Organic Compounds. *ChemInform* **1990**, *21,* 120–126.
29. Etter, M.; MacDonald, J.; Bernstein, J. Graph-Set Analysis of Hydrogen-Bond Patterns in Organic Crystals. *Acta Crystallogr., Sect. B: Struct. Sci.* **1990**, *46*, 256-262.
30. Bernstein, J.; Davis, R.; Shimoni, L.; Chang, N. Cheminform Abstract: Pattern in Hydrogen Bonding: Functionality and Graph Set Analysis in Crystals. *ChemInform* **2010**, *26*, 1555-1573.
31. Hunter, C. Quantifying Intermolecular Interactions: Guidelines for The Molecular Recognition Toolbox. *ChemInform*. **2005**, *36,* 5310-5324.
32. Kumar, S.; Nanda, A. Pharmaceutical Cocrystals: An Overview. *J. Pharm. Sci*. **2017**, *79,* 858-871.
33. Zhang, C.; Xiong, Y.; Jiao, F.; Wang, M.; Li, H. Redefining the Term Of "Cocrystal" And Broadening Its Intention. *Cryst. Growth Des.* **2019**, *19*, 1471-1478.

34. https://www.pharmaexcipients.com/excipient-sources/gras-substances-scogs-database/ accessed on 06/09/2019
35. Karagianni, A.; Malamatari, M.; Kachrimanis, K. Pharmaceutical Cocrystals: New Solid Phase Modification Approaches for The Formulation of Apis. *Pharmaceutics* **2018**, *10*, 18, 1-30.
36. Paul, M.; Desiraju, G. From A Binary to A Quaternary Cocrystal: An Unusual Supramolecular Synthon. *Angew. Chem. Int. Ed.* **2019**, *58*, 12027-12031.
37. Mir, N.; Dubey, R.; Desiraju, G. Four- And Five-Component Molecular Solids: Crystal Engineering Strategies Based on Structural Inequivalence. *IUCrJ* **2016**, *3*, 96-101.
38. Cerreia Vioglio, P.; Chierotti, M.; Gobetto, R. Pharmaceutical Aspects of Salt and Cocrystal Forms of Apis And Characterization Challenges. *Adv. Drug Del. Rev.* **2017**, *117*, 86-110.
39. Kavanagh, O.; Croker, D.; Walker, G.; Zaworotko, M. Pharmaceutical Cocrystals: From Serendipity to Design to Application. *Drug Discov. Today* **2019**, *24*, 796-804.
40. Karimi-Jafari, M.; Padrela, L.; Walker, G.; Croker, D. Creating Cocrystals: A Review of Pharmaceutical Cocrystal Preparation Routes and Applications. *Cryst. Growth Des.* **2018**, *18*, 6370-6387.
41. Schultheiss, N.; Newman, A. Pharmaceutical Cocrystals And Their Physicochemical Properties. *Cryst. Growth Des.* **2009**, *9*, 2950-2967.
42. Amidon, G.; Lennernäs, H.; Shah, V.; Crison, J. A theoretical basis for a biopharmaceutic rug classification: the correlation of in vitro drug product dissolution and in vivo bioavailability *Pharm. Res.* **1995**, *12*, 413-420.
43. Otten, H. Domagk And the Development of The Sulphonamides. *J. Antimicrob. Chemother.* **1986**, *17*, 689-690.

44. Duggirala, N.; Perry, M.; Almarsson, O.; Zaworotko, M. Cheminform Abstract: Pharmaceutical Cocrystals: Along the Path to Improved Medicines. *ChemInform*. **2016**, *47*, 640-655.

45. Cherukuvada, S.; Nangia, A. Eutectics as Improved Pharmaceutical Materials: Design, Properties and Characterization. *Chem. Commun.* **2014**, *50*, 906-923.

46. Healy, A.; Worku, Z.; Kumar, D.; Madi, A. Pharmaceutical Solvates, Hydrates and Amorphous Forms: A Special Emphasis on Cocrystals. *Adv. Drug Del.* Reviews **2017**, *117*, 25-46.

47. Johnston, A.; Florence, A.; Kennedy, A. Chlorothiazide–Pyridine (1/3). *Acta Crystallogr., Sect. E: Struct. Rep. Online* **2008**, *64*, 1105-1106.

48. Yousef, F.; Mansour, O.; Herbali J. Sulfonamides: Historical Discovery Development (Structure-Activity Relationship Notes). *In-vitro In-vivo In-silico Journal* **2018**, *1*, 1-15.

49. Rabiya Parveen, S.; Praveen, S.; Pal, H. A Short Review on Sulphonamides with Antimicrobial Activity. *Int. J. Pharm. Chem.* **2017**, *7*,70-73.

50. Tacic, A.; Nikolic, V.; Nikolic, L.; Savic, I. Antimicrobial Sulfonamide Drugs. *Adv. Tech.* **2017**, *6*, 58-71.

51. Tilles, S. Practical Issues in The Management of Hypersensitivity Reactions: Sulfonamides. *Sout. Med. J.* **2001**, *94*, 817-824.

52. Bolla, G.; Mittapalli, S.; Nangia, A. Modularity and Three-Dimensional Isostructurality Of Novel Synthons in Sulfonamide–Lactam Cocrystals. *IUCrJ* **2015**, *2*, 389-401.

53. Bolla, G.; Nangia, A. Multicomponent Ternary Cocrystals Of the Sulfonamide Group with Pyridine-Amides and Lactams. *Chem. Commun.* **2015**, *51*, 15578-15581.

54. Domingos, S.; Fernandes, A.; Duarte, M.; Piedade, M. New Multicomponent Sulfadimethoxine Crystal Forms: Sulfonamides As Participants in Supramolecular Interactions. *Cryst. Growth Des.* **2016**, *16*, 1879-1892.

55. Seaton, C.; Blagden, N.; Munshi, T.; Scowen, I. Creation of Ternary Multicomponent Crystals by Exploitation of Charge-Transfer Interactions. Chemistry – *Eur. J.* **2013**, *19*, 10663-10671.

56. Pan, X.; Zheng, Y.; Chen, R.; Qiu, S.; Chen, Z.; Rao, W.; Chen, S.; You, Y.; Lü, J.; Xu, L.; Guan, X. Cocrystal Of Sulfamethazine And P-Aminobenzoic Acid: Structural Establishment And Enhanced Antibacterial Properties. *Cryst. Growth Des.* **2019**, *19*, 2455-2460.

57. Harriss, B.; Vella-Zarb, L.; Wilson, C.; Evans, I. Furosemide Cocrystals: Structures, Hydrogen Bonding, And Implications for Properties. *Cryst. Growth Des.* **2013**, *14*, 783-791.

58. Ahuja, D.; Svärd, M.; Rasmuson, Å. Investigation of Solid–Liquid Phase Diagrams of The Sulfamethazine–Salicylic Acid Co-Crystal. *Cryst. Eng. Comm.* **2019**, *21*, 2863-2874.

59. Allu, S.; Bolla, G.; Tothadi, S.; Nangia, A. Supramolecular Synthons in Bumetanide Cocrystals And Ternary Products. *Cryst. Growth Des.* **2017**, *17*, 4225-4236.

60. Goud, N.; Babu, N.; Nangia, A. Sulfonamide−Pyridine-N-Oxide Cocrystals. *Cryst. Growth Des.* **2011**, *11*, 1930-1939.

61. Wang, X.; Zhang, Q.; Jiang, L.; Xu, Y.; Mei, X. Isostructurality In Six Celecoxib Co-Crystals Introduced by Solvent Inclusion. *Cryst. Eng. Comm.* **2014**, *16*, 10959-10968.

62. Wang, J.; Ye, C.; Mei, X. Structural and Physicochemical Aspects of Hydrochlorothiazide Co-Crystals. *Cryst. Eng. Comm.* **2014**, *16*, 6996-7003.

63. Jiang, L.; Huang, Y.; Zhang, Q.; He, H.; Xu, Y.; Mei, X. Preparation and Solid-State Characterization of Dapsone Drug–Drug Co-Crystals. *Cryst. Eng. Comm.* **2014**, *14*, 4562-4573.

64. Yeh, K.; Lee, T. Intensified Crystallization Processes For 1:1 Drug–Drug Cocrystals Of Sulfathiazole–Theophylline, And Sulfathiazole–Sulfanilamide. *Cryst. Growth Des.* **2018**, *18*, 1339-1349.

65. Aljohani, M.; Pallipurath, A.; McArdle, P.; Erxleben, A. A Comprehensive Cocrystal Screening Study of Chlorothiazide. *Cryst. Growth Des.* **2017**, *17*, 5223-5232.

66. Caira, M. Sulfa Drugs as Model Cocrystal Formers. *Mol. Pharmaceutics* **2007***, 4,* 310–316.

Chapter Two - Crystal Landscape of Primary Aromatic Sulfonamides

2. *Crystal Landscape of Primary Aromatic Sulfonamides*

2.1 *Abstract*

The crystal landscape of 22 primary aromatic sulfonamides is described featuring 8 novel sulfonamide crystals as well as 14 previously published. The sulfonamides display similar characteristic intermolecular hydrogen-bonding interactions in the solid state to those observed in their widely studied amide analogues, including $R_2^2(8)$ dimers and C(4) chains. In the crystal, molecules are packed into a three-dimensional supramolecular structure through hydrogen bonds between the two H atoms of the sulfonamide group and the two O atoms of the sulfonyl group of neighboring molecules. Based on the observed solid-state features, the sulfonamide functional group, which is a strong hydrogen-bond donor and acceptor, offers considerable potential as a key moiety for crystal engineering.

2.2 *Introduction*

Sulfonamides, RSO_2NH_2, are a class of organosulfur compounds that are amide derivatives of sulfonic acids (RSO_3H), **Figure 2.1**. Several molecules with the sulfonamide group are found to display antibacterial and antimicrobial properties and intrinsically, have been applied in medicinal therapies for more than 70 years.[1] Benzenesulfonamides make up the core component of most marketed sulfonamide drugs and as such, are currently receiving attention in the crystal engineering community.[2] These compounds are of high significance because they can be utilized to develop supramolecular synthons for the sulfonamide functional group which can be directly applied to sulfonamide drugs in order to improve their solubility, permeability and dissolution.[3]

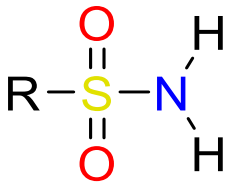


Figure 2.1: The sulfonamide functional group.

The study of intermolecular interactions is the basis of crystal engineering and in the past few years, cocrystallization has been the focus of many research groups, with the purpose of using crystal engineering strategies to develop new crystalline materials with targeted properties.[4] Recently, sulfonamide studies showed that cocrystallization can improve these physicochemical properties with one such example being from *Nangia's* group.[5,6] *Nangia* recently reported four cocrystals, two salts and one salt-cocrystal of the sulfa-drug bumetanide using various GRAS compounds. This paper was one of two studies on bumetanide cocrystals, the initial being a study on bumetanide synthons and ternary products.[5] A bumetanide caprolactam cocrystals, in particular, displayed improved membrane permeability and aqueous solubility nearly 2-fold compared to native bumetanide and, thus, was stipulated to be an alternative formulation for bumetanide.[4] Hence, structural studies on novel sulfonamide synthons as well as studies on the solubility, dissolution rate, and permeability enhancement of new solid forms, particularly salts and cocrystals, have significance in the pharmaceutical industry.[6]

We attempted to cocrystallize several benzenesulfonamides with a library of coformers, but we were only successful in obtaining the sulfonamides. As a result of this, a systematic study of simple primary benzenesulfonamides was undertaken to improve the knowledge pertaining to sulfonamide crystal structures. The compounds investigated are shown in **Figure 2.2**.

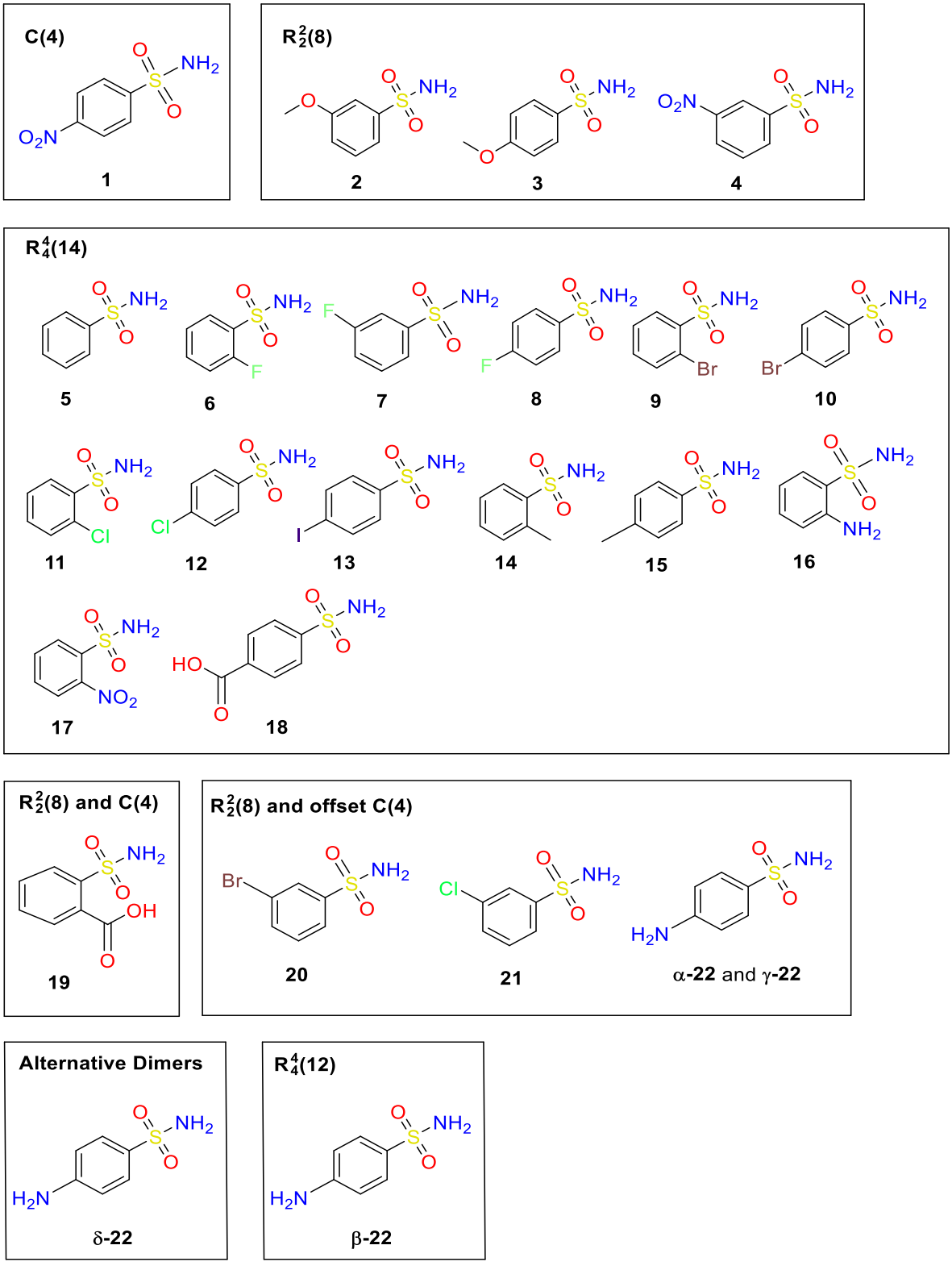


Figure 2.2 Sulfonamides (1−22) investigated in this study and arranged by the hydrogen-bonding motifs observed in their crystal structures, using Etter's graph set notation.[7-9] Compounds **2**, **3**, **6**, **7**, **9**, **17**, **20** and **21** are this work.

2.3 *Experimental*

Materials.

All benzenesulfonamides, coformers and solvents were purchased from commercial outlets and were used as received without further purification.

Grinding Experiments.

Mechanico-chemical grinding experiments were conducted in a Retsch MM400 mixer mill, equipped with stainless steel 5 mL grinding jars and one 2.5 mm stainless steel grinding ball per jar with 2-4 drops of EtOAc. The mill was operated at a rate of 30 Hz for 20 min. The ratio of 1:1 of benzenesulfonamide with the coformers was used in all cases. The ground product was dissolved in 5 mL of EtOH and MeOH.

Physical Measurements.

IR spectra were recorded on a PerkinElmer UATR Two spectrophotometer using a diamond ATR accessory over a range of 400–4000 cm^{-1}. An average of 4 scans was taken for each spectrum obtained with a resolution of 4 cm^{-1}. DSC analysis was performed on a TA Q1000 instrument with a heating rate of 5 °C min^{-1} and a flow rate of 50 m s^{-1}. PXRD data were collected using a STOE STADI-MP diffractometer with Cu $K\alpha_1$ radiation (λ = 1.5406 Å), as previously described.[10] Calculated PXRD patterns were generated from the appropriate crystallographic information files using the THEO function on the STOE WinXPOW software with a pseudo-Voigt profile-shape function and a Gauss component of 0.8. Single-crystal X-ray diffraction data were collected on a Bruker APEX II DUO diffractometer using monochromated Mo Kα radiation (λ = 0.7107 Å). All calculations and refinements were made using the APEX and SHELX software.[11,12] Diagrams were prepared using the Mercury software.[13] The amido hydrogen atoms were found and refined, where possible, and the other hydrogen atoms were placed in calculated positions and allowed to ride on the parent atom. A summary of the crystallographic data is presented in **Table 2.1**.

Table 2.1. Crystallographic Data

	2	**3**	**6**	**7**	**9**	**17**	**20**	**21**
formula	$C_7H_9NO_3S$	$C_7H_9NO_3S$	$C_6H_6FNO_2S$	$C_6H_6FNO_2S$	$C_6H_6BrNO_2S$	$C_6H_6N_2O_4S$	$C_6H_6BrNO_2S$	$C_6H_6ClNO_2S$
MW	187.21	187.21	175.18	175.18	236.09	202.19	236.09	191.63
crystal system	monoclinic	monoclinic	monoclinic	orthorhombic	monoclinic	orthorhombic	monoclinic	monoclinic
space group, *Z*	$P2_1/n$, 4	$P2_1$,2	*Cc*, 4	*Pbca*, 8	*Cc*, 4	*Pccn*, 8	$P2_1/c$, 4	$P2_1/c$, 4
a, Å	7.6978(13)	6.0698(3)	5.0173(10)	8.2818(4)	7.099(2)	8.051(3)	8.4081(6)	8.264(7)
b, Å	8.1766(14)	8.0608(4)	16.209(3)	8.0748(4)	14.822(4)	26.777(10)	14.3373(10)	14.466(14)
c, Å	13.499(2)	8.6323(4)	8.8180(18)	21.6791(11)	7.698(2)	7.694(3)	7.5852(6)	7.446(7)
β, °	91.513(4)	90.8690(10)	91.447(5)	-	91.507(8)	-	116.580(2)	115.060(15)
V, Å^3	849.4(3)	422.31(4)	716.9(3)	1449.77(12)	809.7(4)	1658.7(11)	817.75(10)	806.4(13)
D_c, g cm^{-3}	1.464	1.472	1.623	1.605	1.937	1.619	1.918	1.578
μ, mm^{-1}	0.346	0.348	0.413	0.409	5.280	0.373	5.229	0.678
2θ range, °	2.91-28.50	2.36-26.39	2.51-28.35	1.88-26.51	2.75-28.51	1.52-28.31	2.71-28.33	2.72-28.28
total reflns	14079	6730	5681	10842	7462	14366	15376	14365
obs. reflns., $I>2\sigma(I)$	2132	1727	1733	1502	1995	2055	2034	1988
unique reflns	1772	1670	1583	1339	1888	1723	1831	1830
no. parameters	116	117	109	106	106	124	107	106
R_1 [$I>2\sigma(I)$]	0.0421	0.0302	0.0459	0.0324	0.0235	0.0450	0.0255	0.0316
wR_2 [all data]	0.0971	0.0758	0.1036	0.0535	0.0535	0.1037	0.0535	0.0793
S	1.030	1.072	1.061	1.021	1.021	1.050	1.021	1.060
Flack	-	0.39(12)	0.33(17)	0.052(5)	0.052(5)	-	0.052(5)	-

2.4 *Results & Discussion*

Our initial study used cocrystallization techniques since we were interested in expanding the knowledge pertaining to sulfonamide-coformer cocrystals. However, solubility issues were significant, and the experiments resulted in the characterization of a series of primary aromatic sulfonamides. Sulfonamides **2**, **3**, **6**, **7**, **9**, **20** and **21** were all crystallized from solutions of the products obtained from mechanico-chemical grinding experiments and, in all cases, either a cuboid or plate structure was obtained. The crystal structures of the other sulfonamides have already been described,[14-32] and were obtained from the CSD[33] to allow for a larger systematic analysis. Polymorphism is well documented for sulfonamides.[34-37] We found no evidence of polymorphism for the sulfonamides investigated in this study, except for sulfonamide **17,** which is discussed later. A more comprehensive polymorphic screen may identify new polymorphs of these sulfonamides.

2.4.1 Crystal Structure Analysis and Intermolecular Interactions Observed in Primary Aromatic Sulfonamides.

The crystal structures of all the primary benzenesulfonamides discussed in this study, both new and those previously reported, exhibit the same hydrogen bond motif at the unitary level, namely N-H···O=S C(4) hydrogen bonded chains involving one or both of the sulfonamide hydrogen atoms. The classification in **Figure 2.2**, and discussed below, is based on the binary level hydrogen bonding for the homomeric sulfonamide hydrogen bonding (except for **1**¸ see below). All compounds have $Z' = 1$, except for **13**[19] and one polymorph of **14**,[23] which crystallize with $Z' = 2$. Diagrams of the hydrogen-bonding for all structures are available in the SI.

C(4) Motif.

In compound **1** the sulfonamide C(4) hydrogen bonded chain involves one of the sulfonamide hydrogen atoms and runs parallel to the [010] direction due to an *n*-glide.[14] This glide plane is involved in N-H···O C(9) chains from the other sulfonamide hydrogen atom to one of the oxygen atoms of the nitro group, resulting in an heteromeric $R_4^4(24)$ sheet motif.[14]

$R_2^2(8)$ *Continuous Dimer Motif.*

The second category of hydrogen bonding interactions discussed for these compounds is the infinite continuous $R_2^2(8)$ dimer chain motif described by *Nangia et al*,[3] (earlier described by Tremayne *et al* as $C_2^2(6)$ chains[15]) and shown in **Figure 2.3**. These are seen in compounds **2** (3-OMe) and **3** (4-OMe) from this work and for **4** (3-NO_2).[15] For all three compounds, the dimer chains are related by the 2_1 screw axis along the *b*-axis. In **2** there is weak C−H···O=S hydrogen bonding involving one of the oxygen atoms of the sulfonamide that is bifurcated with an hydrogen atom of the methoxy substituent and an hydrogen atom of the aromatic ring, as well as the other sulfonamide oxygen atom with an aromatic hydrogen atom. In addition to the dimer chains in **3**, there is weak N-H···O hydrogen bonding involving both amido hydrogen atoms with one oxygen atom of the methoxy substituent. Compound **4** has an additional C-H···O=S hydrogen bonding between one of the aromatic hydrogen atoms and an oxygen of the nitro group.[15]

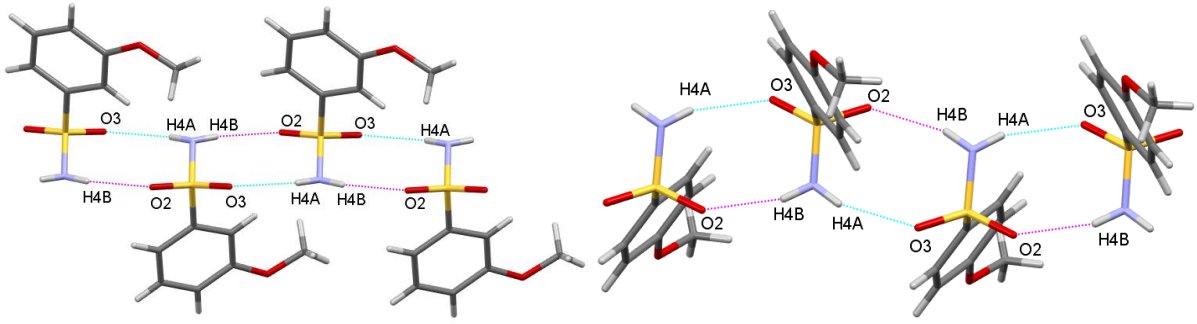


Figure 2.3. The binary level $R_2^2(8)$ chain observed in **2**, left, and **3**, right. The blue and pink colors indicate the unitary level N-H···O=S C(4) hydrogen bonded chains.

$R_4^4(14)$ *Motif.*

The third and largest category of hydrogen-bonding interactions is the $R_4^4(14)$ tetramer motif formed between 4 neighboring sulfonamides. Compound **5** is the parent benzenesulfonamide and the tetramers form 2-D sheets.[16] In addition to the $R_4^4(14)$ tetramer there is a weak C-H···O hydrogen bond from the hydrogen atom para to the sulfonamide group and one of the sulfonyl oxygen atoms. In **6** (2-F) the C(4) chains are related by the 2_1-screw axis along the *b*-axis and the *a*-glide plane, **Figure 2.4**. The tetramers form a zig-zag arrangement along the *b*-axis. There is weak C-H···O hydrogen bonding similar to that seen in **5**, although in this case it is the hydrogen atom ortho to the sulfonamide group that is utilized. In **7** (3-F) the internal hydrogen bonding within the tetramer is unsymmetrical tetramer, **Figure 2.4**, with the O3···H2A distance being 2.6 Å and the O2···H2B distance is 2.8 Å. The tetramers give rise to 2-D hydrogen bonded sheets. The C(4) chains are related by the *c*-glide plane and the C-centering. There is also weak C-H···F hydrogen bonding between both hydrogen atoms that are on the opposite side of the aromatic ring from the F atom.

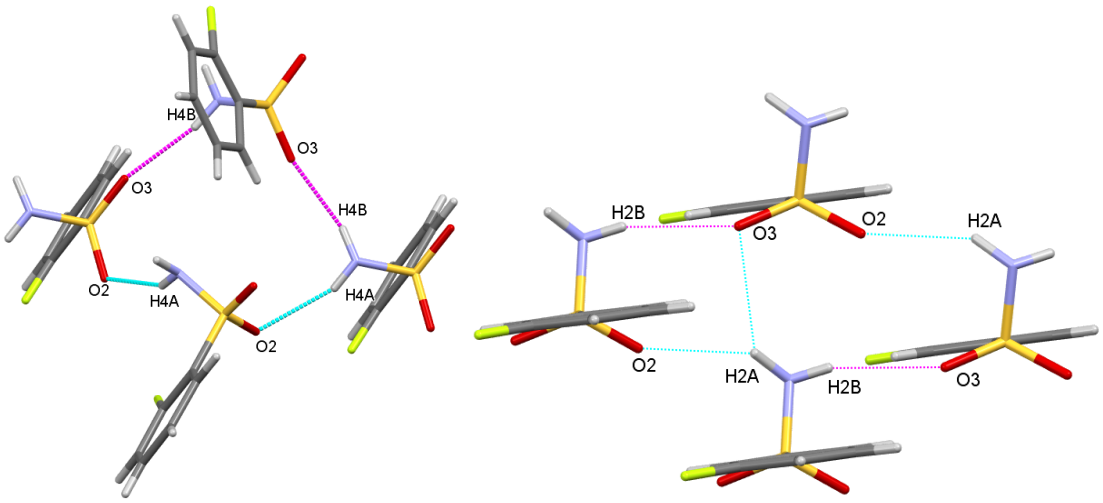


Figure 2.4: The $R_4^4(14)$ motif observed for **6**, left, and **7**, right.

In **8** (4-F) the tetramer forms a zig-zag hydrogen bonded network with similarities to that seen in **6**.[17,18] There is weak C-H···O hydrogen bonding from one of the oxygen atoms of the sulfonyl group to a hydrogen atom on the aromatic ring and a C-H···F interaction. The 2-Br derivative **9** has 2-D sheets of tetramers with weak C-H···O hydrogen bonding (**Figure 2.5)**. In **10** (4-Br) the tetramers form 2-D sheets that are joined together via S=O···Br halogen bonding between the bromine and the sulfonyl group.[18,19] Compounds **11** (2-Cl) and **12** (4-Cl) have similar intermolecular interactions to the bromine analogues **9** and **10,** respectively.[18-20] The tetramers in **13** (4-I) also form 2-D sheets that are joined by halogen bonding (I···O=S).[18] The $R_2^2(6)$ motif described by *Nangia et al* is a subset of the tetramers, see SI.[3]

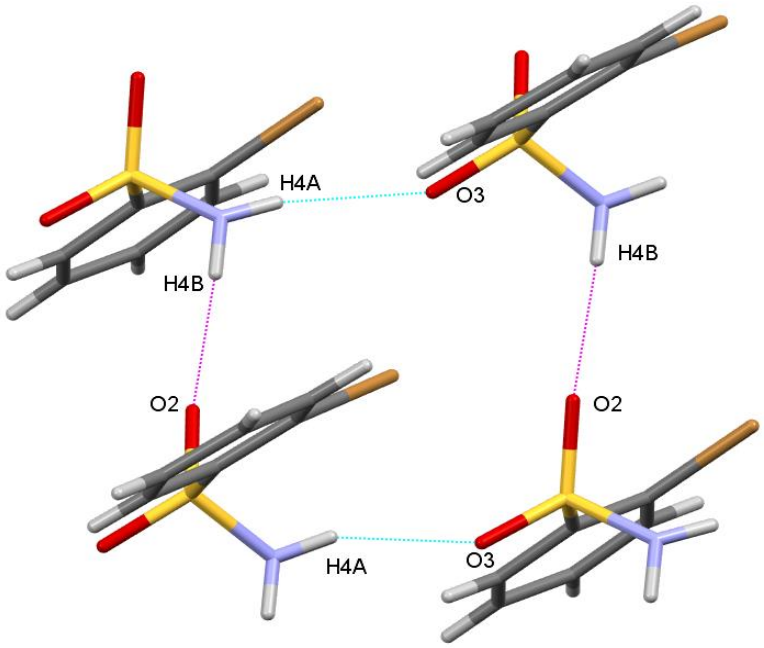


Figure 2.5: The $R_4^4(14)$ motif observed for compound **9**.

The tetramers in **14** (2-Me) form an interconnected network in all three directions with weak C-H···O involving an aromatic hydrogen atom and a sulfonyl oxygen atom.[15] Both polymorphs of **15** (4-Me) have 2-Ds sheet of tetramers, although only one of them has additional C-H···O hydrogen bonding involving the hydrogen atom ortho to the sulfonamide substituent and a sulfonyl oxygen atom.[19,21,22] There are 2-D sheets of tetramers in **16** (2-NH_2) with π-π interactions between adjacent aromatic rings.[24,25]

We have identified a new polymorph of **17** (2-NO_2) in which, rather than having just one $R_4^4(14)$ motif involving four molecules, there are two $R_4^4(14)$ motifs involving six molecules (**Figure 2.6)**. Overall, there is a hydrogen bonded channel down the *c*-axis. There are also two weak C-H···O hydrogen bonds involving the hydrogen atoms on the opposite side of the nitro group and the sulfonyl oxygen atoms of two different molecules. The C(4) chains are related by the 2_1-screw axis along the *b*-axis and the glide plane perpendicular to the *a*-axis. This contrasts

with the previously reported structure of **17** in which the tetramers form 2-D hydrogen bonded sheets.[26]

The experimental PXRD for **17** obtained direct from the supplier was compared with the calculated PXRD patterns based on the CIFs for the two polymorphs. This revealed that the supplied polymorph is the new polymorph reported in this work (see SI).

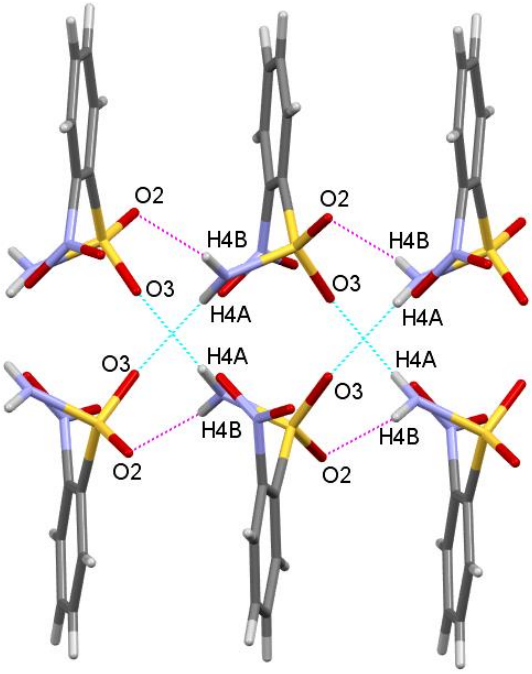


Figure 2.6: The six molecules forming two $R_4^4(14)$ tetramers in **17.**

In **18** there is the well-known carboxylic acid dimer present as well as the tetramer.[27]

$R_2^2(8)$ + *C(4) Motif.*

Another set of hydrogen-bonding interactions observed in these compounds is the infinite ladder motif formed between neighboring sulfonamide functional groups, which is similar to that observed in primary amides. This ladder motif is a combination of the individual $R_2^2(8)$ dimer and

C(4) chain hydrogen-bond motifs. This can be seen in compound **19** (2-CO_2H) where the combination gives rise to a $R_4^4(12)$ motif.[28]

Centrosymmetric Dimer and Offset C(4).

The fifth set of interactions observed is the centrosymmetric $R_2^2(8)$ dimer with an offset C(4) chain formed between neighboring sulfonamide as observed in **20** (3-Br) and **21** (3-Cl) (this work). The offset dimer means it is not possible to form the ladder motif seen in **19**. Instead, for the isomorphous **20** and **21** the dimers assemble into $R_6^6(20)$ hexamer rings **(Figure 2.7**) that form 2-D hydrogen bonded sheets. The C(4) chains are related by the 2_1-screw axis and the *c*-glide plane. Compound **22** (4-NH_2) has four known polymorphs. The α and γ polymorphs have $R_2^2(8)$ dimers and four of these form $R_6^4(16)$ that assemble into 2-D sheets.[29,30]

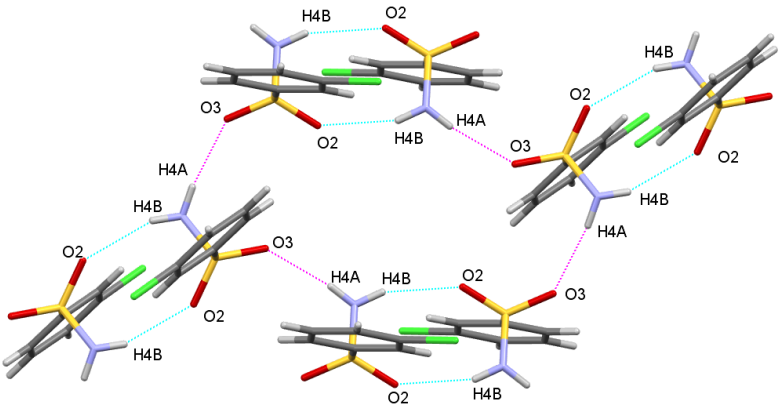


Figure 2.7: The $R_2^2(8)$ dimer and $R_6^6(20)$ hexamer rings present in the 2-D hydrogen bonded sheets in **20** and **21**.

Alternative Dimers.

The δ polymorph of **22** was described by Gelbrich *et al* as consisting of $R_2^2(8)$ dimers, four of which form $R_6^4(16)$ that assemble into 2-D sheets.[31] These were also categorized by *Nangia et al* as alternative dimers since the $R_2^2(8)$ dimers alternate in the chain.[3]

$R_4^4(12)$ *Motif.*

The β polymorph of **22** forms tetramers that differ from those discussed previously.[32] The $R_4^4(14)$ tetramers involved all atoms (H,N,O and S) of at least one sulfonamide functional group, whereas this tetramer utilizes only two atoms (H and N, or O and S) of each sulfonamide molecule, see SI.

2.5 *Conclusion*

Primary sulfonamides display similar characteristic hydrogen-bonding motifs to those observed in their widely studied amide analogues, including $R_2^2(8)$ dimers and C(4) chains. The analysis of the structural features across these aromatic sulfonamides showed that 60% of the sulfonamides crystallized with the $R_4^4(14)$ motif. This is observed in the parent compound, benzenesulfonamide, and is not retained with substitution on the aromatic ring, mainly, but not exclusively, when the substituent is a halide or methyl group, especially when para-substitution occurs. It is also observed in some cases when one competing hydrogen bond donor or acceptor is present, for example when the one-dimensional carboxylic acid motif is possible, as seen in **18**.

References

1. Tacic, A.; Nikolic, V.; Nikolic, L.; Savic, I. Antimicrobial Sulfonamide Drugs. *Advanced technologies* **2017**, *6*, 58-71.

2. Goud, N.; Babu, N.; Nangia, A. Sulfonamide−Pyridine-N-Oxide Cocrystals. *Cryst. Growth Des*. **2011**, 11, 1930-1939.

3. Bolla, G.; Mittapalli, S.; Nangia, A. Modularity and Three-Dimensional Isostructurality of Novel Synthons in Sulfonamide–Lactam Cocrystals. *IUCrJ* **2015**, *2*, 389-401.

4. Bolla, G.; Nangia, A. Multicomponent Ternary Cocrystals Of the Sulfonamide Group with Pyridine-Amides and Lactams. *Chem. Commun.* **2015**, 51, 15578-15581.

5. Allu, S.; Bolla, G.; Tothadi, S.; Nangia, A. Supramolecular Synthons in Bumetanide Cocrystals and Ternary Products. *Cryst. Growth Des.* **2017**, *17*, 4225-4236.

6. Allu, S.; Bolla, G.; Tothadi, S.; Nangia, A. Novel Pharmaceutical Cocrystals and Salts of Bumetanide. *Cryst. Growth Des*. **2019**, *20*, 793-803.

7. Etter, M.; MacDonald, J.; Bernstein, J. Graph-Set Analysis Of Hydrogen-Bond Patterns In Organic Crystals. *Acta Crystallogr., Sect. B: Struct. Sci.*, **1990**, *46*, 256-262.

8. Bernstein, J.; Shimoni, L.; Davis, R.; Chang, N. Graph Set Analysis Of Hydrogen-Bond Patterns In Organic Crystals. Recent Developments And Applications. *Acta Crystallogr., Sect. A: Found. Crystallogr.*, **1993**, *49*, 164-164.

9. Bernstein, J.; Davis, R.; Shimoni, L.; Chang, N. Patterns In Hydrogen Bonding: Functionality And Graph Set Analysis In Crystals. *Angew. Chem., Int. Ed. Engl.*, **1995**, *34*, 1555-1573.

10. Eccles, K. S.; Elcoate, C. J.; Maguire, A. R.; Lawrence, S. E. Unzipping the Dimer in Primary Amides by Cocrystallization with Sulfoxides *Cryst. Growth Des*. **2011**, *11*, 4433−4439.

11. APEX2 v2009.3-0; Bruker AXS: Madison, WI, **2009**.

12. Sheldrick, G. M. A Short History of SHELX *Acta Cryst*. **2008**, *A64*, 112−122.

13. Macrae, C.; Sovago, I.; Cottrell, S.; Galek, P.; McCabe, P.; Pidcock, E.; Platings, M.; Shields, G.; Stevens, J.; Towler, M.; Wood, P. Mercury 4.0: From Visualization To Analysis, Design And Prediction. *J. Appl. Crystallogr.* **2020**, *53*, 226-235.

14. Zhou, T.; Zhang, Q.; Chen, G.; Zhou, Z. Redetermination Of 4-Nitrobenzenesulfonamide. *Acta Crystallogr., Sect. E: Struct. Rep. Online* **2004**, *60*, 1767-1768.

15. Tremayne, M.; Seaton, C.; Glidewell, C. Structures of Three Substituted Arenesulfonamides from X-Ray Powder Diffraction Data using the Differential Evolution Technique. *Acta Crystallogr., Sect. B: Struct. Sci.* **2002**, *58*, 823-834.

16. Gowda, B.; Nayak, R.; Kožíšek, J.; Tokarčík, M.; Fuess, H. Benzenesulfonamide. *Acta Crystallogr., Sect. E: Struct. Rep. Online* **2007**, *63*, 2967-2967.

17. Jones, P.; Weinkauf, A. Crystal Structure of p-Fluorobenzene-Sulphonamide, $C_6H_6FNO_2S$. *Z. Kristallogr. Cryst. Mater.* **1993**, *208*, 128-129.

18. Thimme Gowda, B.; Jyothi, K.; Kožíšek, J.; Fuess, H. Crystal Structure Studies On p-Substitutedbenzenesulphonamides 4-X-$C_6H_4SO_2NH_2$ (X = CH_3, NH_2 F, Cl or Br). *Z. Naturforsch. A* **2003**, *58*, 656-660.

19. Zerbe, E.; Moers, O.; Jones, P.; Blaschette, A. Intermolecular Interactions in the Crystal Structures Of 4-Halobenzenesulfonamides (Halogen = Fluorine, Chlorine, Bromine, Iodine) and 4-Methylbenzenesulfonamide. *Z. Naturforsch. B* **2005**, *60*, 125-138.

20. Gowda, B.; Foro, S.; Shakuntala, K.; Fuess, H. 2-Chlorobenzenesulfonamide. *Acta Crystallogr., Sect. E: Struct. Rep. Online* **2009**, *65*, 2144-2144.

21. Vijay-Kumar, S.; Senadhi, S.; Rao, L. Structure of *p*-Methylbenzene Sulfonamide. *Z. Kristallogr. Cryst. Mater.* **1992**, *202*, 1-6.

22. Lightfoot, P.; Tremayne, M.; Glidewell, C.; Harris, K.; Bruce, P. Investigation and Rationalisation of Hydrogen Bonding Patterns in Sulfonylamino Compounds and Related Materials: Crystal Structure Determination of Microcrystalline Solids from Powder X-Ray Diffraction Data. *J. Chem. Soc., Perkin Trans.* 2 **1993**, *9*, 1625-1630.

23. Tatiana N. Drebushchak, Natalia A. Pankrushina, Aleksandr N. Mikheev, Manfred K. A. Thumm, *Cryst. Eng. Comm.*, **2013**, 15, 3582-3586.

24. Le Bars, M.; Alléaume, M. 2-Aminobenzenesulfonamide. *C. R. Acad. Sci.* **1972**, 275, 187-187.

25. Flörke, U.; Saeed, A. *o*-Sulfanilamide. https://dx.doi.org/10.5517/ccdc.csd.cc1ywxf5 (accessed Apr 28, 2020).

26. Cheng, H.; Zhang, S.; Huang, C. 2-Nitrobenzenesulfonamide. *Acta Crystallogr., Sect. E: Struct. Rep. Online* **2007**, *63*, 1979-1980.

27. Ng, S. Crystal Structure Of *p*-Sulfamoylbenzoic Acid, $H_2NSO_2C_6H_4COOH$. *Z. Kristallogr. Cryst. Mater.* **1997**, *212*, 282-282.

28. Siddiqui, W.; Ahmad, S.; Siddiqui, H.; Tariq, M.; Parvez, M. O-Sulfamoylbenzoic Acid. *Acta Crystallogr., Sect. E: Struct. Rep. Online* **2007**, *63*, 4117-4117.

29. O'Connor, B.; Maslen, E. The Crystal Structure of α-Sulphanilamide. *Acta Crystallogr.,* **1965**, *18*, 363-366.

30. Alléaume, M.; Decap, J. Affinement Tridimensionnel Du Sulfanilamide γ. *Acta Crystallogr.,* **1965**, *19*, 934-938.

31. Gelbrich, T.; Bingham, A.; Threlfall, T.; Hursthouse, M. δ-Sulfanilamide. *Acta Crystallogr., Sect. C: Cryst. Struct. Commun.* **2008**, *64*, 205-207.

32. Alléaume, M.; Decap, J. Affinement Tridimensionnel Du Sulfanilamide β. *Acta Crystallogr.,* **1965**, *18*, 731-736.

33. C. R. Groom, I. J. Bruno, M. P. Lightfoot and S. C. Ward, Acta Cryst. (2016). B72, 171-179

34. Munroe, Á.; Rasmuson, Å.; Hodnett, B.; Croker, D. Relative Stabilities of The Five Polymorphs of Sulfathiazole. *Cryst. Growth Des*. **2012**, *12*, 2825-2835.

35. Yeh, K.; Lee, T. Intensified Crystallization Processes For 1:1 Drug–Drug Cocrystals Of Sulfathiazole–Theophylline, And Sulfathiazole–Sulfanilamide. *Cryst. Growth Des*. **2018**, *18*, 1339-1349.

36. Grossjohann, C.; Serrano, D.; Paluch, K.; O'Connell, P.; Vella-Zarb, L.; Manesiotis, P.; McCabe, T.; Tajber, L.; Corrigan, O.; Healy, A. Polymorphism in Sulfadimidine/4-Aminosalicylic Acid Cocrystals: Solid-State Characterization and Physicochemical Properties. *J. Pharm. Sci*. **2015**, *104*, 1385-1398.

37. Sangtani, E.; Sahu, S.; Thorat, S.; Gawade, R.; Jha, K.; Munshi, P.; Gonnade, R. Furosemide Cocrystals With Pyridines: An Interesting Case of Color Cocrystal Polymorphism. *Cryst. Growth Des*. **2015**, *15*, 5858-5872.

Supplementary Information for Crystal Landscape of Primary Aromatic Sulfonamides

Analytical data for 3-methoxybenzenesulfonamide, **2**	82
Analytical data for 4-methoxybenzeensulfonamide, **3**	85
Analytical data for 2-fluorobenzenesulfonamide, **6**	87
Analytical data for 3-fluorobenzensulfonamide, **7**	90
Analytical data for 2-bromobenzenesulfonamide, **9**	94
Analytical data for 2-nitrobenzenesulfonamide, **17**	98
Analytical data for 3-bromobenzenesulfonamide, **20**	101
Analytical data for 3-chlorobenzenesulfonamide, **21**	104
Hydrogen bonding in **2**,**3**,**6**,**7**,**9**,**17**,**20,** and **21**	107
Hydrogen Bonding in previously published sulfonamides: **1**,[1] **4**,[2] **5**,[3] **8**,[4] **10**,[4] **11**,[5] **12**,[4] **13**,[4] **14**,[6] **15**,[7] **16**,[8] **17**,[9] **18**,[10] **19**,[11] **22**,[12-15]	108

Note: The DSC curves for compounds **6** (Figure S14), **7** (Figure S20), **17** (Figure S32), **20** (Figure S38) and **21** (Figure S44) have more than one endotherm as our initial study used cocrystallization techniques for sulfonamide-coformer crystal formation. These DSC curves were obtained from suspected cocrystal samples however, only starting materials were observed. These endotherms do no indicate polymorphism in the samples.

Analytical data for 3-methoxybenzenesulfonamide, **2**

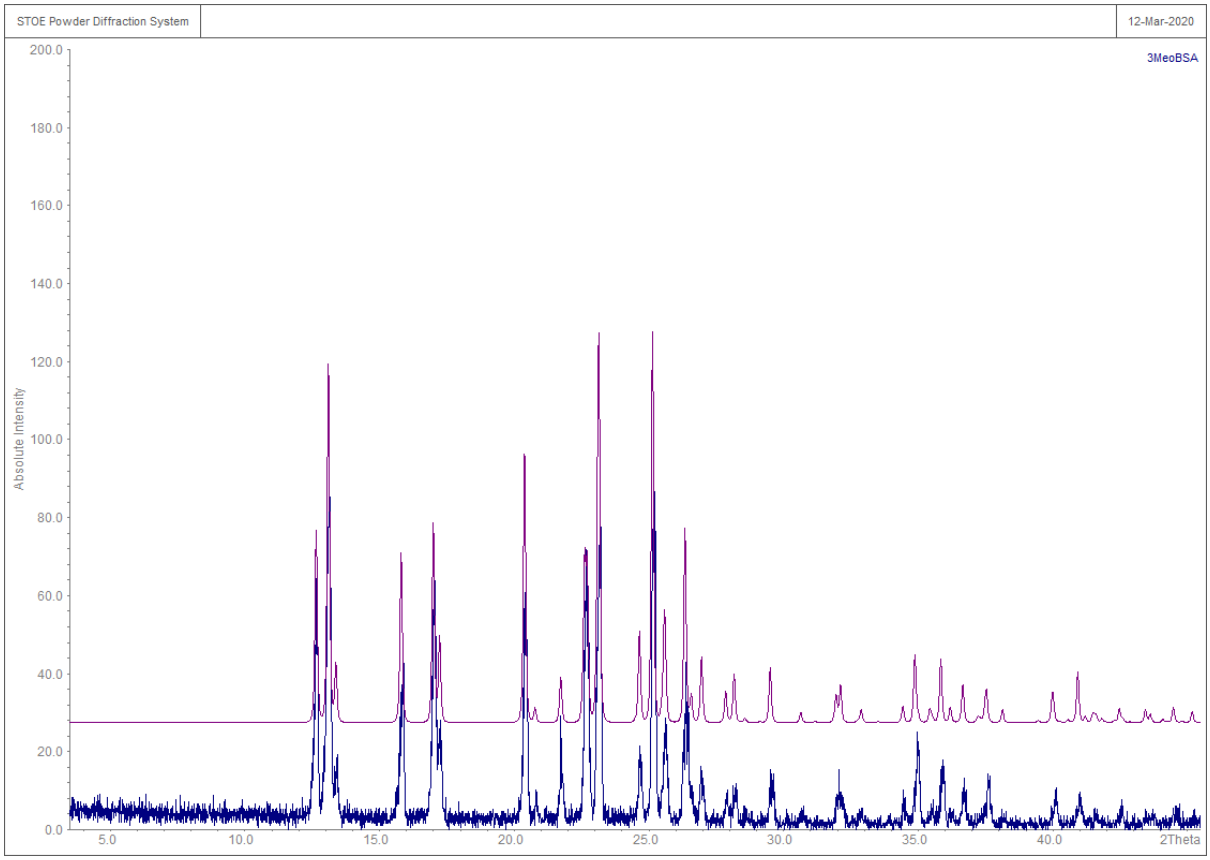


Figure S1: Experimental (blue) and theoretical (purple) PXRD data of **2**.

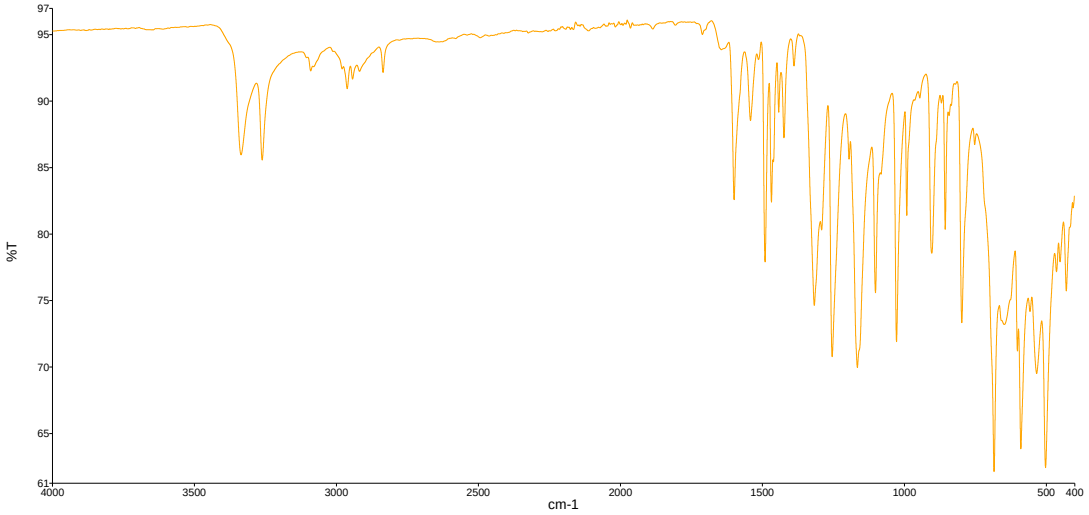


Figure S2: IR spectra of **2**.

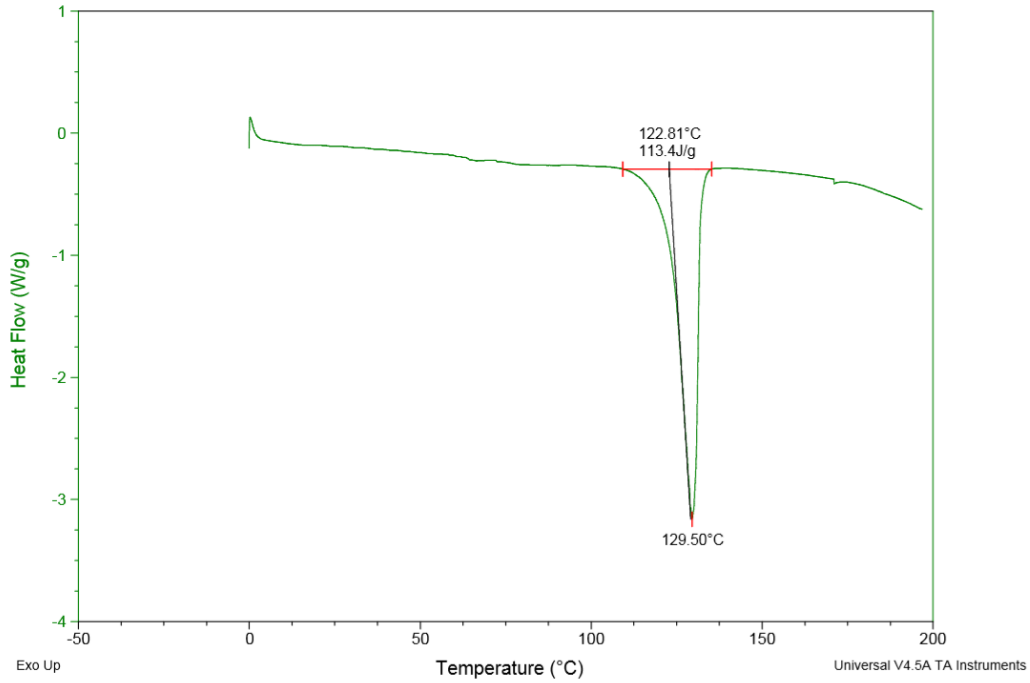


Figure S3: DSC data of **2**.

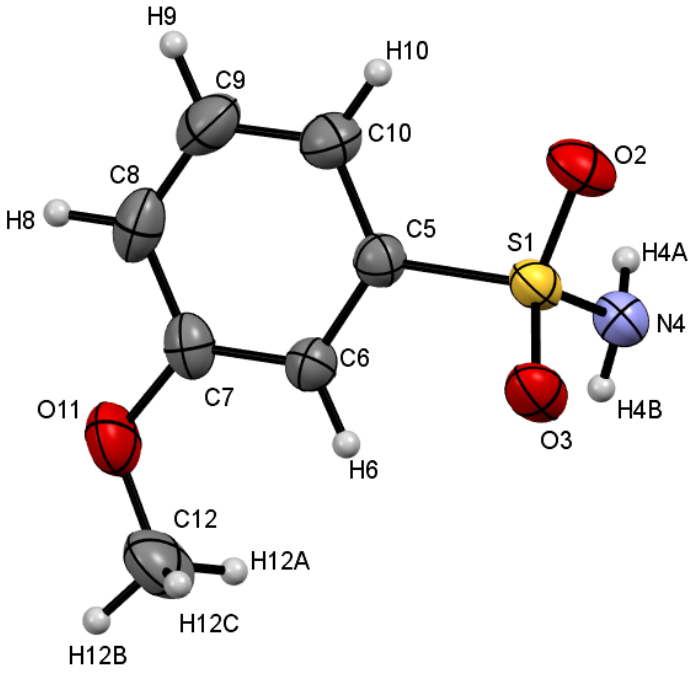


Figure S4: ORTEP diagram of **2**, with numbering scheme. Thermal ellipsoids are drawn at the 50% level.

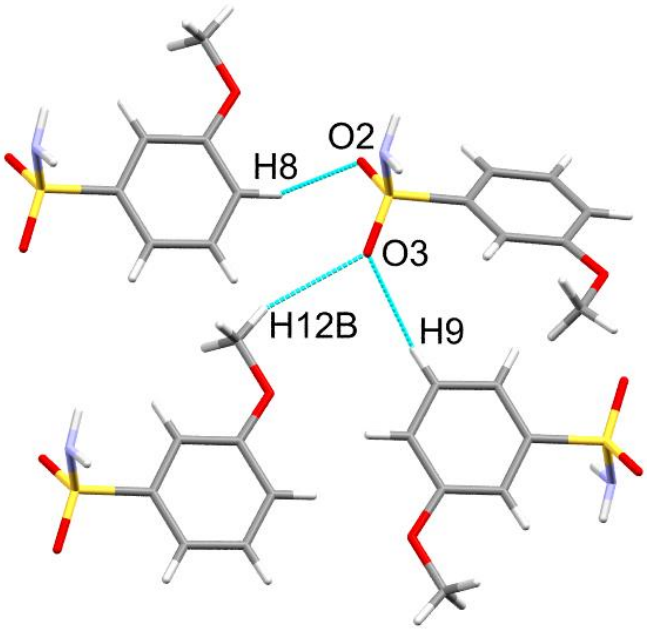


Figure S5: Weak C-H···O=S hydrogen bonding in **2**.

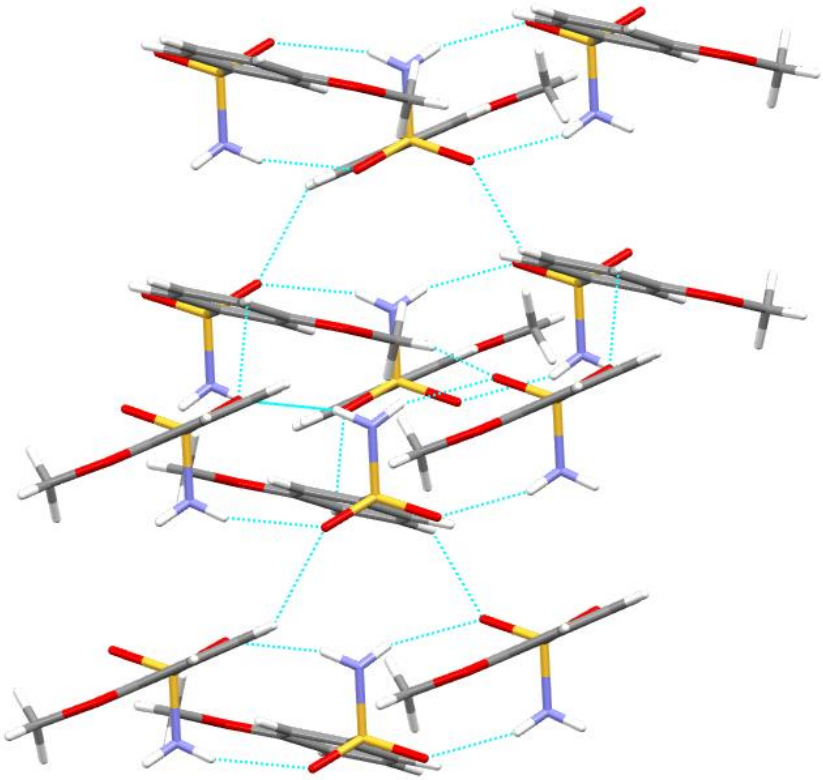


Figure S6: Packing diagram of **2**.

Analytical data for 4-methoxybenzenesulfonamide, **3**

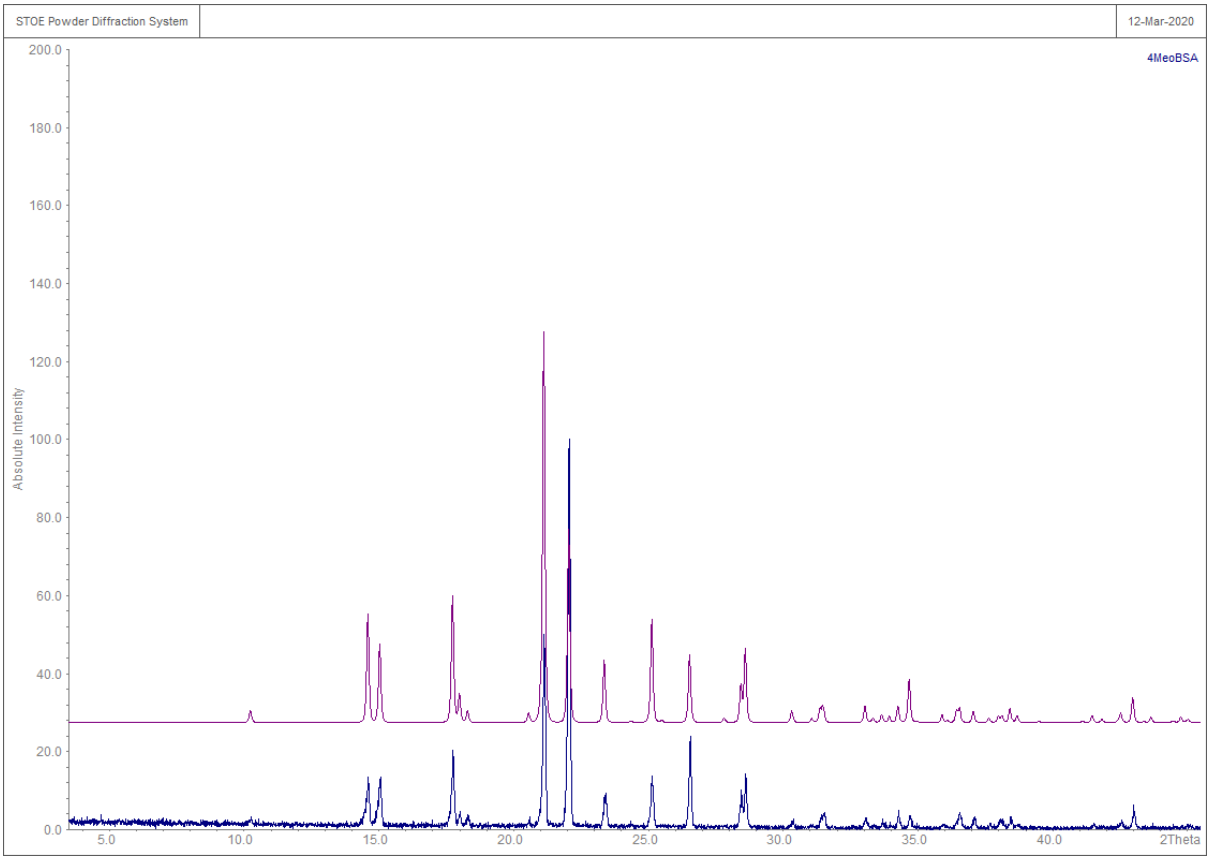


Figure S7: Experimental (blue) and theoretical (purple) PXRD data of **3**.

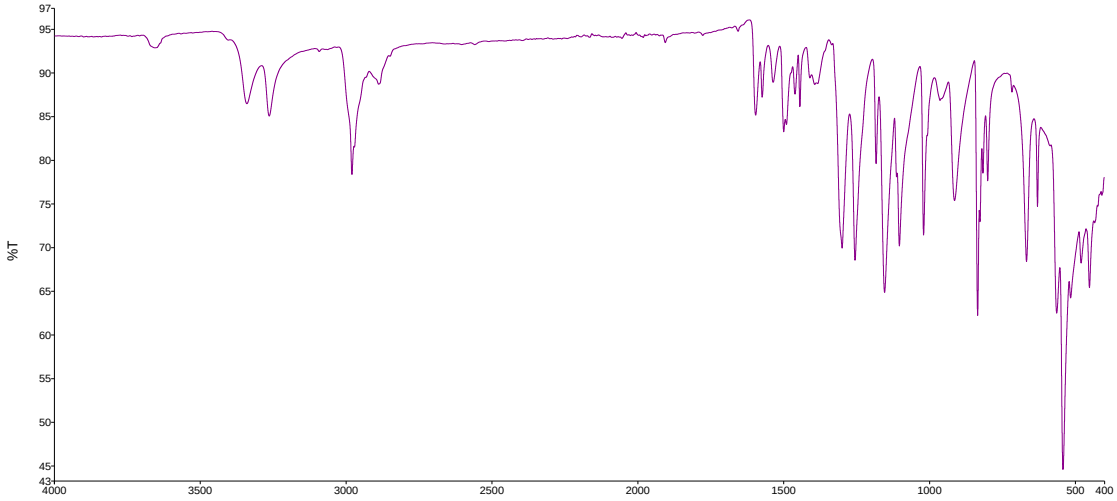


Figure S8: IR spectra of **3**.

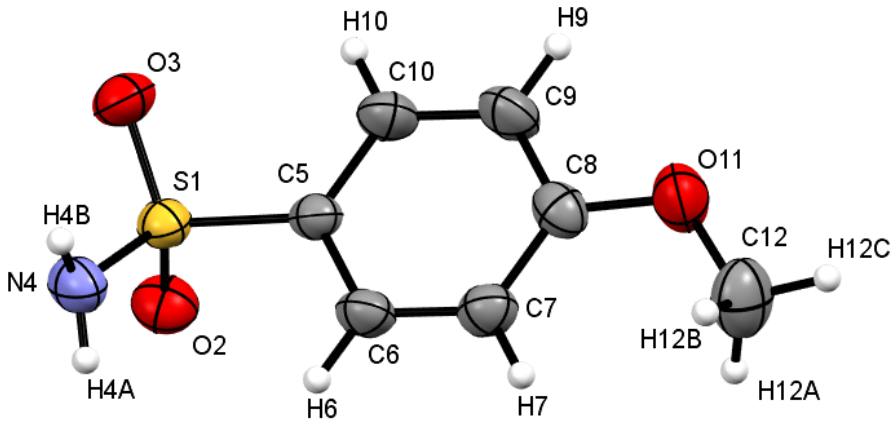


Figure S9: ORTEP diagram of **3**, with numbering scheme. Thermal ellipsoids are drawn at the 50% level.

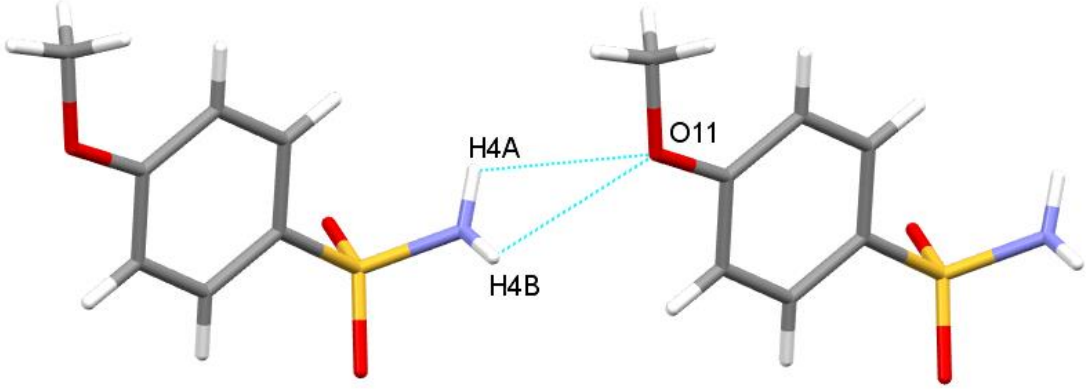


Figure S10: Additional N-H···O hydrogen bonding in **3**.

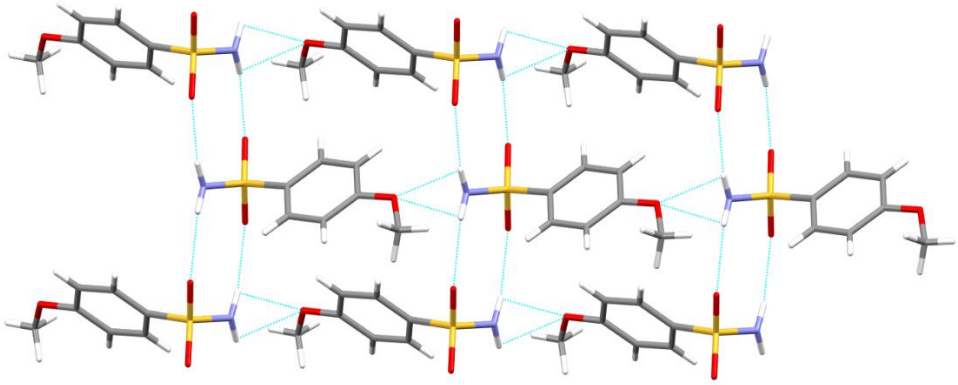


Figure S11: Packing diagram of **3**.

Analytical data for 2-fluorobenzenesulfonamide, **6**

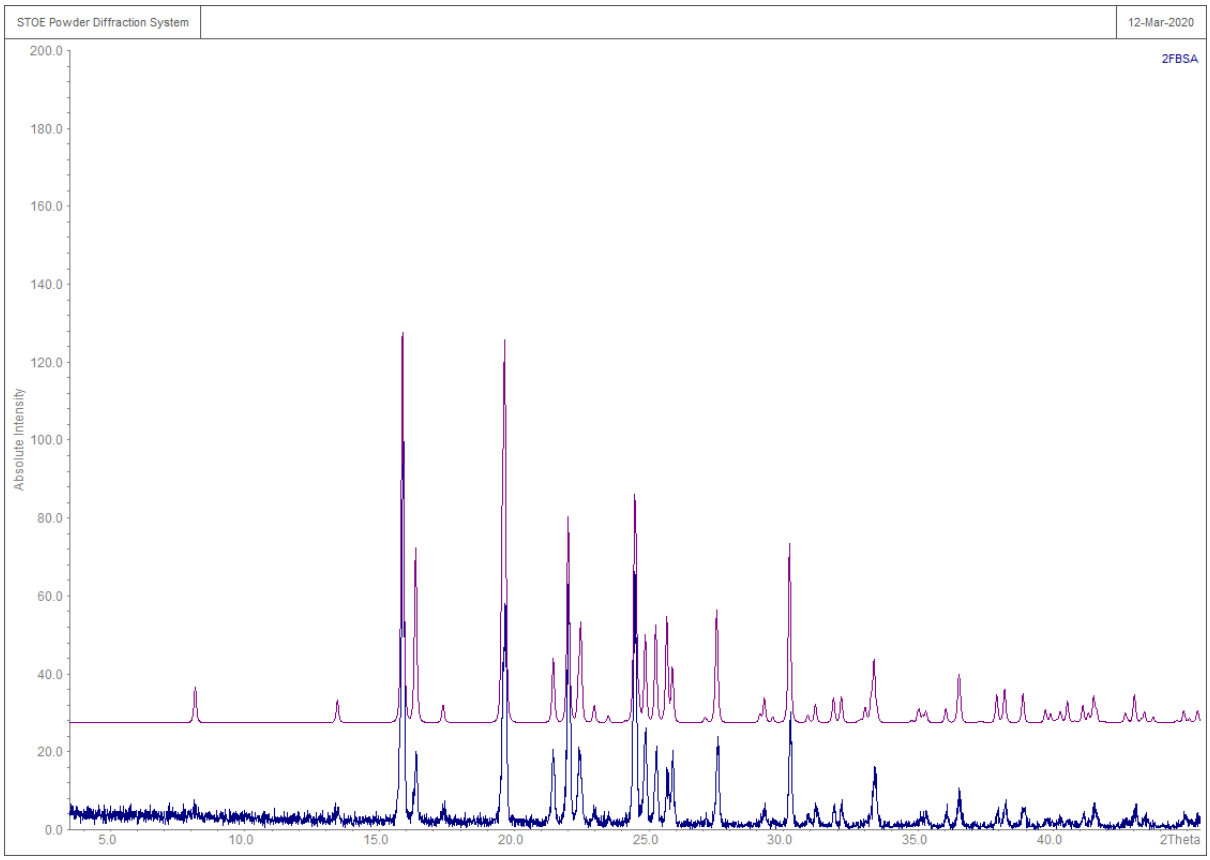


Figure S12: Experimental (blue) and theoretical (purple) PXRD data of **6**.

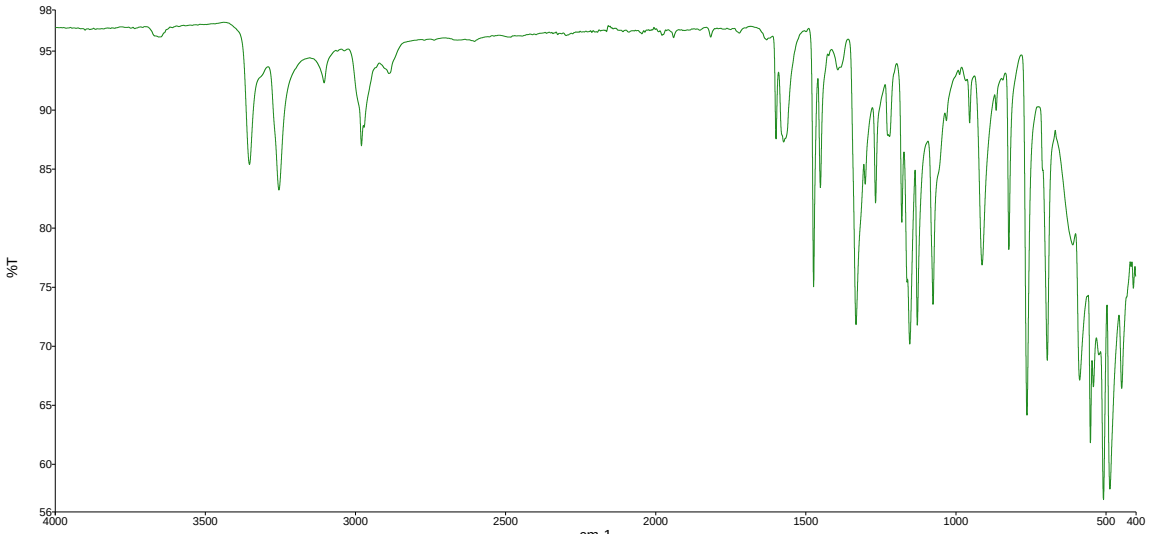


Figure S13: IR spectra of **6**.

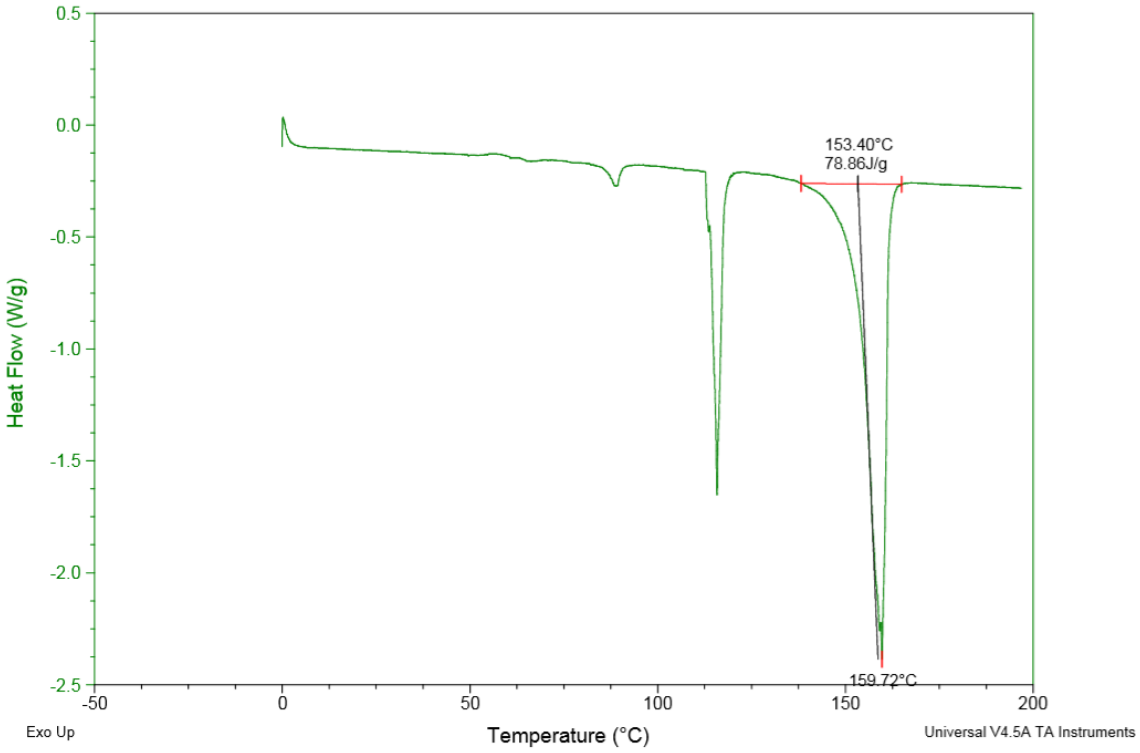


Figure S14: DSC data of **6**.

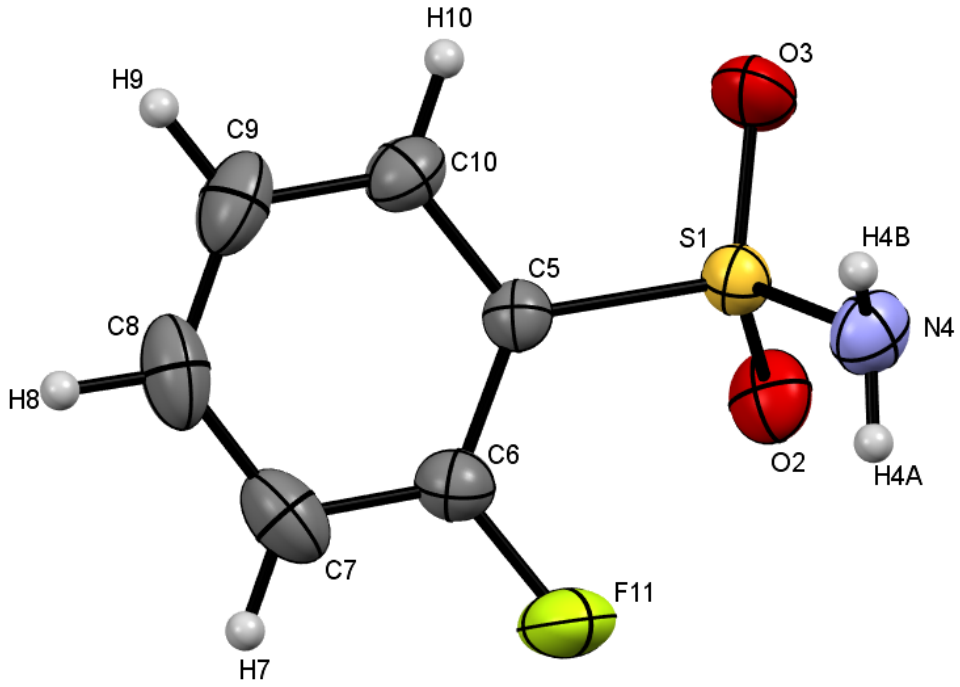


Figure S15: ORTEP diagram of **6**, with numbering scheme. Thermal ellipsoids are drawn at the 50% level.

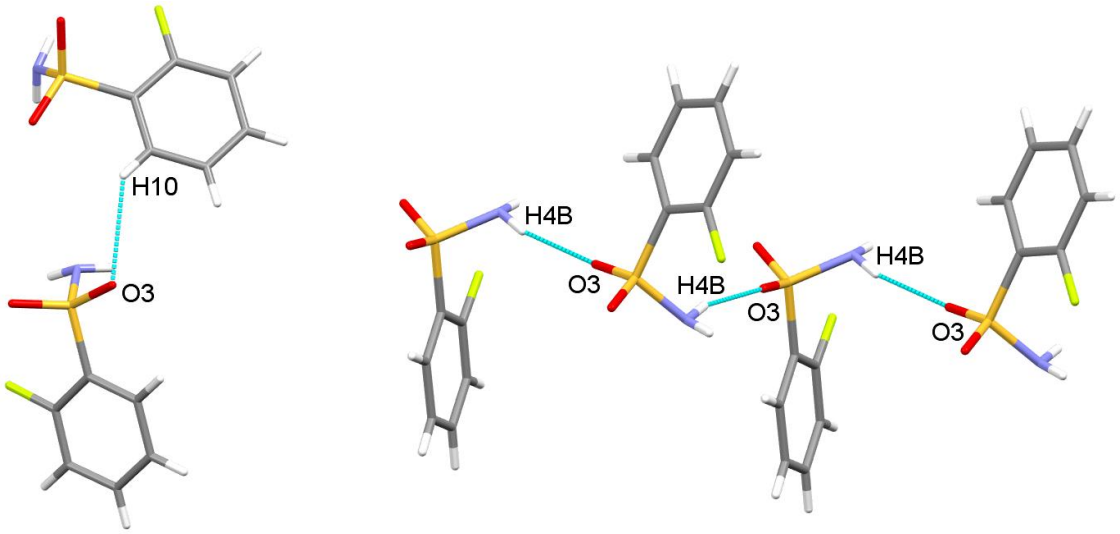


Figure S16: Hydrogen bonding in **6**.

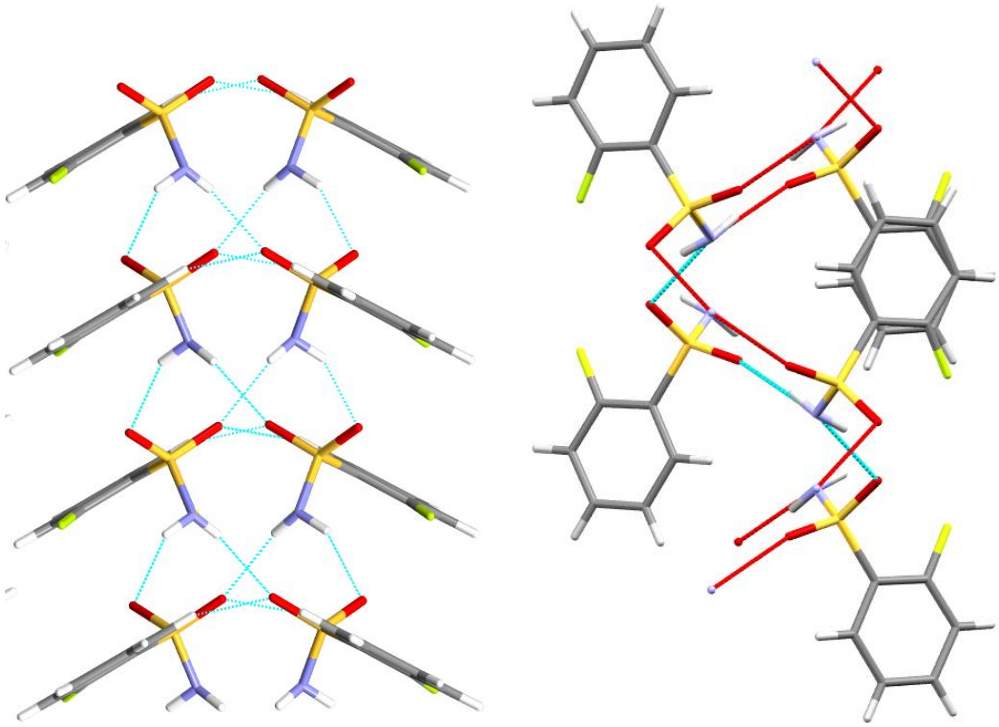


Figure S17: Packing diagrams of **6** showing the zig-zag arrangement formed by the tetramers. View along the *b*-axis, right.

Analytical data for 3-fluorobenzenesulfonamide, **7**

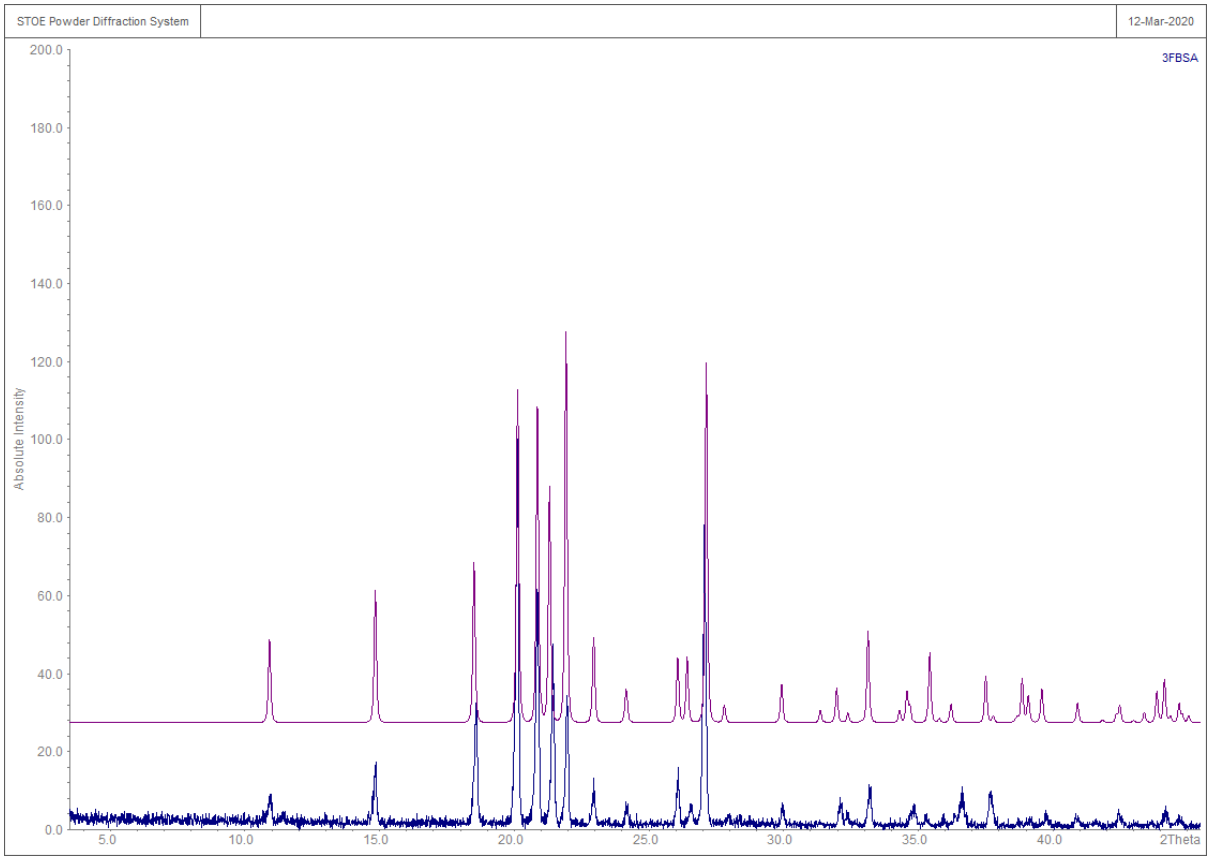


Figure S18: Experimental (blue) and theoretical (purple) PXRD data of **7**.

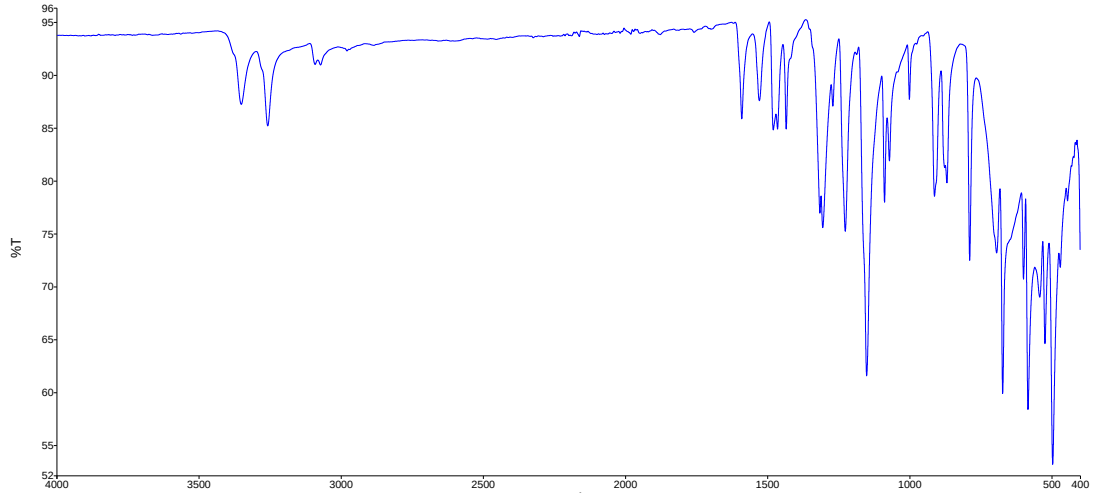


Figure S19: IR spectra of **7**.

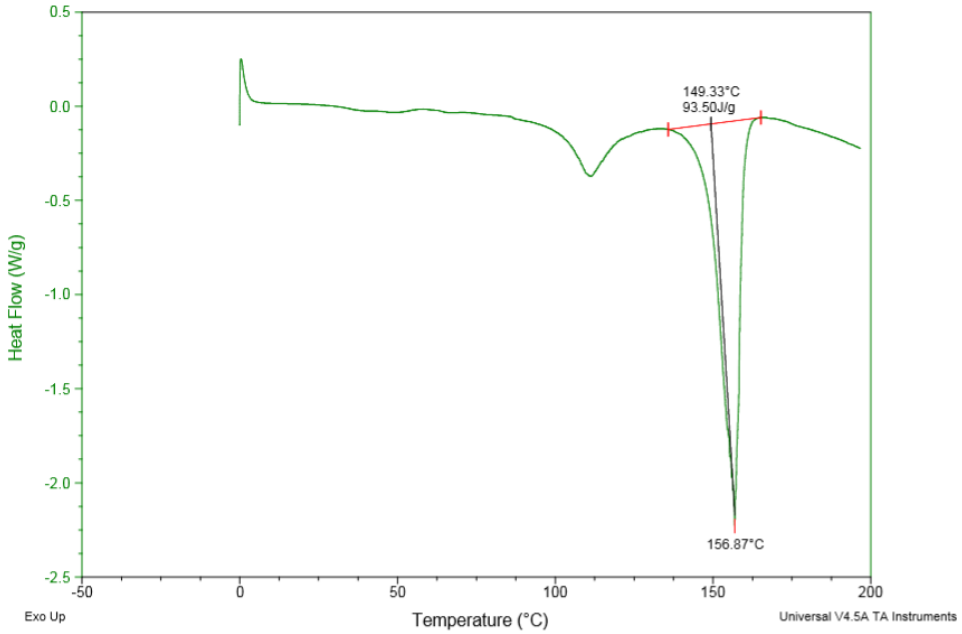


Figure S20: DSC spectra of **7**.

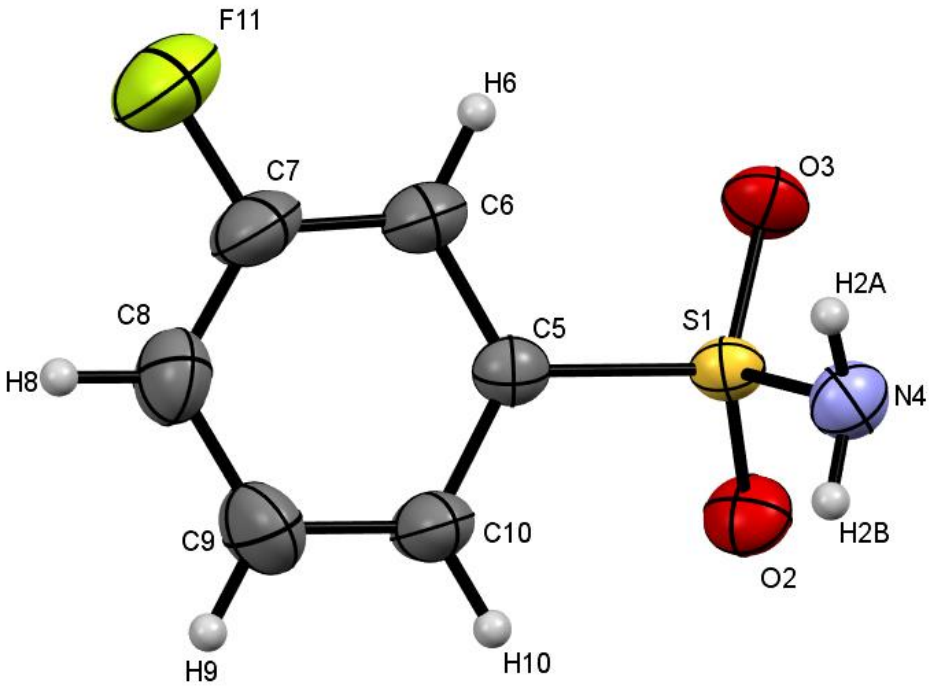


Figure S21: ORTEP diagram of **7**, with numbering scheme. Thermal ellipsoids are drawn at the 50% level.

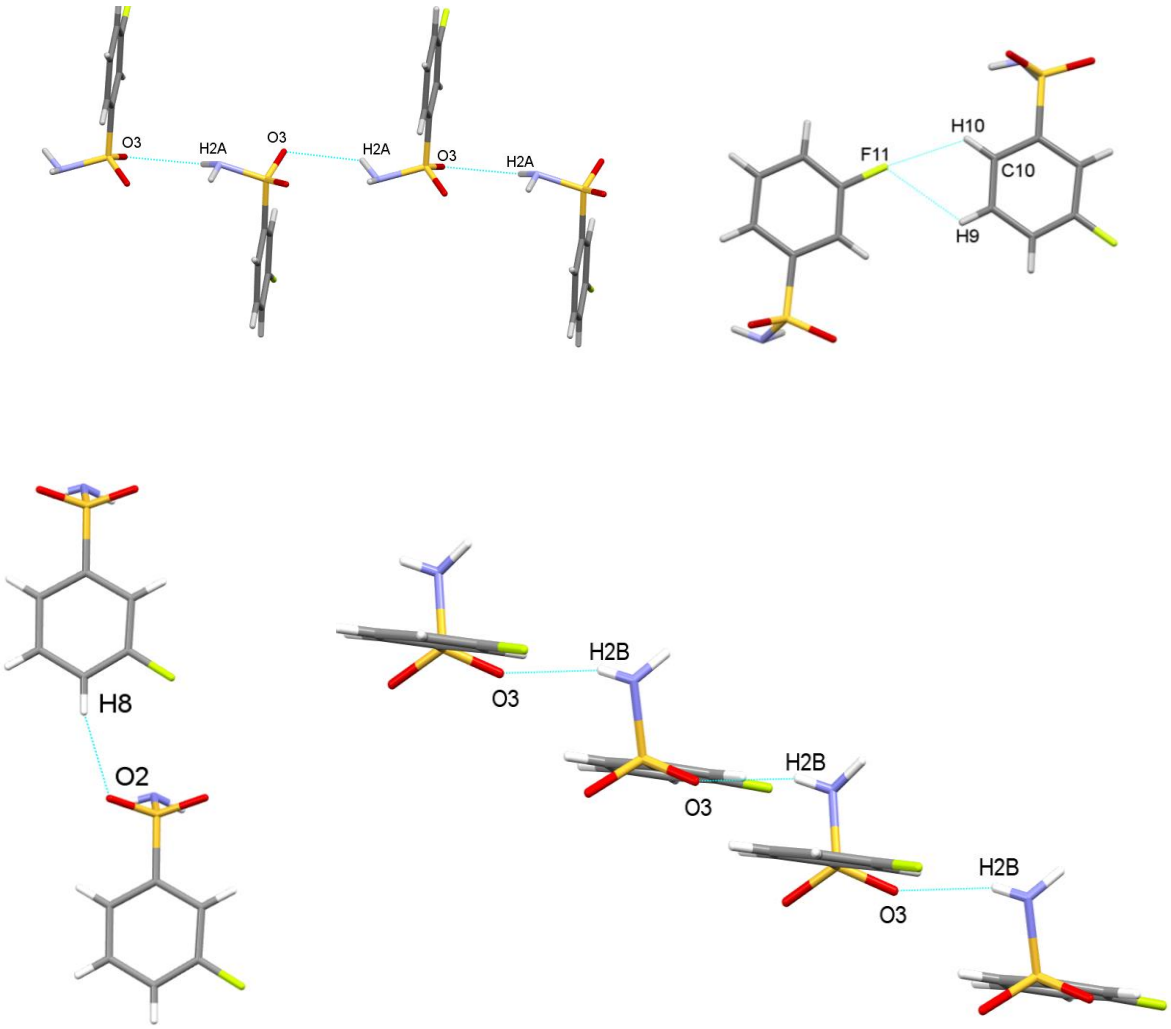


Figure S22: Hydrogen bonding in **7**.

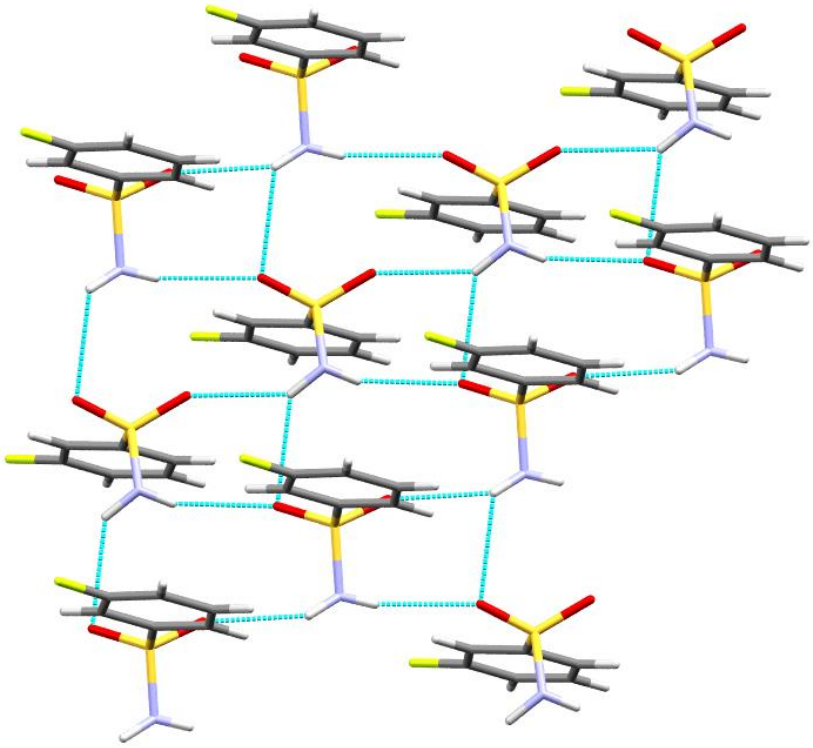


Figure S23: Packing diagram of **7**.

Analytical data for 2-bromobenzenesulfonamide, **9**

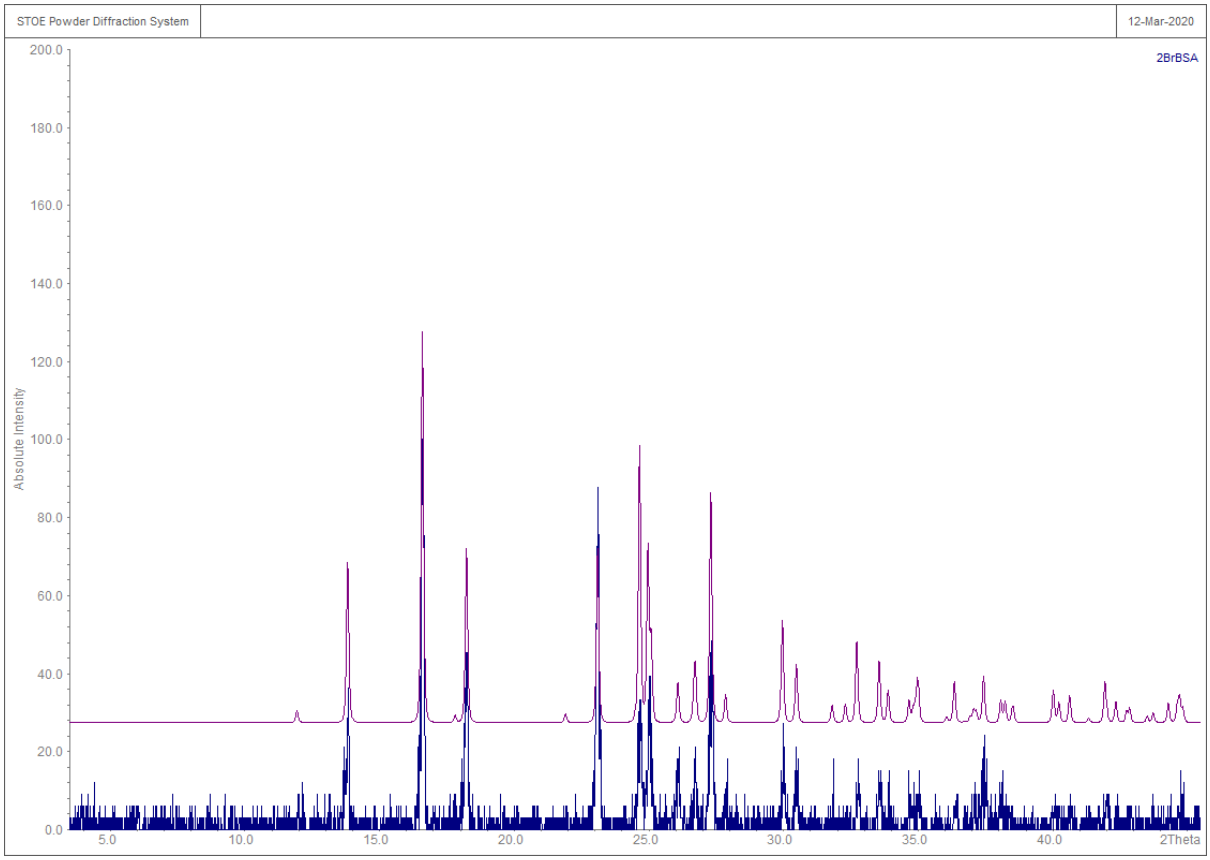


Figure S24: Experimental (blue) and theoretical (purple) PXRD data of **9**.



Figure S25: IR spectra of **9**.

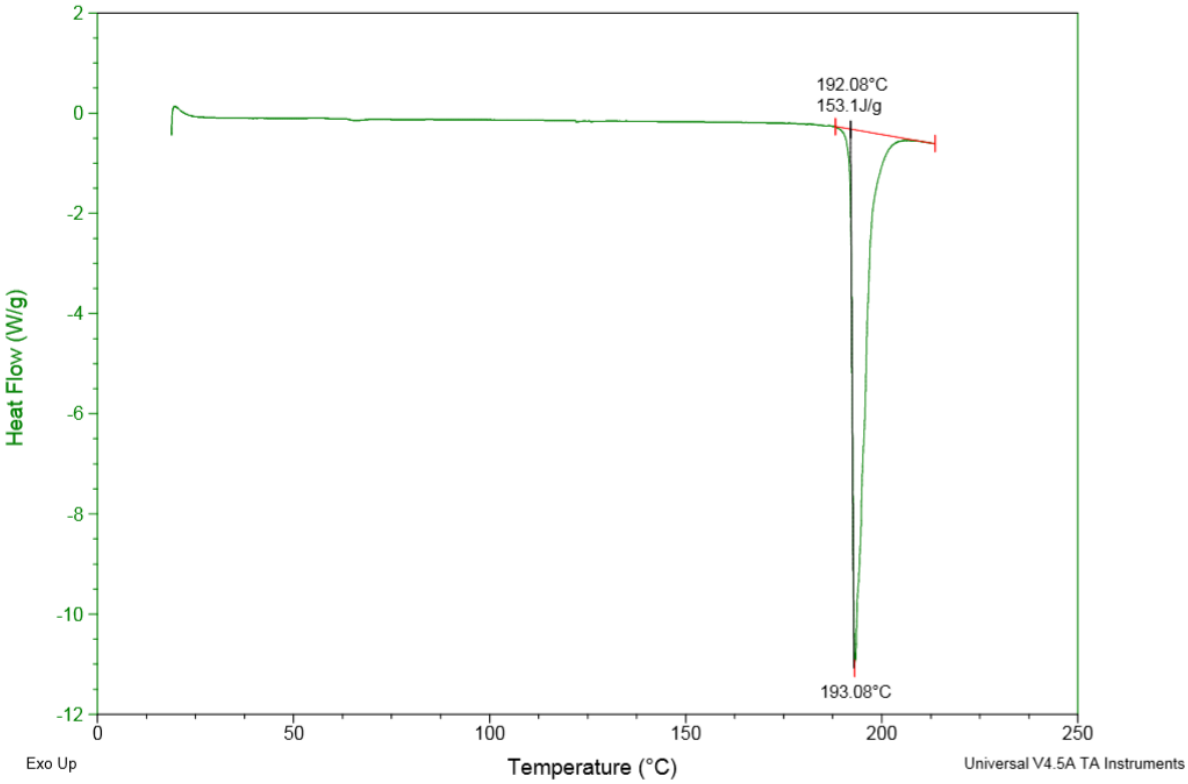


Figure S26: DSC spectra of **9**.

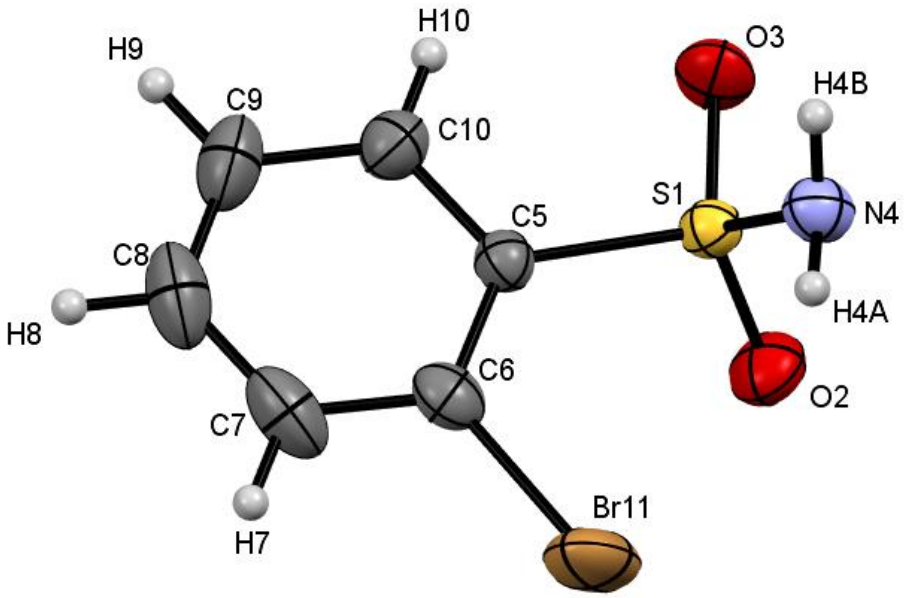


Figure S27: ORTEP diagram of **9**, with numbering scheme. Thermal ellipsoids are drawn at the 50% level.

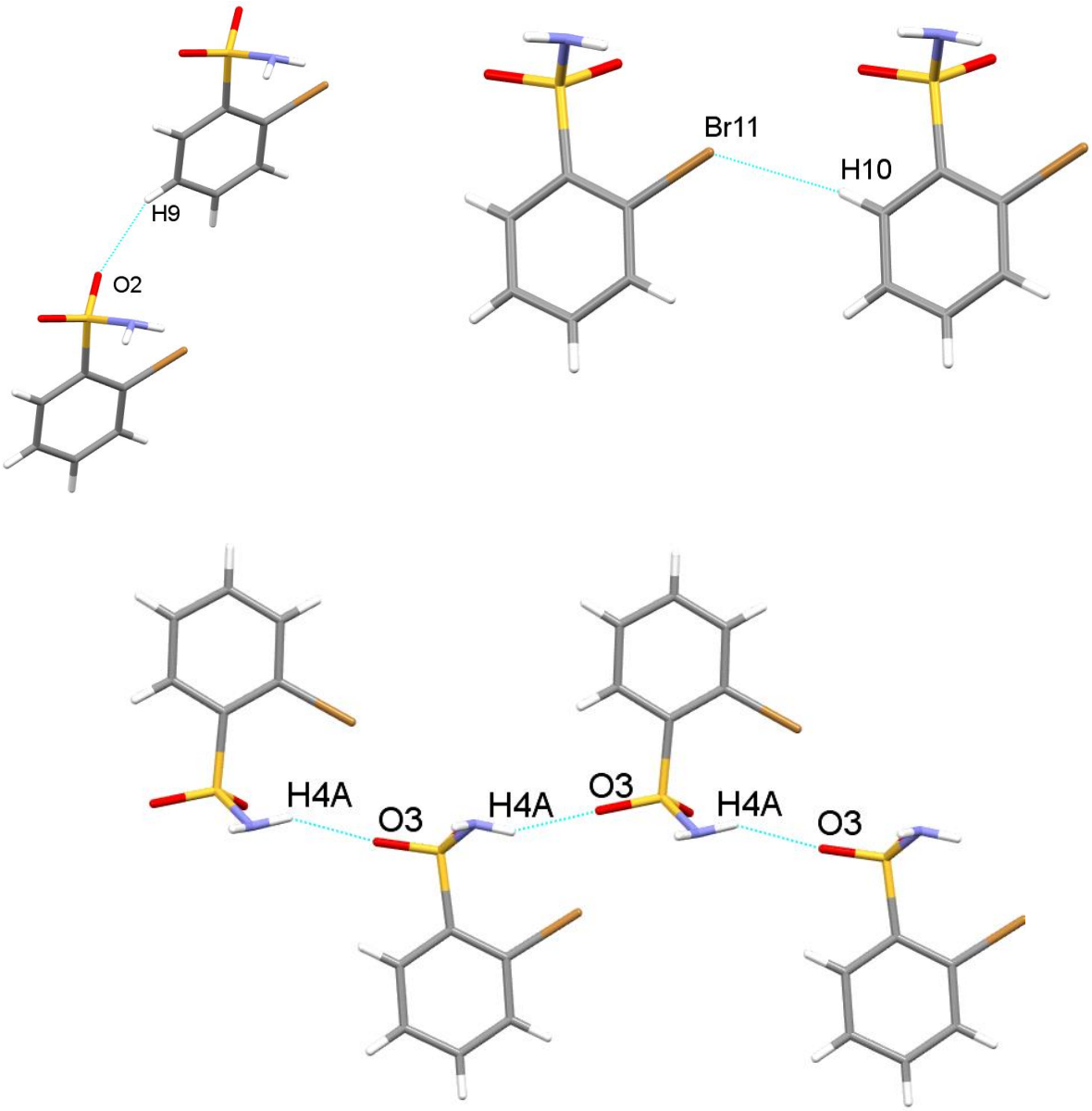


Figure S28: Hydrogen bonding in **9**.

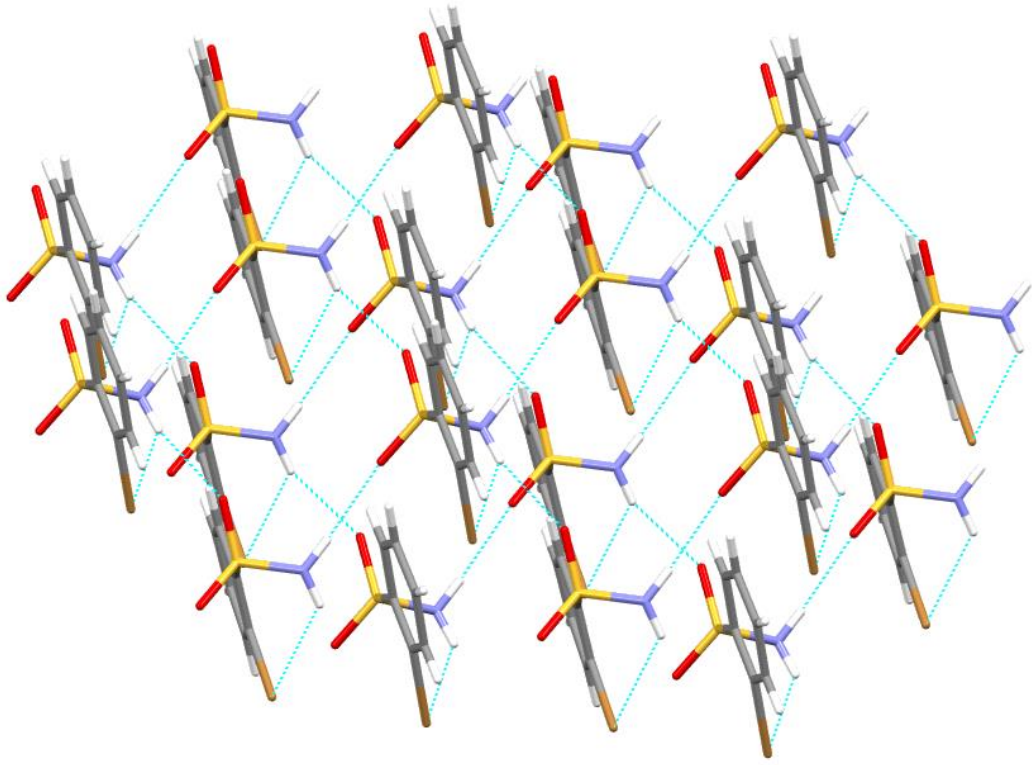


Figure S29: Packing diagram of **9**.

Analytical data for 2-nitrobenzenesulfonamide, **17**

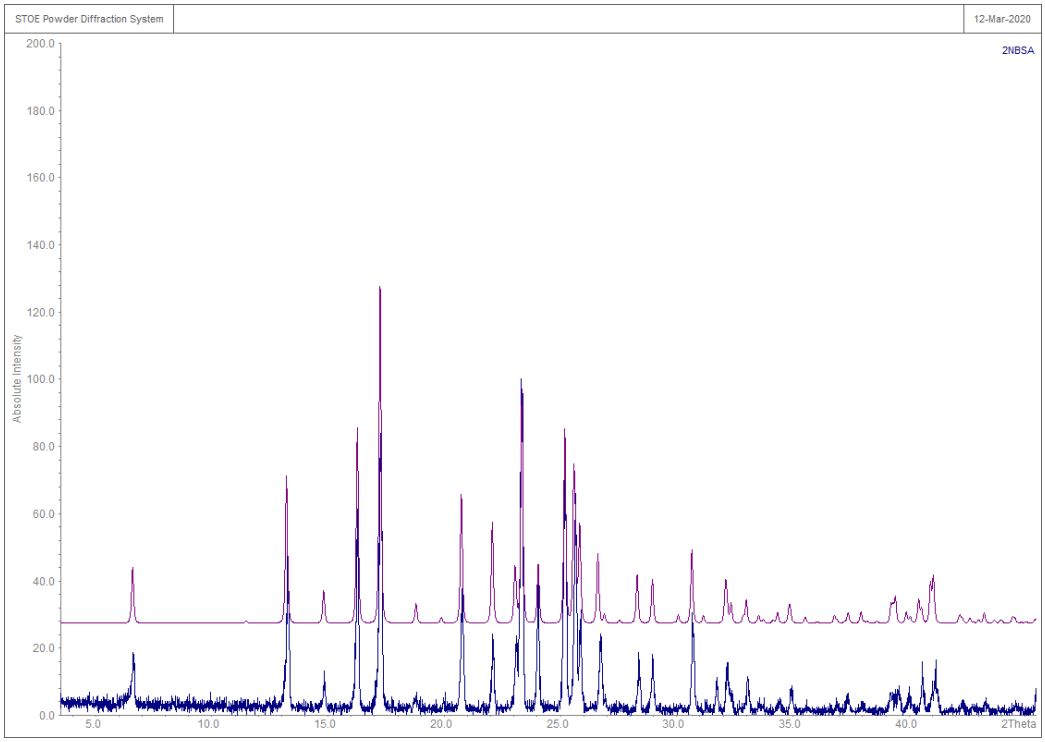


Figure S30: Experimental (blue) and theoretical (purple) PXRD data of **17**.

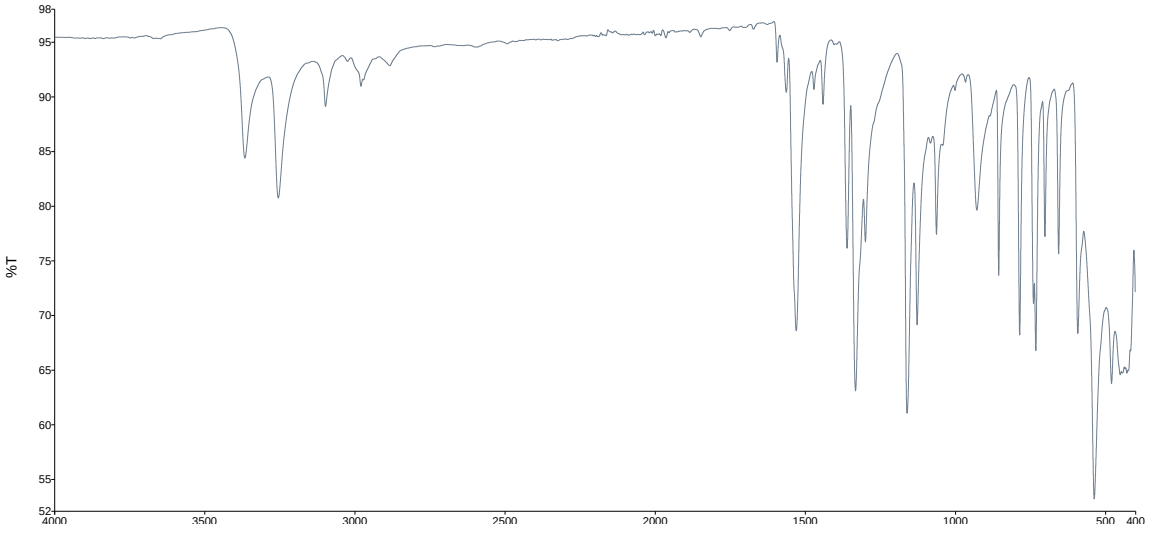


Figure S31: IR spectra of **17**.

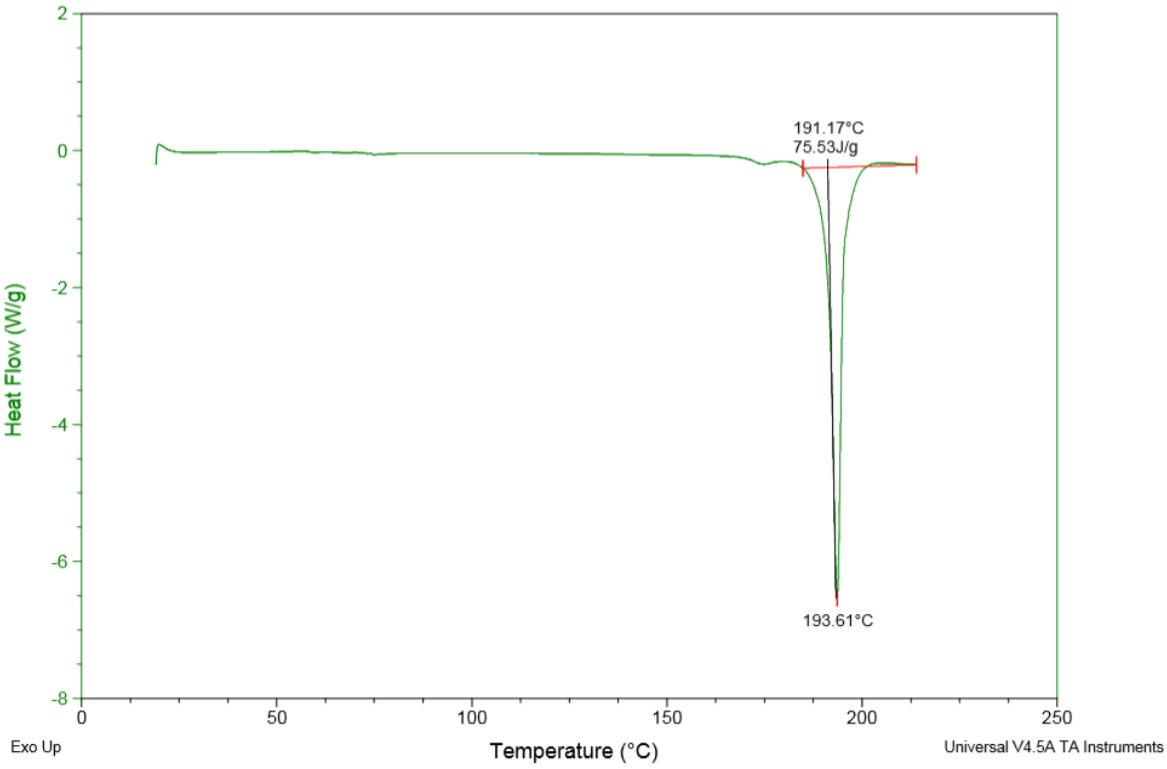


Figure S32: DSC spectra of **17**.

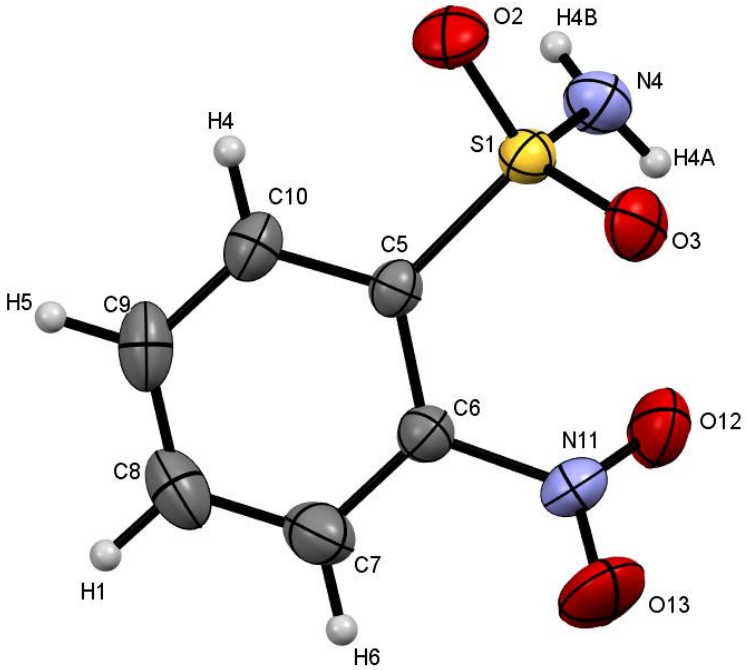


Figure S33: ORTEP diagram of **17**, with numbering scheme. Thermal ellipsoids are drawn at the 50% level.

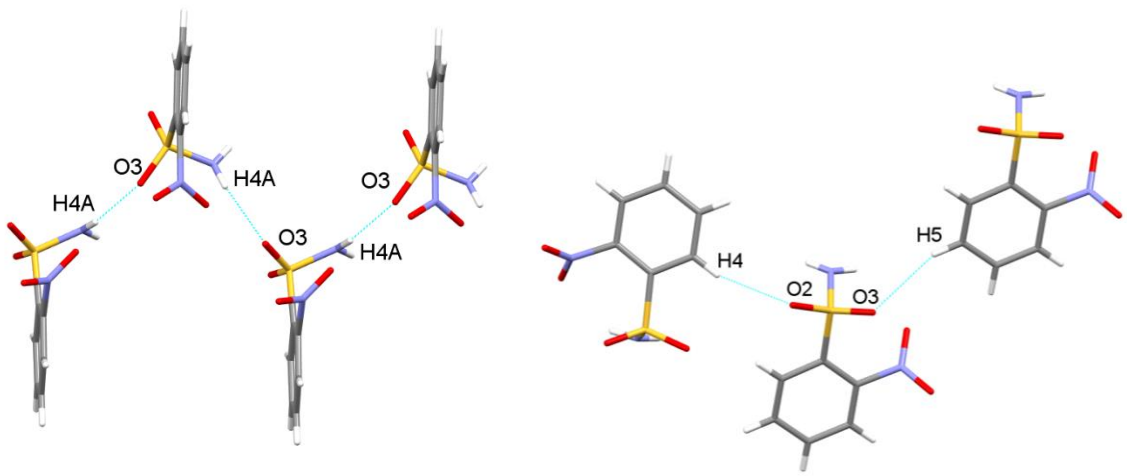


Figure S34: Hydrogen bonding in **17**.

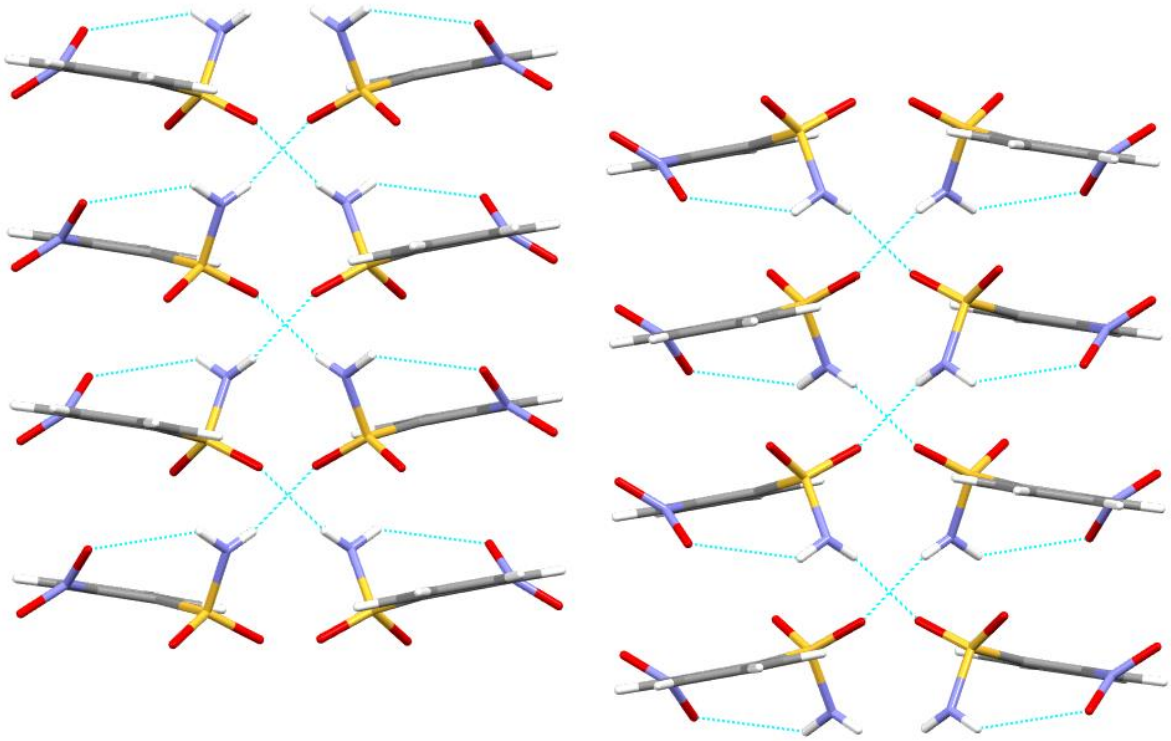


Figure S35: Packing diagram of **17**.

Analytical data for 3-bromobenzenesulfonamide, **20**

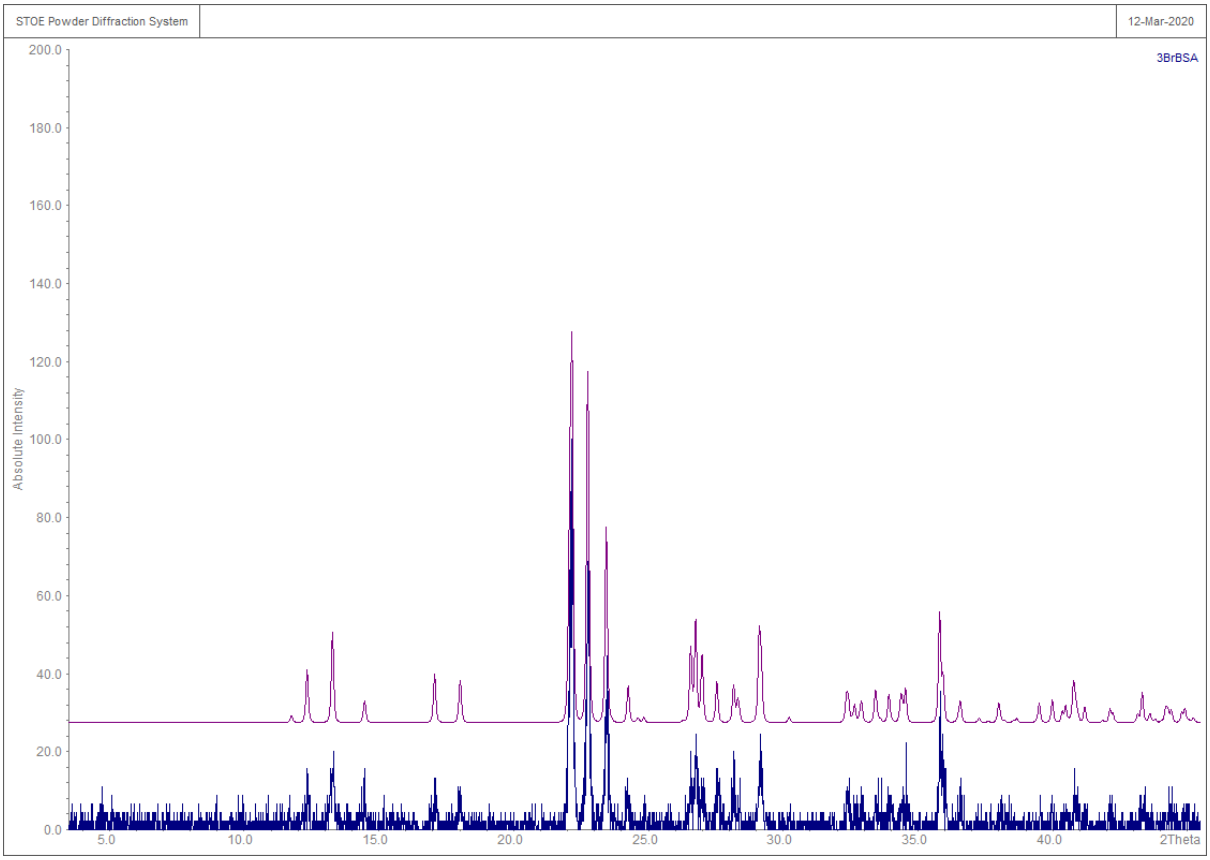


Figure S36: Experimental (blue) and theoretical (purple) PXRD data of **20**.

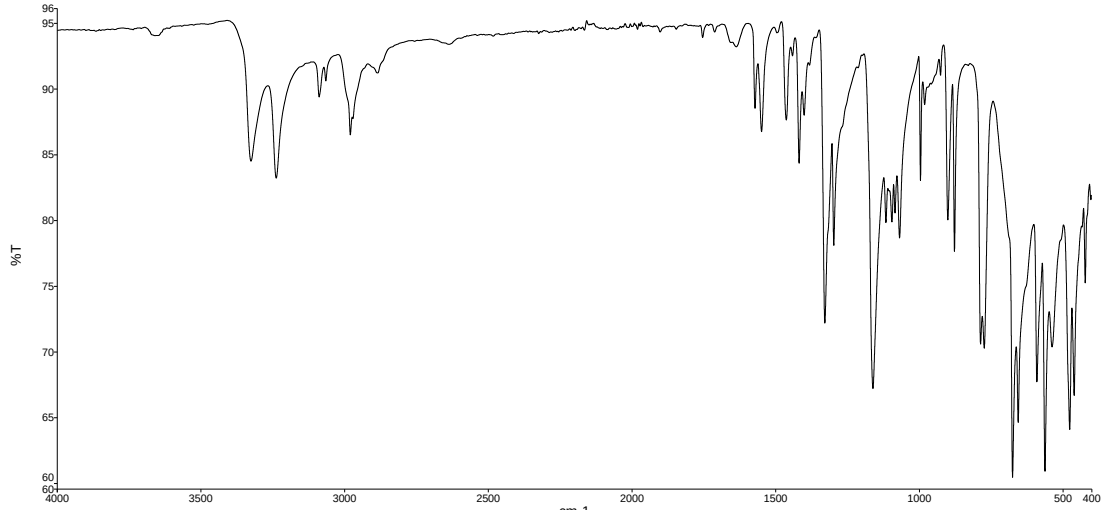


Figure S37: IR spectra of **20**.

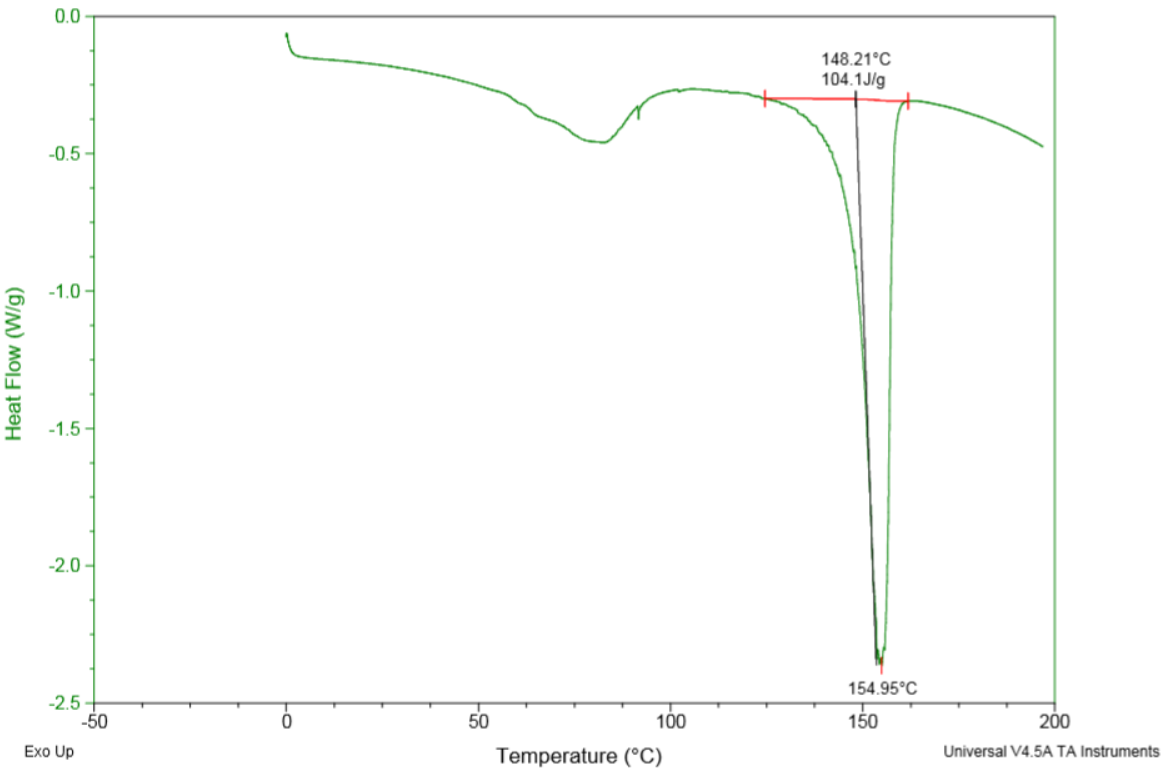


Figure S38: DSC spectra of **20**.

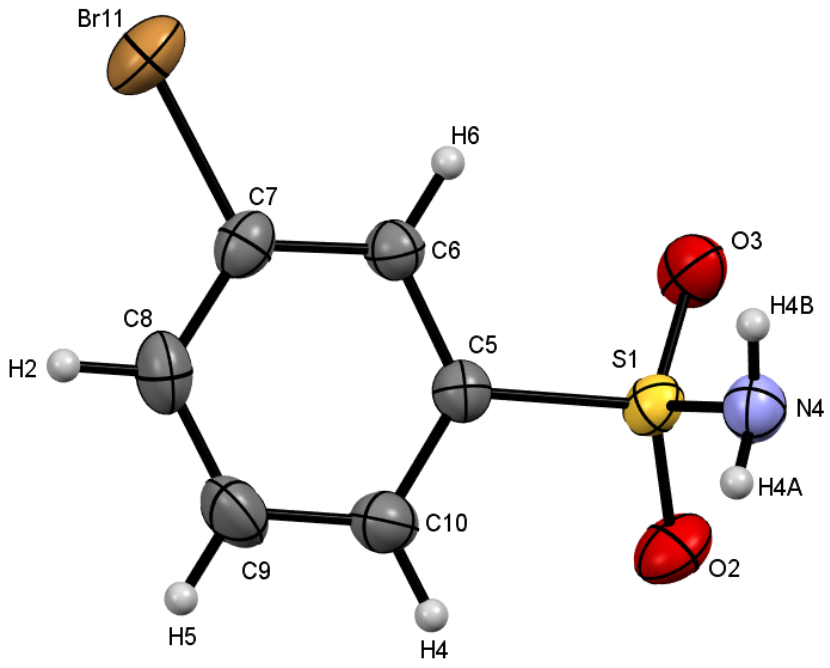


Figure S39: ORTEP diagram of **20**, with numbering scheme. Thermal ellipsoids are drawn at the 50% level.

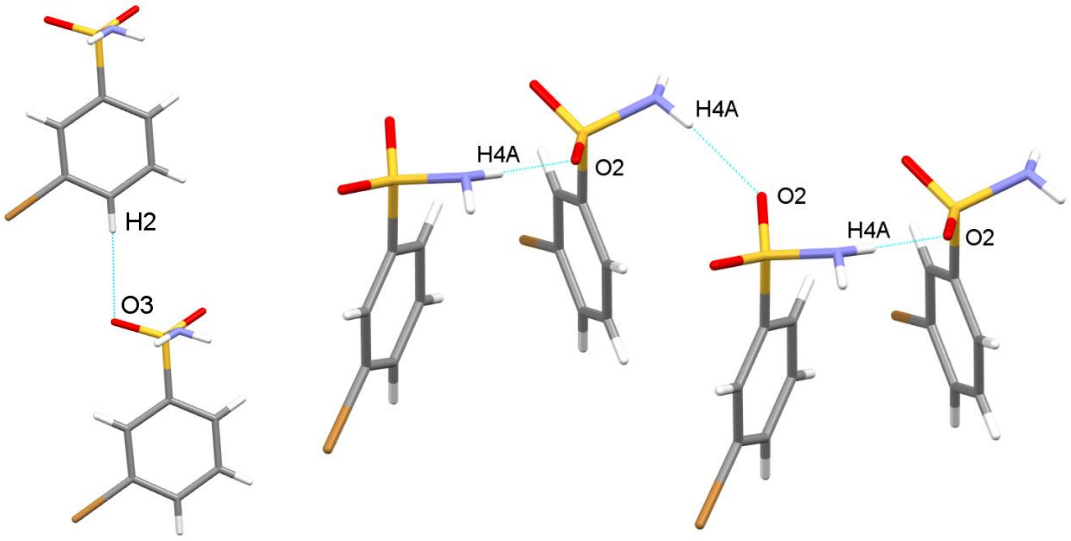


Figure S40: Hydrogen bonding in **20**.

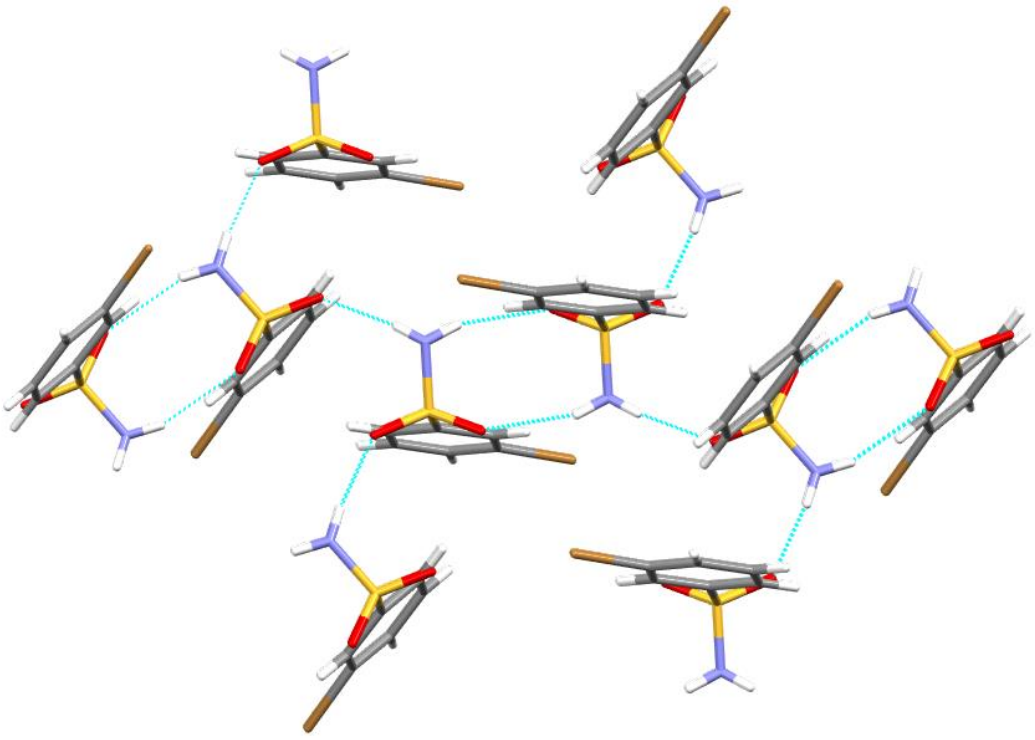


Figure S41: Packing diagram of **20**.

Analytical data for 3-chlorobenzenesulfonamide, **21**

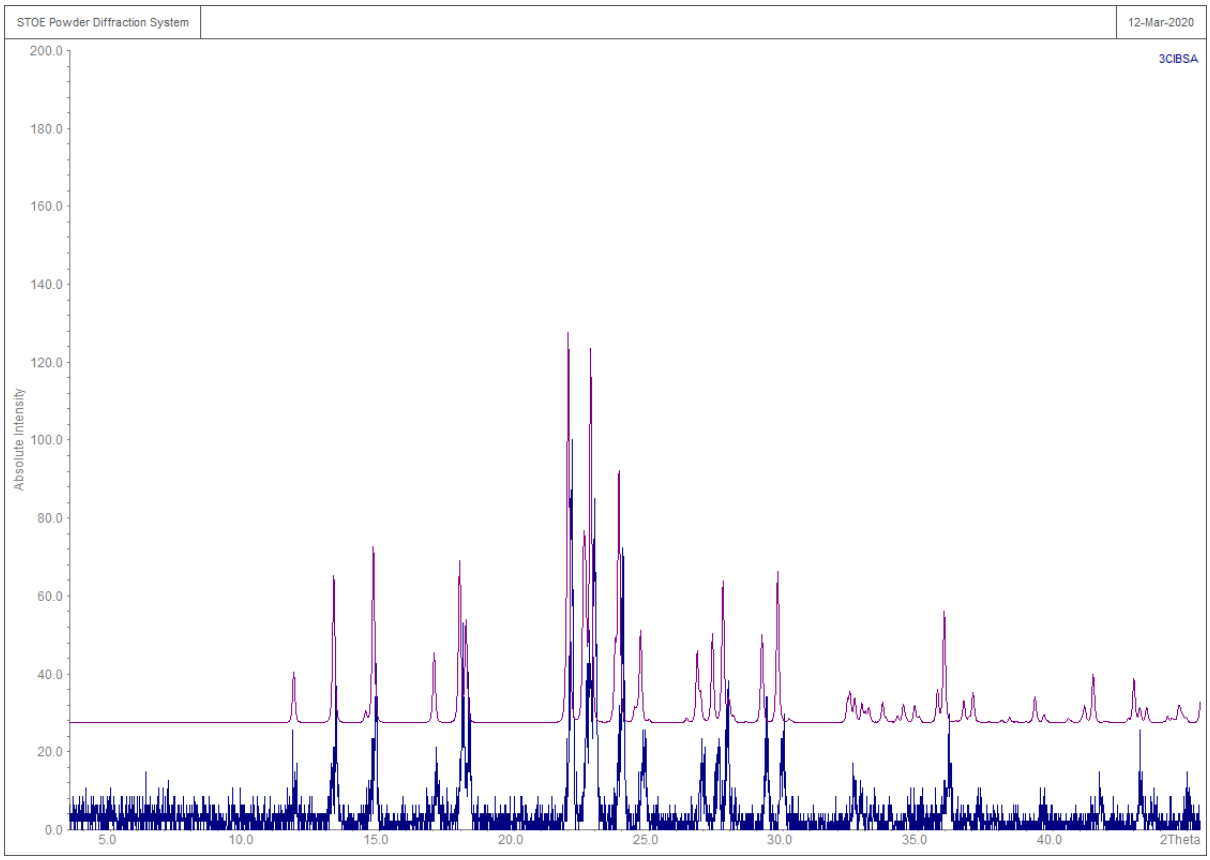


Figure S42: Experimental (blue) and theoretical (purple) PXRD data of **21**.

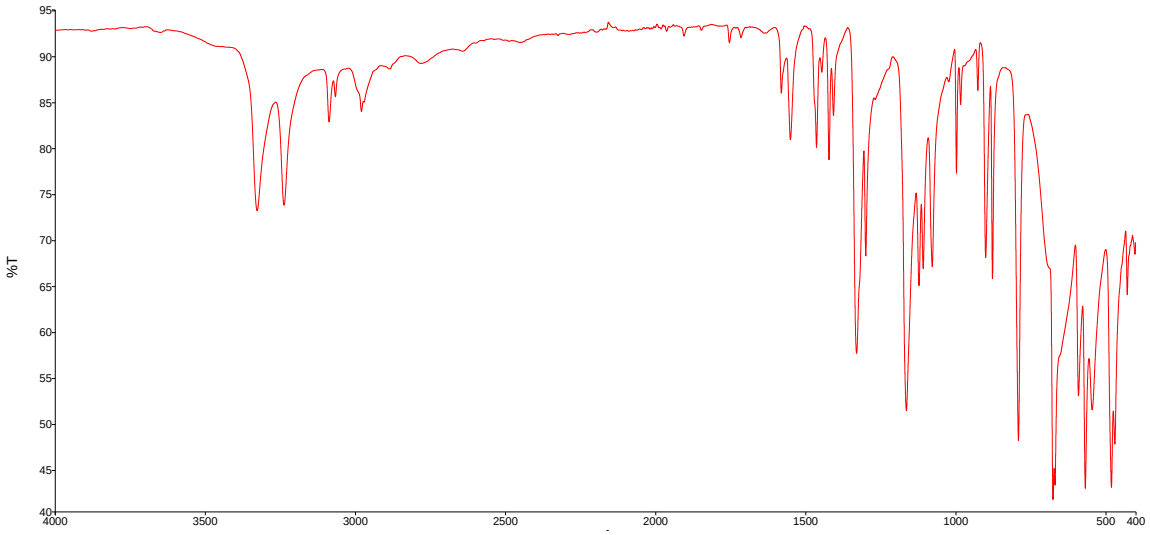


Figure S43: IR spectra of **21**.

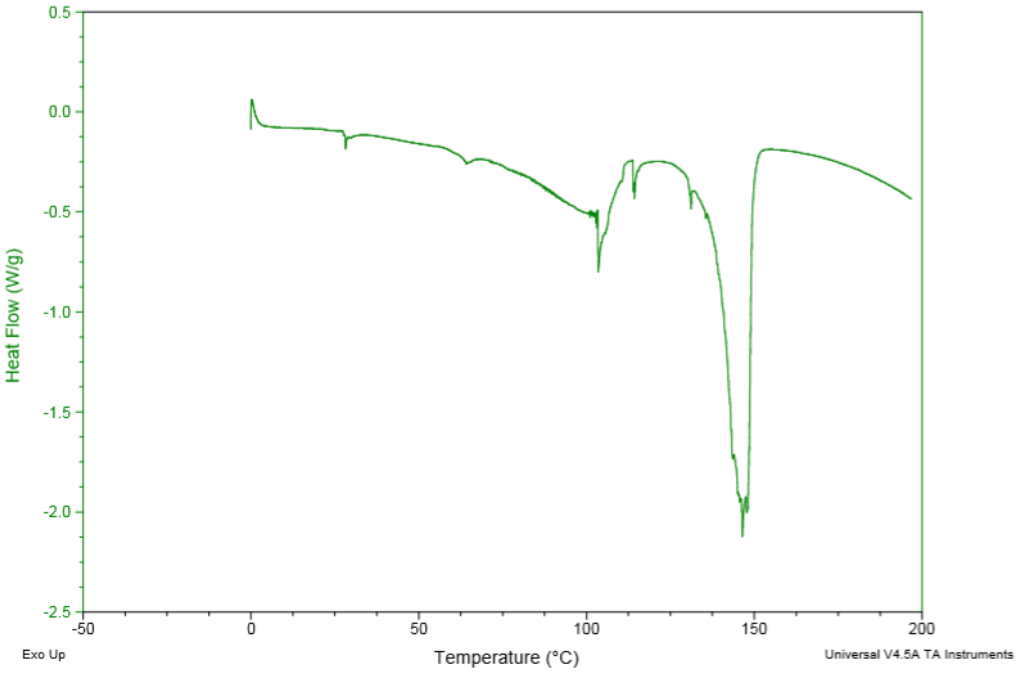


Figure S44: DSC spectra of **21**.

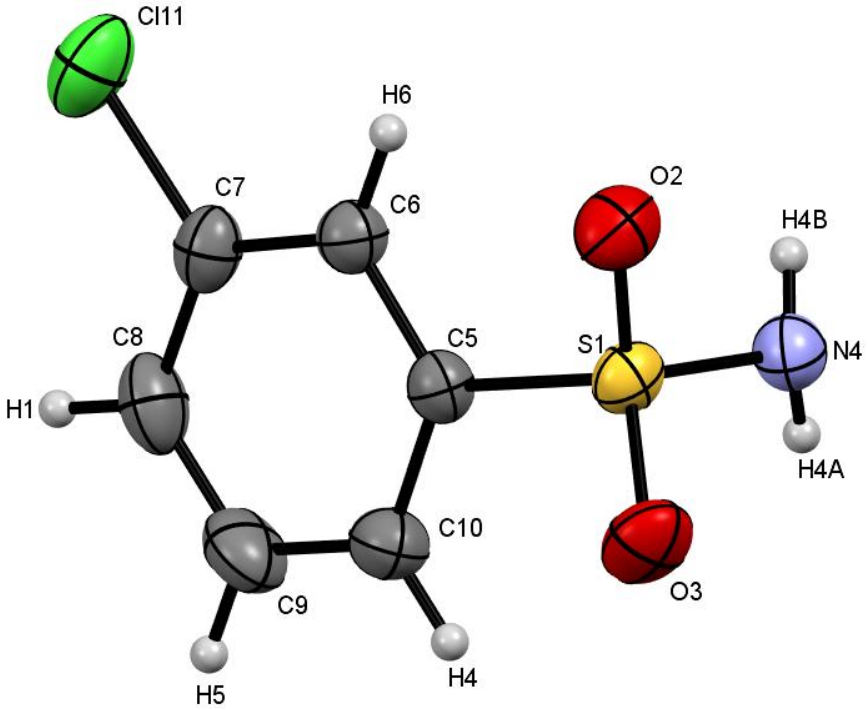


Figure S45: ORTEP diagram of **21**, with numbering scheme. Thermal ellipsoids are drawn at the 50% level.

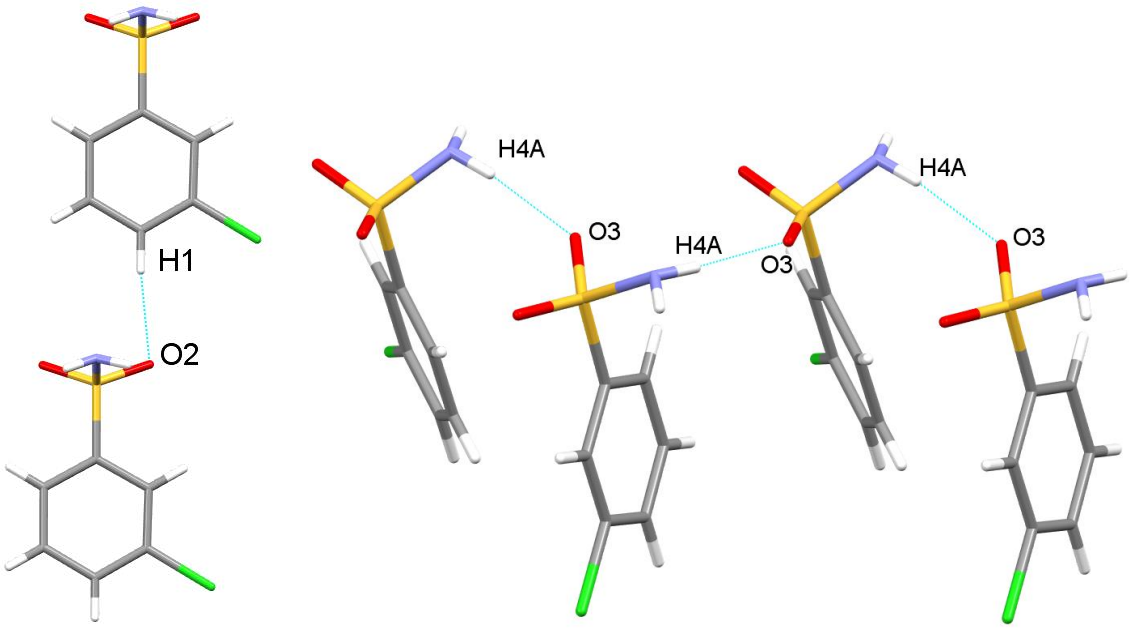


Figure S46: Hydrogen bonding in **21**.

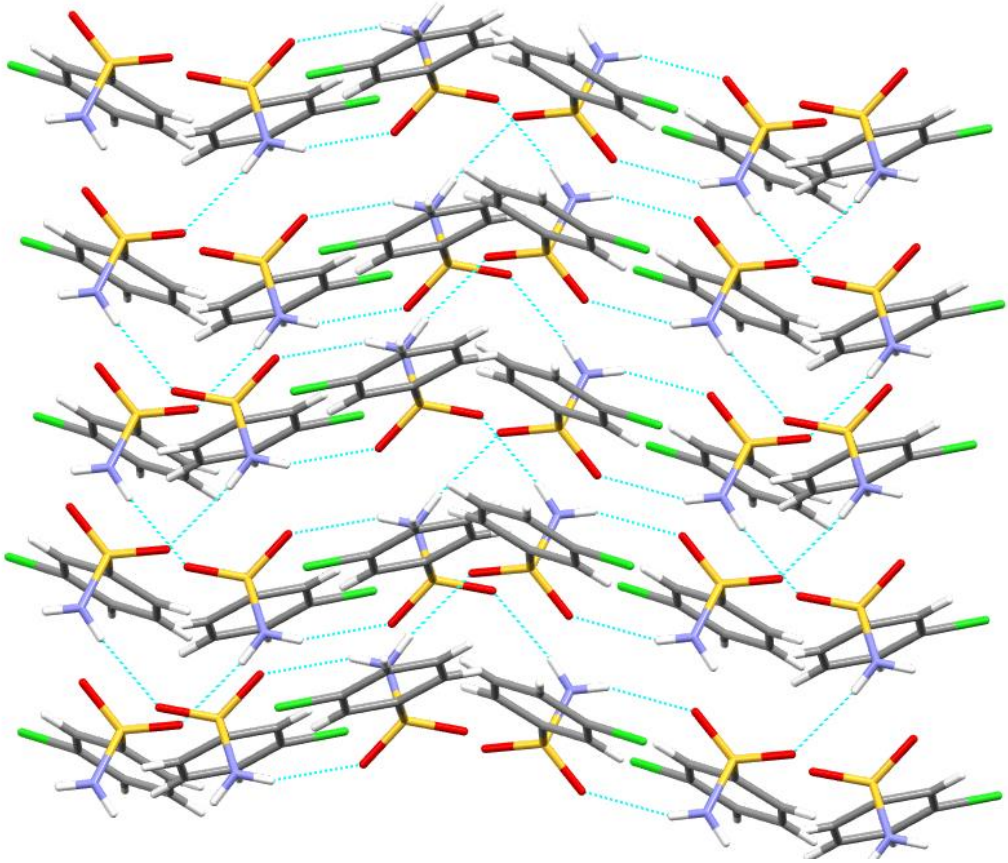


Figure S47: Packing diagram of **21**.

Table S1: Hydrogen bonds in benzenesulfonamide analogues.

compound	motif	interaction	graph set	D-H···A	D···A (Å)	H···A (Å)	D-H···A (°)
2	dimer	N4-H4A···O3	$R_2^2(8)$	0.840	2.232	3.0183	156.1
		N4-H4B···O2	$R_2^2(8)$	0.844	2.157	2.9646	160.1
3	dimer	N4-H4A···O3	$R_2^2(8)$	0.845	2.17	2.969	158
		N4-H4B···O2	$R_2^2(8)$	0.849	2.14	2.960	162
6	tetramer	N4-H4A···O2	$R_4^4(14)$	0.843	2.211	2.9828	152
		N4-H4B···O3	$R_4^4(14)$	0.852	2.139	2.9698	165
		C8-H8···O2	C(4)	0.93	2.53	3.388	154.3
		C10-H10···F11	-	0.93	2.47	3.115	126.8
7	tetramer	N4-H2A···O2	$R_4^4(14)$	0.95	2.34	3.119	138
		N4-H2A···O3	$R_4^4(14)$	0.95	3.57	3.265	131
		N4-H2B···O3	$R_4^4(14)$	0.83	2.35	3.134	158
		N4-H4A···O3	$R_4^4(14)$	0.851	2.19	2.949	148
9	tetramer	N4-H4A···Br11	-	0.851	2.89	3.471	127
		N4-H4B···O2	$R_4^4(14)$	0.847	2.147	2.992	175
		N4-H4A···O3	$R_4^4(14)$	0.87	2.13	2.933	154
17	tetramer	N4-H4A···O12	$R_4^4(14)$	0.87	2.53	3.101	125
		N4-H4B···O2	$R_4^4(14)$	0.78	2.21	2.983	169
		N4-H4A···O2	$R_2^2(8)$ & C(4)	0.847	2.166	3.009	173
20	dimer & offset C(4)	N4-H4B···O3	$R_2^2(8)$ & C(4)	0.847	2.224	3.019	157
		C8-H2···O3	C(4)	0.93	2.59	3.437	151.5
		C10-H4···Br11	-	0.93	3.06	3.6938	126.9
		N4-H4A···O3	$R_2^2(8)$ & C(4)	0.849	2.158	3.002	172.4
21	dimer & offset C(4)	N4-H4B···O2	$R_2^2(8)$ & C(4)	0.841	2.218	3.013	157.7
		C8-H1···O2	C(4)	0.93	2.6	3.438	151

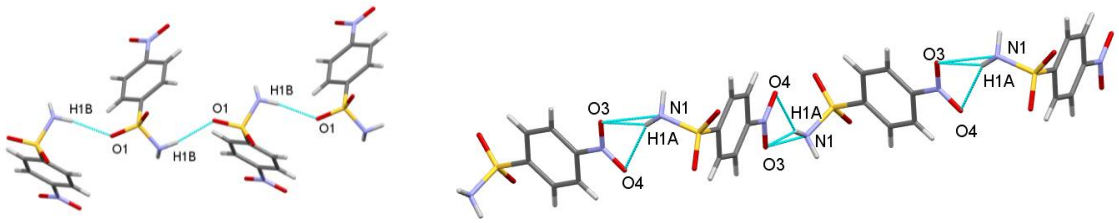


Figure S48: Hydrogen bonding in **1**. The blue hydrogen bonding indicates the C(4) hydrogen bonding at the unitary level. The C(4) chains are related by the 2_1-fold screw axis along the b-axis and a glide plane perpendicular to the b-axis.[1]

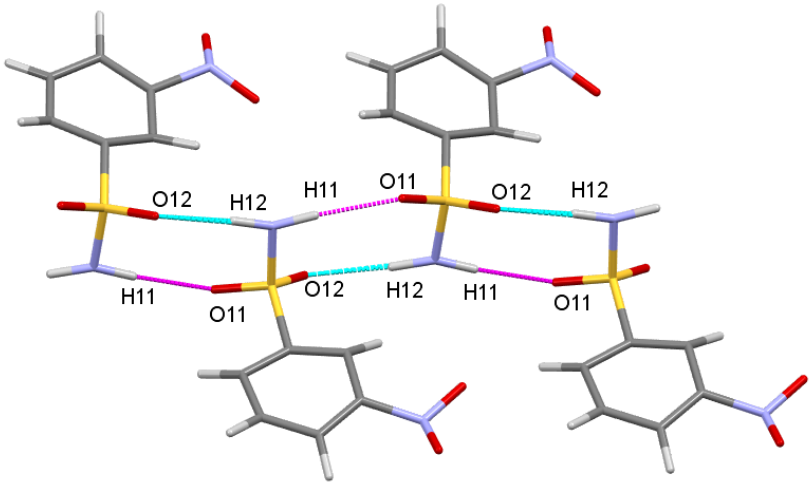


Figure S49: Hydrogen bonding in **4**. The blue hydrogen bonding indicates the C(4) hydrogen bonding at the unitary level. The C(4) chains are related by the 2_1-fold screw axis along the b-axis.[2]

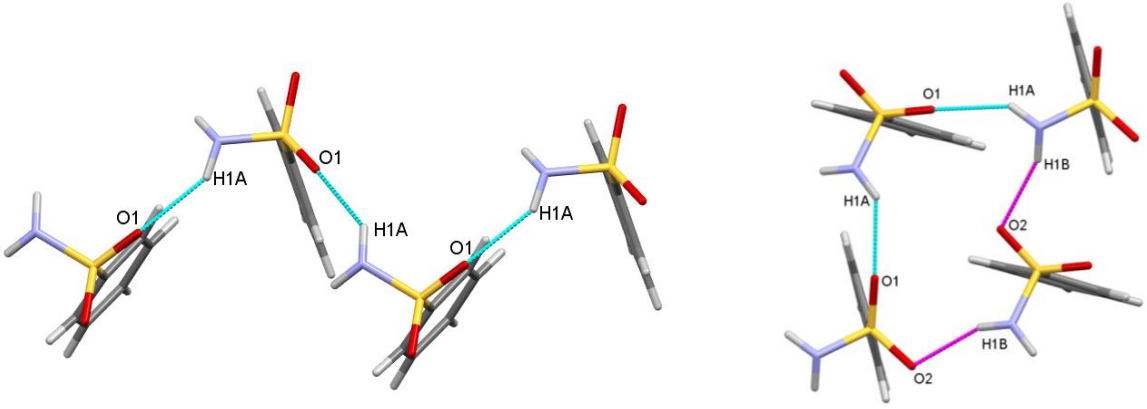


Figure S50: Hydrogen bonding in **5.** The blue and pink hydrogen bonding indicates the individual C(4) hydrogen bonding at the unitary level. The C(4) chains are related by the *c*-glide plane.[3]

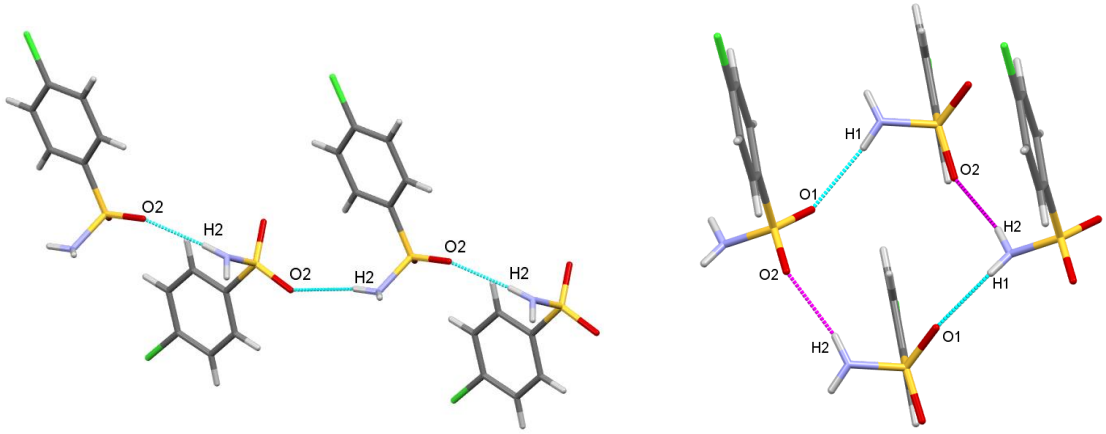


Figure S51: Hydrogen bonding in **8**. The blue and pink hydrogen bonding indicates the individual C(4) hydrogen bonding at the unitary level. The C(4) chains are related by the 2_1-screw axis and the *a* glide plane.[4]

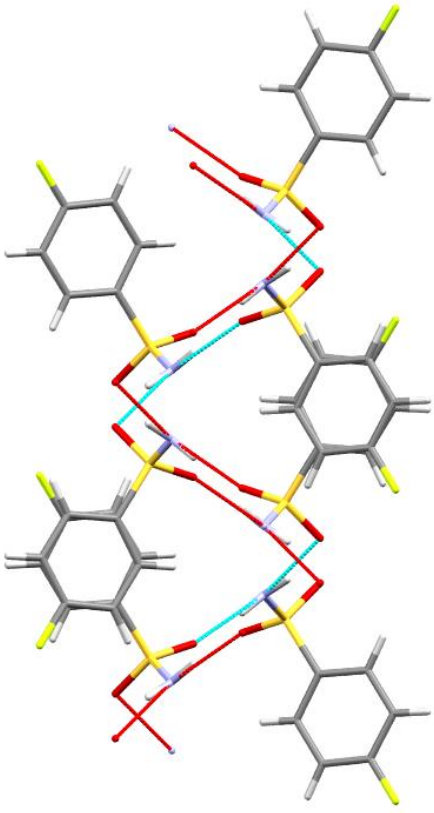


Figure S52: View of along the *b*-axis in **8** showing the zif-zag arrangement of the tetramers.

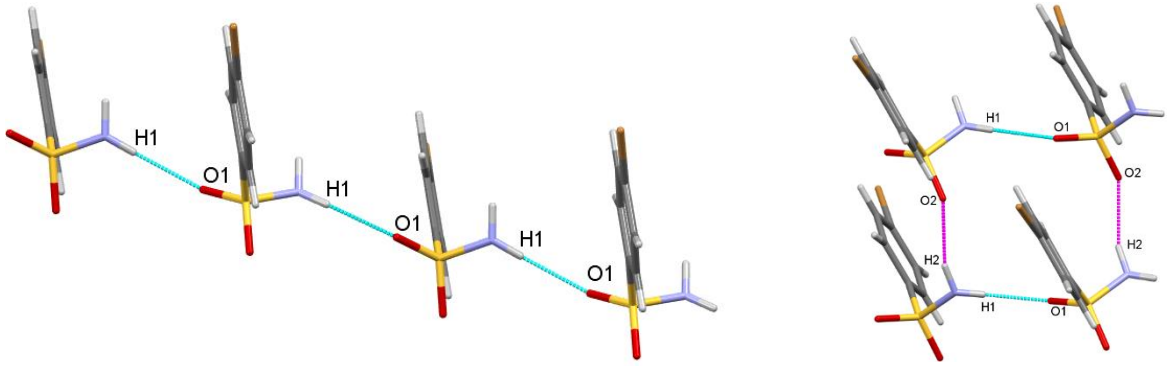


Figure S53: Hydrogen bonding in **10**. The blue and pink hydrogen bonding indicates the individual C(4) hydrogen bonding at the unitary level. The C(4) chains are related by the 2_1-screw axis and the *n* glide plane.[4]

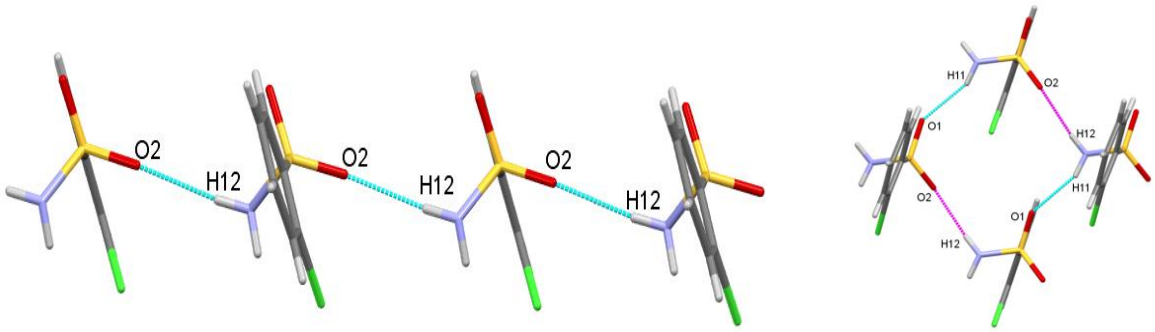


Figure S54: Hydrogen bonding in **11**. The blue and pink hydrogen bonding indicates the individual C(4) hydrogen bonding at the unitary level. The C(4) chains are related by the *c* glide plane and the C centering.[5]

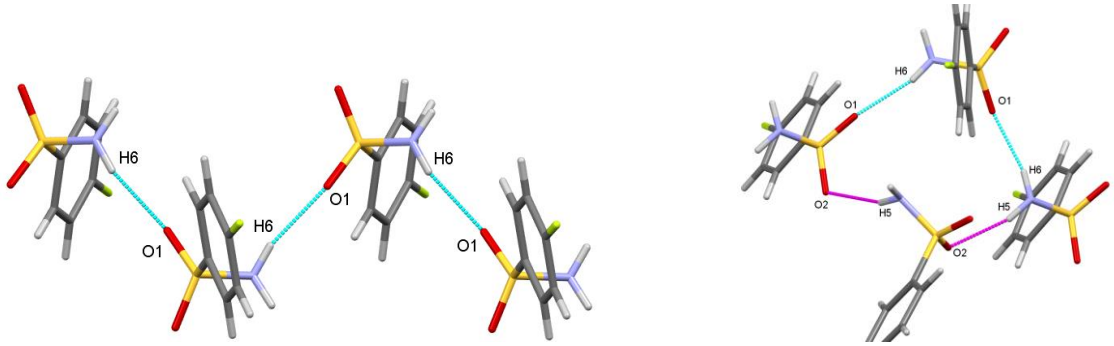


Figure S55: Hydrogen bonding in **12**. The blue and pink hydrogen bonding indicates the individual C(4) hydrogen bonding at the unitary level. The C(4) chains are related by the 2_1-screw axis and the *n* glide plane.[4]

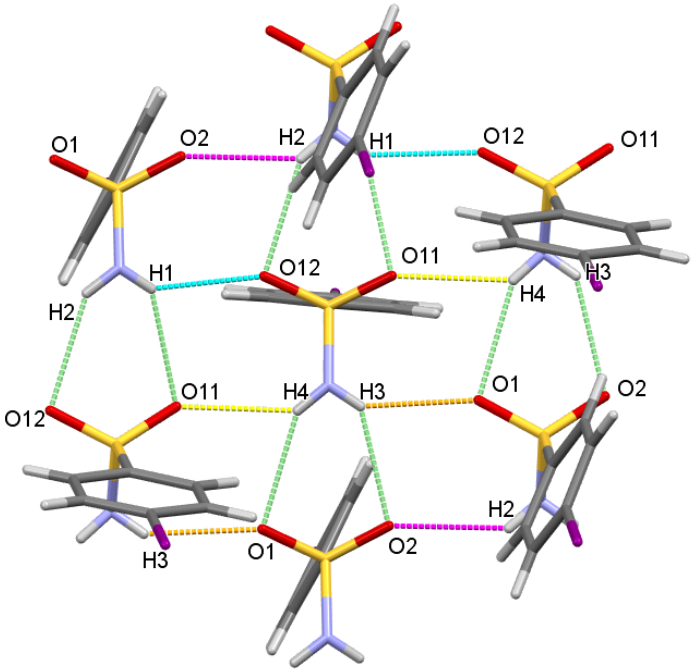


Figure S56: Hydrogen bonding in **13**. The blue, yellow, orange and pink hydrogen bonding indicates the individual C(4) hydrogen bonding at the unitary level and the green hydrogen bonding indicates the $R_2^2(6)$ hydrogen bonding at the binary level. The C(4) chains are related by a glide plane perpendicular to the b-axis.[4]

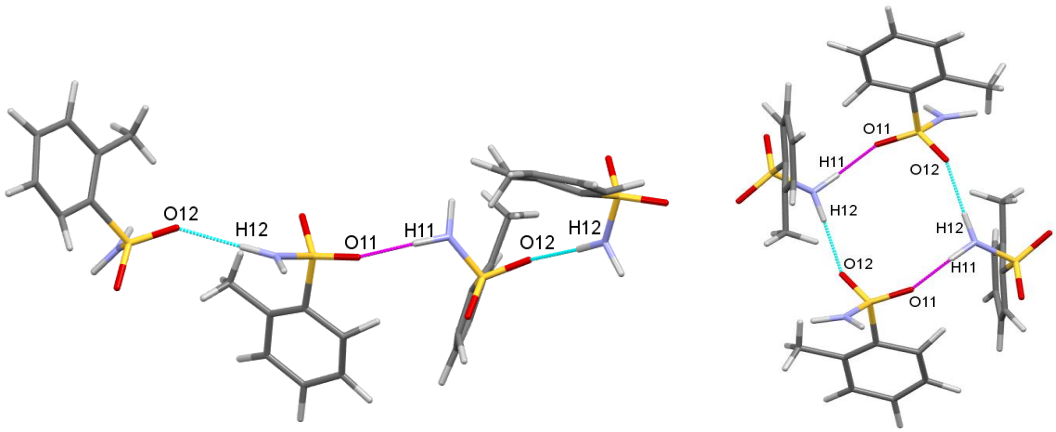


Figure S57: Hydrogen bonding in **14**. The blue and pink hydrogen bonding indicates the individual C(4) hydrogen bonding at the unitary level. The C(4) chains are related by the 4_1-fold screw axis along the c-axis and a glide plane perpendicular to the c-axis. There is also a $2_{1\text{-rotation}}$ axis and a 2_1 rotoinversion axis along the c-axis.[6]

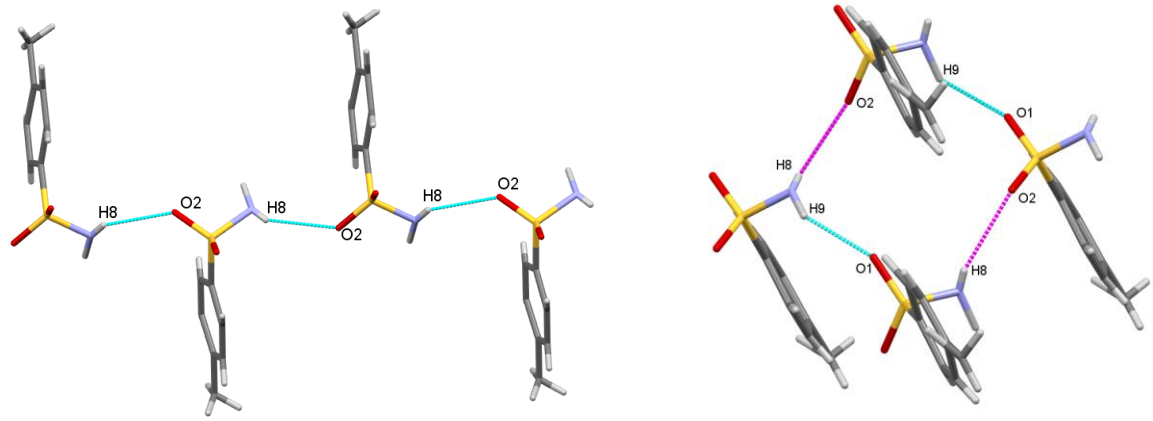


Figure S58: Hydrogen bonding in **15**. The blue and pink hydrogen bonding indicates the individual C(4) hydrogen bonding at the unitary level. The C(4) chains are related by the 2_1-fold screw axis along the b-axis and a glide plane perpendicular to the b-axis.[7]

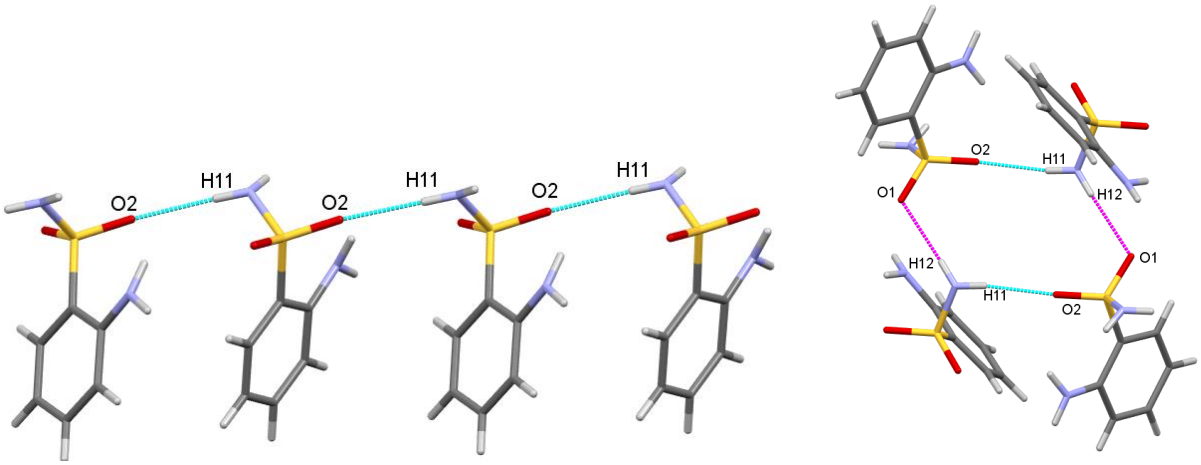


Figure S59: Hydrogen bonding in **16**. The blue and pink hydrogen bonding indicates the individual C(4) hydrogen bonding at the unitary level. The C(4) chains are related by the 2_1-fold screw axis along the b-axis and a glide plane perpendicular to the b-axis.[8]

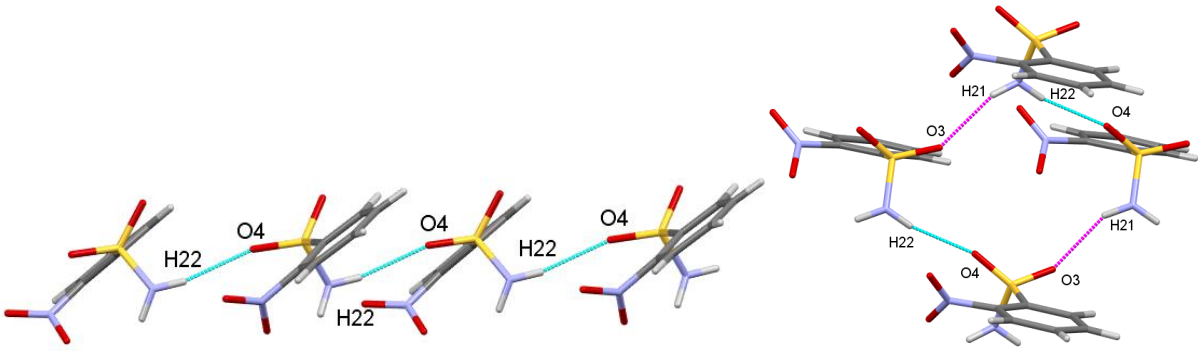


Figure S60: Hydrogen bonding in **17 (TIBPAW)**. The blue and pink hydrogen bonding indicates the individual C(4) hydrogen bonding at the unitary level. The C(4) chains are related by the glide plane perpendicular to the b-axis.[9]

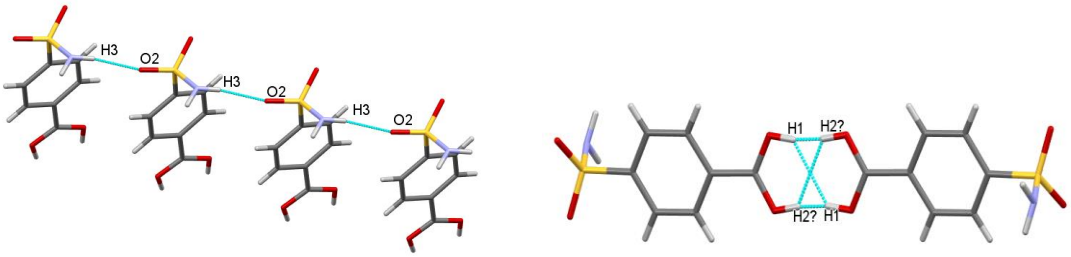


Figure S61: Hydrogen bonding in **18**. The blue hydrogen bonding indicates the C(4) hydrogen bonding at the unitary level. The C(4) chains are related by the 2_1-fold screw axis along the b-axis and a glide plane perpendicular to the b-axis.[10]

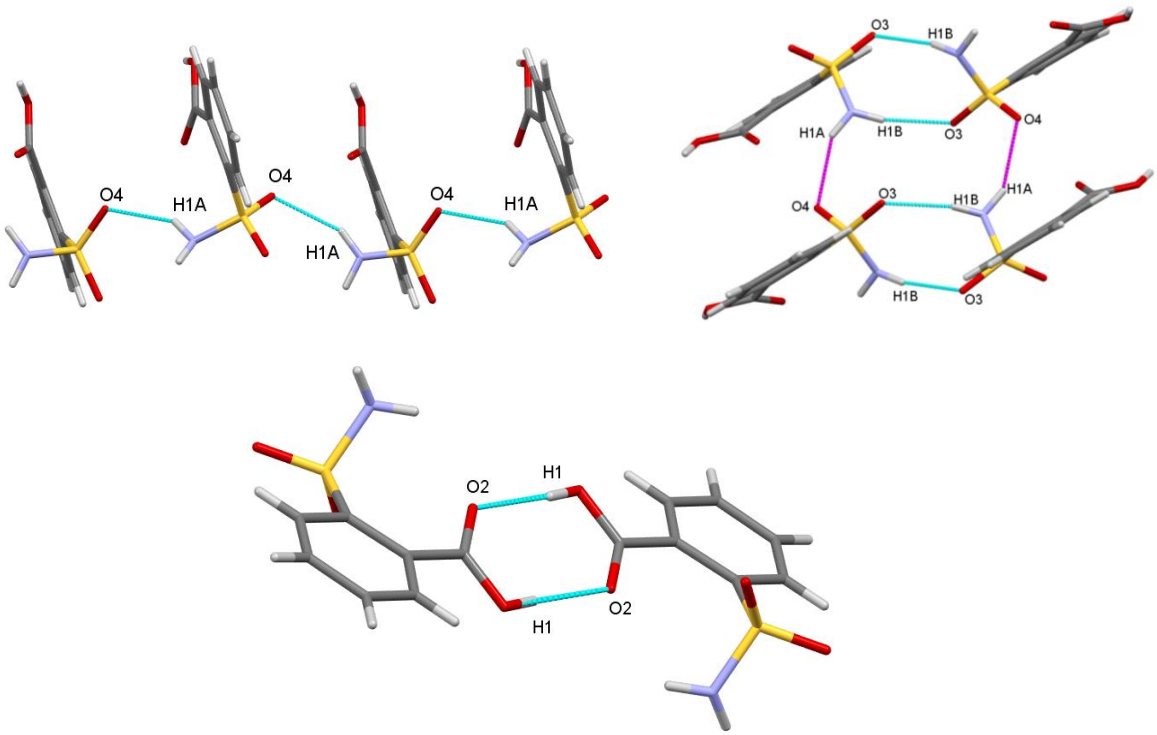


Figure S62: Hydrogen bonding in **19**. The blue and pink hydrogen bonding indicates the individual C(4) hydrogen bonding at the unitary level. The C(4) chains are related by the 2_1-fold screw axis along the b-axis and a glide plane perpendicular to the b-axis. There is also a 2_1-fold rotation axis along the b-axis.[15]

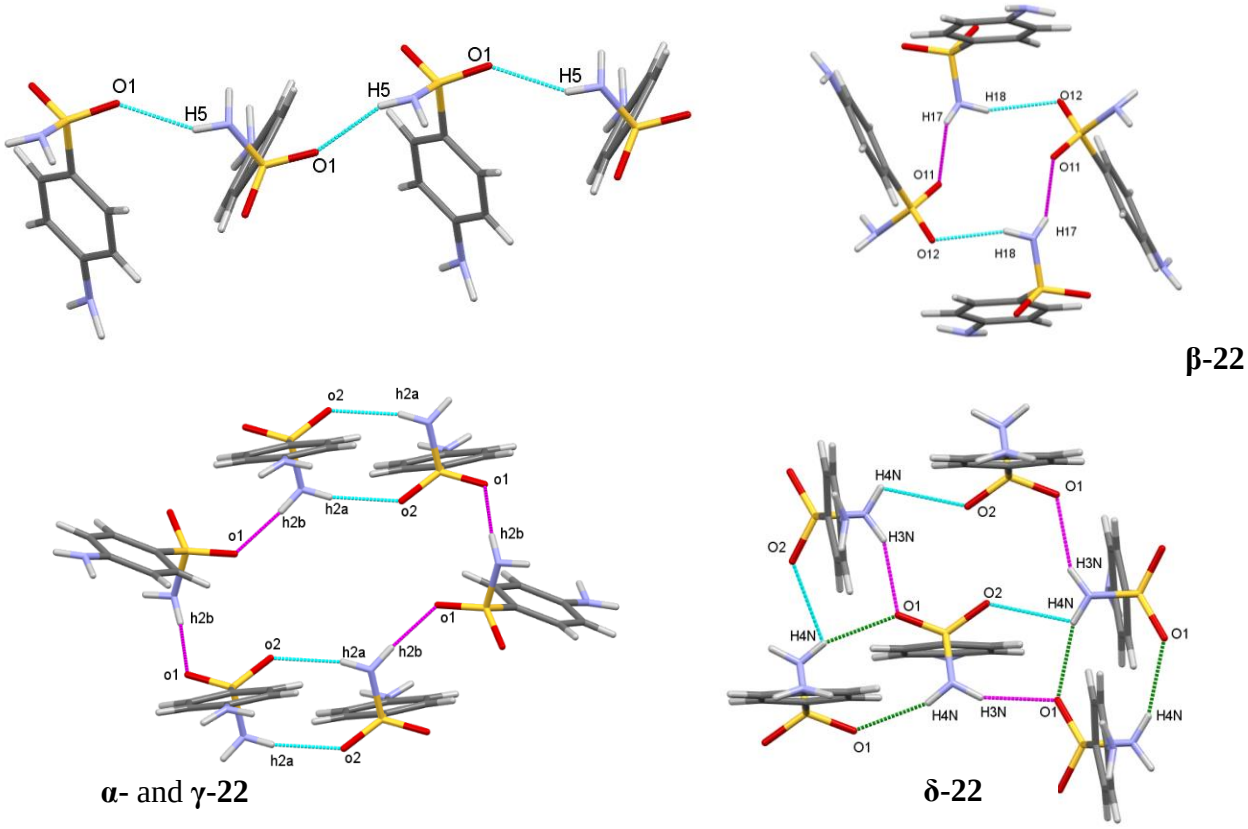


Figure S63: Hydrogen bonding in **22**. The blue and pink hydrogen bonding indicates the individual C(4) hydrogen bonding at the unitary level. The C(4) chains are related by the 2_1-fold screw axis along the b-axis and a glide plane perpendicular to the b-axis.[11-14]

References

1. Zhou, T.; Zhang, Q.; Chen, G.; Zhou, Z. Redetermination Of 4-Nitrobenzenesulfonamide. *Acta Crystallogr., Sect. E: Struct. Rep. Online* **2004**, *60*, 1767-1768.

2. Tremayne, M.; Seaton, C.; Glidewell, C. Structures of Three Substituted Arenesulfonamides from X-Ray Powder Diffraction Data using the Differential Evolution Technique. Acta Crystallogr., Sect. B: Struct. Sci. 2002, 58, 823-834.

3. Gowda, B.; Nayak, R.; Kožíšek, J.; Tokarčík, M.; Fuess, H. Benzenesulfonamide. *Acta Crystallogr., Sect. E: Struct. Rep. Online* **2007**, *63*, 2967-2967.

4. Zerbe, E.; Moers, O.; Jones, P.; Blaschette, A. Intermolecular Interactions in the Crystal Structures Of 4-Halobenzenesulfonamides (Halogen = Fluorine, Chlorine, Bromine, Iodine) and 4-Methylbenzenesulfonamide. *Z. Naturforsch. B* **2005**, *60*, 125-138.

5. Gowda, B.; Foro, S.; Shakuntala, K.; Fuess, H. 2-Chlorobenzenesulfonamide. *Acta Crystallogr., Sect. E: Struct. Rep. Online* **2009**, *65*, 2144-2144.

6. Gowda, B.; Foro, S.; Shakuntala, K.; Fuess, H. O-Toluenesulfonamide: A Redetermination. *Acta Crystallogr., Sect. E: Struct. Rep. Online* **2009**, *65*, 2258-2258.

7. Thimme Gowda, B.; Jyothi, K.; Kožíšek, J.; Fuess, H. Crystal Structure Studies On p-Substitutedbenzenesulphonamides 4-X-$C_6H_4SO_2NH_2$ (X = CH_3, NH_2 F, Cl or Br). *Z. Naturforsch. A* **2003**, *58*, 656-660.

8. Flörke, U.; Saeed, A. CCDC 1814288: Experimental Crystal Structure Determination - o-Sulfanilamide. https://dx.doi.org/10.5517/ccdc.csd.cc1ywxf5 (accessed Apr 17, 2020).

9. Cheng, H.; Zhang, S.; Huang, C. 2-Nitrobenzenesulfonamide. *Acta Crystallogr., Sect. E: Struct. Rep. Online* **2007**, *63*, 1979-1980.

10. Ng, S. Crystal Structure Of p-Sulfamoylbenzoic Acid, $H_2NSO_2C_6H_4COOH$. *Z. Kristallogr. Cryst. Mater.* **1997**, *212*, 282-282.

11. Siddiqui, W.; Ahmad, S.; Siddiqui, H.; Tariq, M.; Parvez, M. O-Sulfamoylbenzoic Acid. *Acta Crystallogr., Sect. E: Struct. Rep. Online* **2007**, *63*, 4117-4117.

12. Alléaume, M.; Decap, J. Affinement Tridimensionnel Du Sulfanilamide B. *Acta Crystallogr.,* **1965**, *18*, 731-736.

13. O'Connor, B.; Maslen, E. The Crystal Structure of α-Sulphanilamide. *Acta Crystallogr.,* **1965**, *18*, 363-366.

14. Alléaume, M.; Decap, J. Affinement Tridimensionnel Du Sulfanilamide γ. *Acta Crystallogr.,* **1965**, *19*, 934-938.

15. Gelbrich, T.; Bingham, A.; Threlfall, T.; Hursthouse, M. δ-Sulfanilamide. *Acta Crystallogr., Sect. C: Cryst. Struct. Commun.* **2008**, *64*, 205-207.

Chapter Three – Cocrystallization of Primary Aromatic Sulfonamides

3. Cocrystallization of Primary Aromatic Sulfonamides

3.1 *Abstract*

The design of novel supramolecular synthons for functional groups relevant to drugs is an essential prerequisite for applying crystal engineering in the development of novel pharmaceutical cocrystals. It has been convincingly shown over the past two decades that molecular level control and modulation can influence the physicochemical properties of drug cocrystals. Whereas considerable advances have been reported on the design of cocrystals for carboxylic acids and carboxamide functional groups, the sulfonamide group, which is a cornerstone of sulfa drugs, is relatively unexplored for reproducible heterosynthon-directed crystal engineering. This study investigated 18 primary aromatic sulfonamides and 20 coformers which resulted in the structural characterisation of a cocrystal of 4-methylbenzene sulfonamide with succinic acid in a 1:1 stoichiometric ratio that has dimer-dimer and tetramer synthons. We also obtained an additional two crystalline samples which have both been fully characterized by IR, NMR, DSC and PXRD and are likely to be cocrystals, namely 4-nitrobenzene sulfonamide with caprolactam and 4-methoxybenzene sulfonamide with valerolactam. ^{1}H NMR analysis confirms that these crystalline materials contain both the sulfonamide and the coformer.

3.2 *Introduction*

Research into the sulfonamide functional group has intensified over the last number of years due to the ability of sulfonamides to form different intermolecular S=O···H and N−H···O hydrogen-bonds.[1] However, one of the major issue's researchers are currently facing is procuring enough structural data on supramolecular synthons and crystal landscape of the

sulfonamide group and as such, sulfonamides remain a structural gap in the CSD despite SO_2NH_2 being the key functional group in the most populated sulfa drugs category.[2] The reason for this is due to the sulfonamide groups conformational flexibility, having two O acceptors and two NH donors and, thus, is able to form a more stable homo dimer.[3] This issue is currently being addressed through cocrystallization and salt studies in the *Nangia* research group.[1-6] In general, salts and cocrystals are necessary to improve the physiochemical properties of drugs affected by issues such as solubility, bioavailability dissolution rate, and stability. Cocrystallization is a standard strategy to tailor physicochemical properties of drugs based on their chemical constituents and supramolecular structure through crystal engineering.[7-9] It allows for an increased yield, control over polymorphism, better product crystallinity and applies to a significantly larger scope of cocrystal coformers and nucleation through seeding. It also involves a rapid screening and analysis process.[10-12] Sulfonamide drugs are predominantly limited by their physicochemical properties of low solubility and, hence, the design of soluble cocrystals and salts is essential in the current bacterial resistance crisis.

To lessen the structural gap, we conducted a systematic review of multiple simple primary aromatic sulfonamides, which revealed many interesting facts about sulfonamide crystal formation as discussed in **Chapter 2**. This work complements a synthon study undertaken by Nangia's group in 2015 in which they categorized all sulfonamides in the CSD.[1] With our systematic review and Nangia's extensive cocrystal research taken into consideration we employed a crystal engineering approach in order to explore cocrystal formation of primary aromatic sulfonamides, **Figure 3.1**, to attempt to identify novel synthons in a non-competitive environment. This study explored both GRAS and non-GRAS compounds, **Figure 3.2**. GRAS coformers are useful for potential sulfonamide drug development and non-GRAS compounds are useful for providing a wider dataset for analysis such as comparing crystal packing and solubility in relation to the structure-forming synthons.[13] We were successful in obtaining

structural analysis of one cocrystal comprised of 4-methybenzenesulfonamide and succinimide in a 1:1 ratio. An additional two cocrystals were identified and characterized, yet not analysed by SCXRD due to the COVID-19 pandemic.

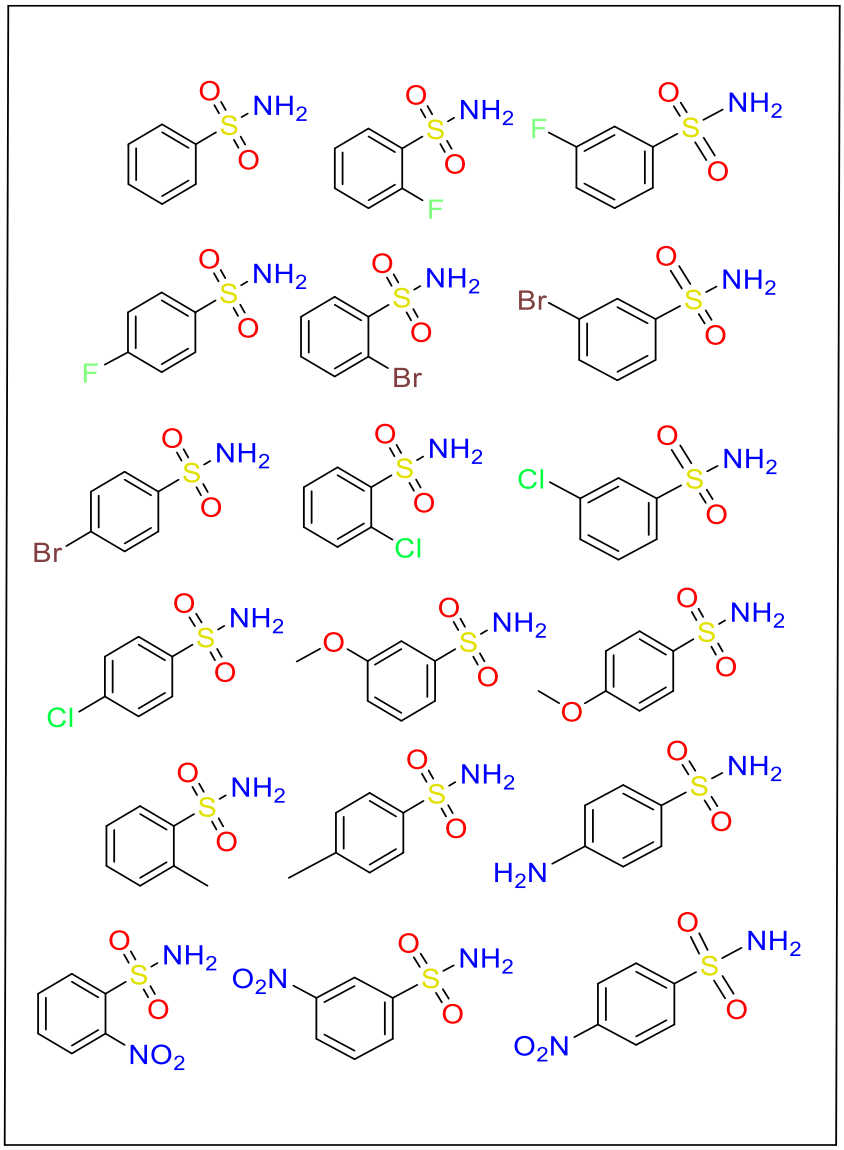


Figure 3.1: The primary aromatic sulfonamides examined in this study

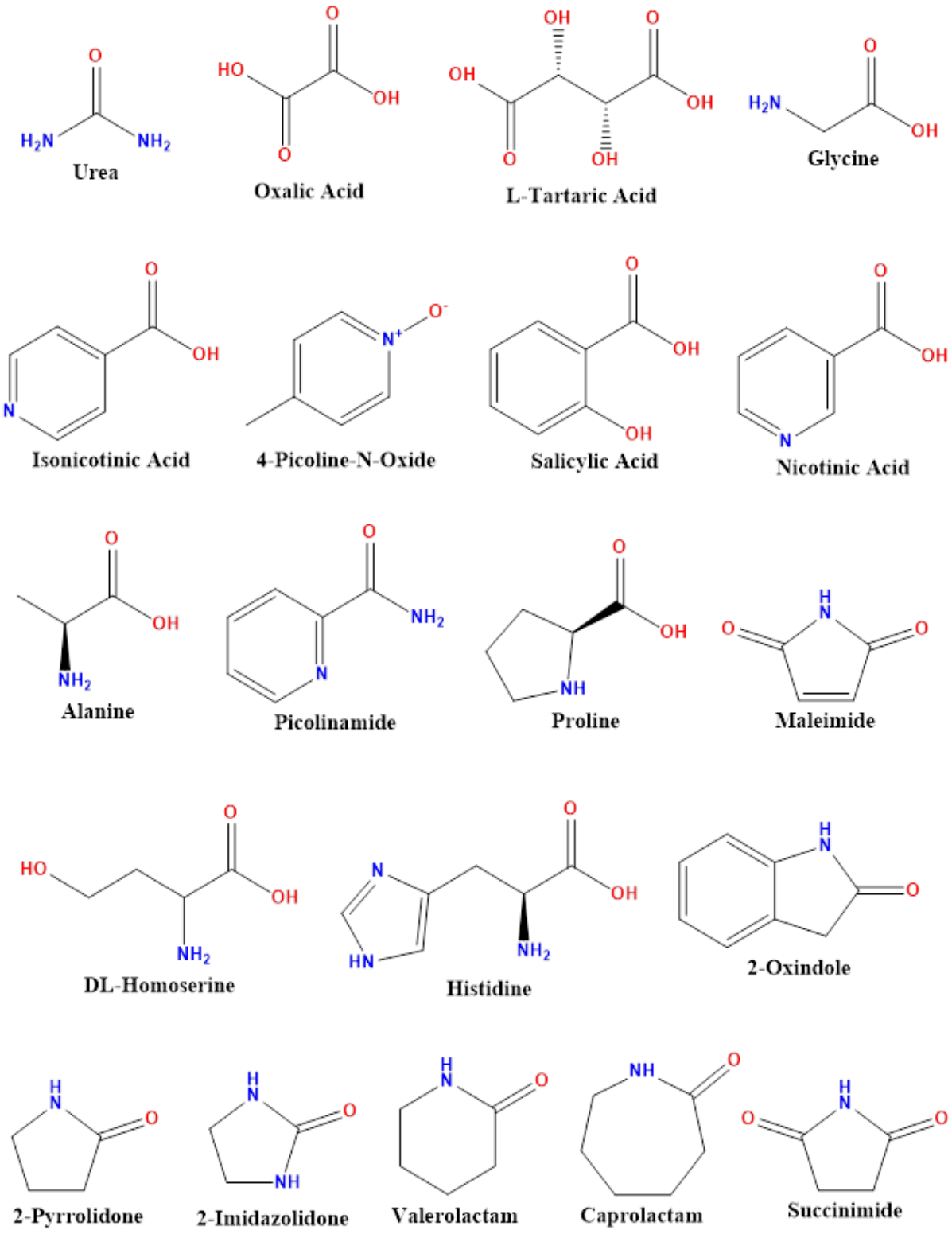


Figure 3.2: GRAS and non-GRAS coformers used in this study.

3.3 Experimental

Materials.

All benzenesulfonamides were purchased from Fluorochem and were used as received without further purification. All coformers and solvents were purchased from commercial outlets and used as received.

Grinding Experiments.

Mechanical grinding experiments were conducted using a Retsch MM400 Mixer mill, equipped with stainless steel 5 mL grinding jars and one 2.5 mm stainless steel grinding ball per jar. 2-6 drops of ethyl acetate were added once both reagents were in the jar. The mill was operated at a rate of 30 Hz for 20 min. A 1:1 ratio of benzenesulfonamide and coformer was used. In most cases a powdered material was isolated and analyzed by PXRD and IR, although some experiments resulted in solvates or an oil/paste, see SI.

Crystallization Experiments.

The ground products obtained from the grinding experiments were dissolved in solvent in a 10 mL sample vial and allowed to crystallize at room temperature for a period of days.

4-MeBSA–SNI (1:1). 4-Me-BSA (100 mg, 0.584 mmol) and SNI (57.87 mg, 0.584 mmol) were used. Colourless, good quality single crystals were harvested by slow evaporation from ethyl acetate over 2-3 weeks; m.p. 92-95 °C.

4-OMeBSA–VLM (1:1). 4-OMe-BSA (100 mg, 0.534 mmol) and VLM (52.95 mg, 0.534 mmol) were used. Colourless, good quality single crystals were harvested by slow evaporation from MeOH under ambient conditions after 2-3 weeks; m.p. 71-73 °C.

4-NBSA–CPR (1:1). 4-HN_2-BSA (100 mg, 0.495 mmol) and CPR (55.97 mg, 0.495 mmol) were used. Colourless, good quality single crystals were harvested by slow evaporation 60% EtOAc – 40% cyclohexane under ambient conditions after 2-3 weeks; m.p. 97-99 °C.

Physical Measurements

Infrared spectra were recorded on a PerkinElmer UATR Two spectrophotometer using a diamond ATR accessory over a range of 400–4000 cm^{-1}. An average of 4 scans was taken for each spectrum obtained with a resolution of 4 cm^{-1}. Thermal analysis was recorded on a TI DSC Q1000 instrument. Samples (2–6 mg) were crimped in nonhermetic aluminium pans and scanned from 30 to 300 °C at a heating rate of 5 °C min^{-1} under a continuously purged dry nitrogen atmosphere flowing at 50 mL min^{-1}. All PXRD data were collected using a STOE STADI MP diffractometer with Cu Kα radiation using a linear PSD over the 2θ range of 3.5-45.5°, with a step size equal to 2° and step time equal to 90 s. The samples were prepared as transmission foils and the data were viewed via STOE WinXPOW POWDAT. Single-crystal X-ray diffraction data were collected on a Bruker APEX II DUO with monochromated Mo Kα radiation (λ = 0.7107 Å), as previously described.[14] All calculations and refinements were made using APEX software.[15,16] All diagrams were prepared using Mercury software.[17] The amido hydrogen atoms were found and refined, where possible, and the other hydrogen atoms were placed in calculated positions and allowed to ride on the parent atom. The crystallographic data for 4-Me-BSA-SNI are given in **Table 3.1**.

Table 3.1: Crystal Data for 4-MeBSA-SNI.

	4-MeBSA-SNI
formula	$C_{11}H_{14}N_2O_4S$
MW	270.30
crystal system	triclinic
space group, Z	P-1, 2
a, Å	8.0484(12)
b, Å	8.8614(13)
c, Å	10.1275(14)
α, °	108.461(3)
β, °	104.132(3)
γ, °	95.529(4)
V, Å^3	652.44(16)
D_c, g cm^{-3}	1.376
μ, mm^{-1}	0.256
2θ range, °	2.22, 28.38
total reflns	25324
obs. reflns., I >2σ(I)	3245
unique reflns	2823
no. parameters	170
R_1 [I >2σ(I)]	0.0462
wR_2 [all data]	0.1158
S	1.027

3.4 *Results*

The 4-methylbenzenesulfonamide-succinimide cocrystal revealed a very interesting supramolecular structure known as a dimer-dimer synthon.[1] A dimer-dimer synthon contains 2 independent dimers linked by a C(4) motif. In this molecule 2 independent succinimide molecules formed a $R_2^2(8)$ dimer whilst 2 independent sulfonamide molecules also formed a $R_2^2(8)$ dimer connected by a C(4) motif as illustrated in the top of **Figure** 3.**3**. Also observed in this crystal system was a tetramer ring. This was not surprising as our systematic review in **Chapter 2** revealed that 4-methylbenzenesulfonamdie formed a $R_4^4(14)$ tetramer motif

between 4 independent sulfonamide molecules. In the lattice, 2 of the sulfonamides are substituted for succinimide to form a $R_4^2(10)$ tetramer ring, see **Figure 3.3**.

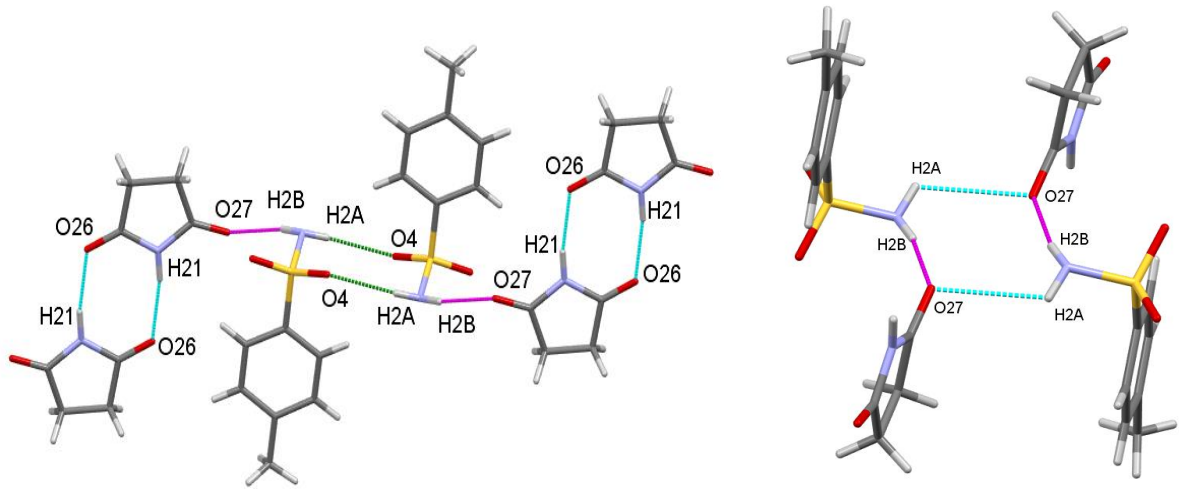


Figure 3.3: Syn N-H catemer and succinimide/sulfonamide dimers, (top) and tetramer ring (bottom).

To complement this study we performed a Hirshfeld surface analysis of the novel cocrystal 4-MeBSA-SNI.[18] The Hirshfeld surface analysis translates the electron density into molecular fragments and also volume around a molecule in a manner similar to the van der Waals surface, or an outer surface of the electron density in a crystal structure.[18] The Hirshfeld surface is related to the molecule and the proximity of its nearest neighbours and this allows easy identification of characteristic strong and weak interactions throughout the structure. It explains the nature of intermolecular interactions within a crystal structure using a two-dimensional fingerprint plot consisting of spikes and wings. The 4-MeBSA–SNI cocrystal two-dimensional finger plots with all types of interactions are shown in **Figure 3.4**.

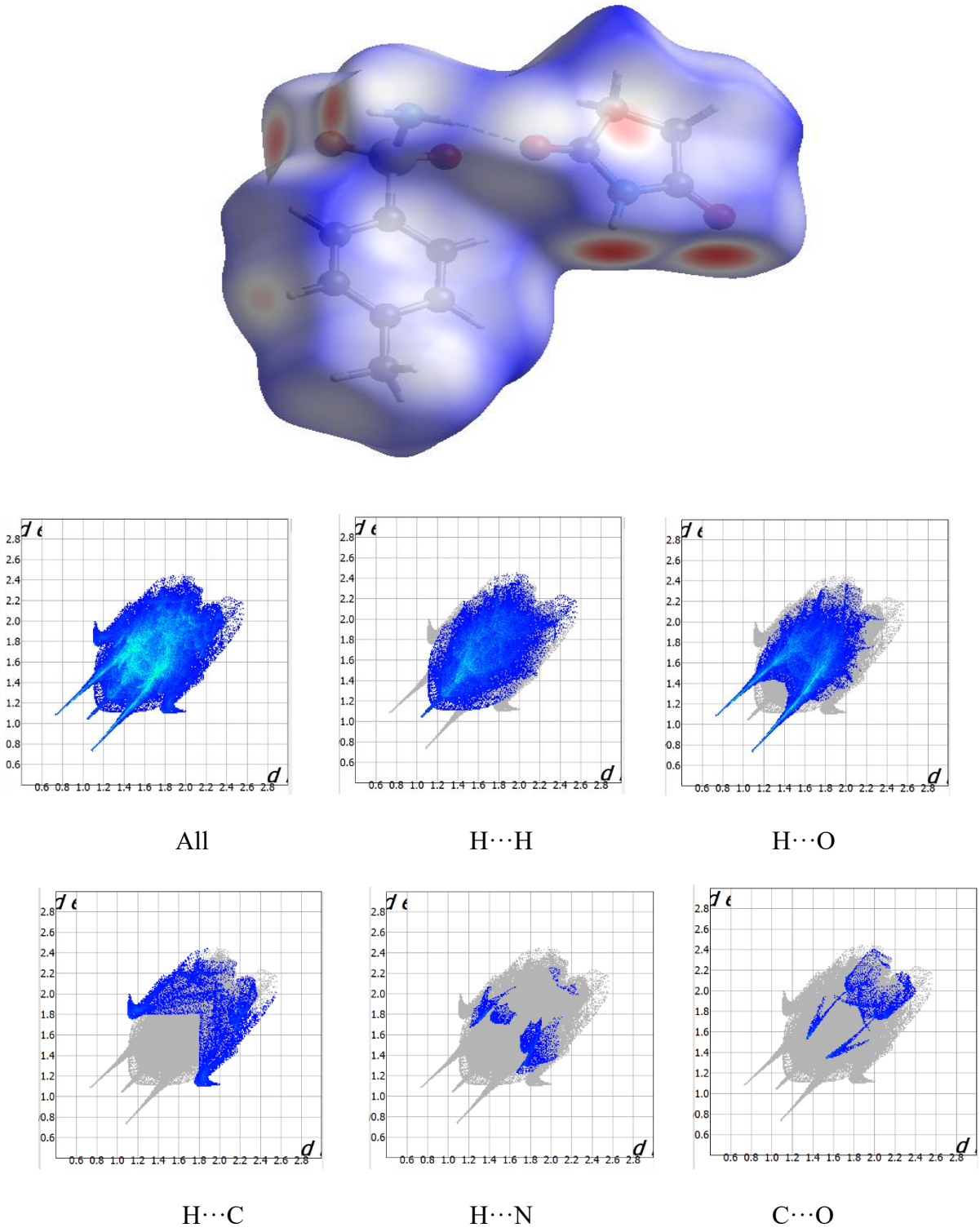


Figure 3.4: Hirshfeld surfaces of the 4-MeBSASNI cocrystals, top, and 2D fingerprint plots of the intermolecular contacts in the 4-Me-BSASNI cocrystals, bottom.

The strong spikes at 0.6–1.0 Å correspond to H···O interactions and the weak spikes between 1.1 and 1.2 Å for H···N hydrogen bonds. The other H···X, H···H, H···C interactions

occur between 1.3 and 2.4 Å in the wings region. The strong H···O interaction is the major contributor in the structure of the 4-MeBSA–SNI cocrystal. The hydrogen bonds found in the 4-MeBSA-SNI cocrystals are provided in **Table 3.2**.

Table 3.2: Hydrogen bonds in the sulfonamide cocrystals.

	NAME	D-H···A	D···A (Å)	H···A (Å)	D-H···A (°)
4-MeBSA-SNI	N2-H2A···O4	0.840	2.275	3.083	161
	N2-H2B···O27	0.844	2.094	2.9206	166
	N21-H21···O26	0.86	1.99	2.841	169.1

We also obtained an additional two crystalline samples which have both been fully characterized by IR, NMR, DSC and PXRD and have been determined are likely to be cocrystals. These are 4-NBSA-CPR and 4-OMeBSA-VLM, which exhibit all the necessary characteristics of a cocrystal having peak shifts in the IR graph, one peak in the DSC graph that is lower than that of the starting materials and a new powder pattern that does not correlate to any reported polymorphs. ^{1}H NMR analysis confirms that these crystalline materials contain both the sulfonamide and the coformer compounds, see SI.

3.5 *Discussion*

This research project was designed to create a variety of sulfonamide cocrystals utilising the three main coformers used in the literature to identify novel sulfonamide synthons that could be exploited for pharmaceutical development. The carboxylic acids and amino acids make up the majority of the coformers used as there has not been a reported sulfonamide-cocrystal containing these coformers. Carboxylic acids and amino acids have been used in the past for pharmaceutical development and as such, we wanted to examine this for the sulfonamide

functional group. The remaining compounds were chosen because they were either a lactam, which as mentioned, has shown great success in sulfonamide cocrystal formation, or they had a functional group like that of a lactam. We elected not to use any pyridines as they are not GRAS and chose two inorganic coformers as they were readily available in the laboratory. As part of the screening process we also used several solvents namely water, methanol, ethanol, ethanol-water, ethyl acetate, THF, ethyl acetate-THF, cyclohexane and ethyl acetate-cyclohexane.

Novel cocrystals were characterised by FT-IR spectroscopy. The sulfonamide and coformer functional groups (C=O / NH / OH) exhibit different stretching frequency as outlined in **Table 3.3**. These various stretching frequencies are very similar to that of previously published sulfonamide-lactam cocrystals from the Nangia group. As such, the caprolactam and valerolactam cocrystals will more than likely exhibit one of the synthons outlined in Nangia's 2015 cocrystal study.[1]

Table 3.3: Selected functional group stretching frequencies (cm^{-1}) of reagents and cocrystals.

	C=O	Acid/ Hydroxyl /Amide	NH in SO_2NH_2
4-MeBSA	-	**3322**	**3235**
SNI	**1683**	-	-
4-MeBSA-SNI	**1695**	**3335**	**3229**
4-OMeBSA	-	**3338**	**3262**
VLM	**1656**	-	-
4-OMeBSA-VLM	**1645**	**3292**	**3268**
4-NBSA	-	**3332**	**3246**
CPR	**1652**	-	-
4-NBSA-CPR	**1614**	**3386**	-

Another piece of evidence for cocrystal formation is DSC. These results convey cocrystal formation when compared to the starting components. In all cases the cocrystals exhibit lower melting points than their individual components, see **Table 3.4**.

Table 3.4: Comparison between cocrystal melting points and starting materials.

COMPOUND NAME	M.P. °C	COMPOUND NAME	M.P. °C	ΔH, J G^{-1}
4-MeBSA	136 - 139	4-MeBSA-SNI	92.84 - 95.02	130.8
4-OMeBSA	111-115	4-OMeBSA-VLM [a]	71.19 - 73.34	71.92
4-NBSA	178-180	4-NBSA-CPR [a]	97.15 - 98.53	99.91
SNI	121-126			
VLM	38 – 40			
CPR	68			

[a] new solid form labelled for simplicity as cocrystal, awaiting structural analysis

3.6 *Conclusion*

One new solid form of a sulfonamide cocrystal with succinimide was prepared and fully characterized. The cocrystal structure has two different synthons: dimer-dimer and tetramer. Two new solid forms of a sulfonamide cocrystal with caprolactam and valerolactam were prepared and partially characterized. Analysis by SCXRD is expected to be performed after the end of the COVID-19 quarantine. These new solid forms involve 4-OMeBSA and 4-NBSA, which adopt less common supramolecular motifs in their crystal structures than the most common $R_4^4(14)$ tetramer. It is too early to know whether this is significant in understanding the cocrystallization behaviour of primary benzenesulfonamides.

References

1. Bolla, G.; Mittapalli, S.; Nangia, A. Modularity and Three-Dimensional Isostructurality Of Novel Synthons in Sulfonamide–Lactam Cocrystals. *IUCrJ* **2015**, *2*, 389-401.
2. Bolla, G.; Nangia, A. Supramolecular Synthon Hierarchy in Sulfonamide Cocrystals With Syn-Amides And N-Oxides. *IUCrJ* **2019**, *6*, 751-760.
3. Allu, S.; Bolla, G.; Tothadi, S.; Nangia, A. Novel Pharmaceutical Cocrystals And Salts Of Bumetanide. *Cryst. Growth Des.* **2019**, *20*, 793-803.
4. Bolla, G.; Nangia, A. Multicomponent Ternary Cocrystals Of the Sulfonamide Group with Pyridine-Amides and Lactams. *Chem. Commun.* **2015**, *51*, 15578-15581.
5. Goud, N.; Babu, N.; Nangia, A. Sulfonamide−Pyridine-N-Oxide Cocrystals. *Cryst. Growth Des.* **2011**, *11*, 1930-1939.
6. Allu, S.; Bolla, G.; Tothadi, S.; Nangia, A. Supramolecular Synthons in Bumetanide Cocrystals and Ternary Products. *Cryst. Growth Des.* **2017**, *17*, 4225-4236.
7. Yeh, K.; Lee, T. Intensified Crystallization Processes For 1:1 Drug–Drug Cocrystals Of Sulfathiazole–Theophylline, And Sulfathiazole–Sulfanilamide. *Cryst. Growth Des.* **2018**, *18*, 1339-1349.
8. Suresh, K.; Minkov, V.; Namila, K.; Derevyannikova, E.; Losev, E.; Nangia, A.; Boldyreva, E. Novel Synthons In Sulfamethizole Cocrystals: Structure–Property Relations And Solubility. *Cryst. Growth Des.* **2015**, *15*, 3498-3510.
9. Croker, D.; Foreman, M.; Hogan, B.; Maguire, N.; Elcoate, C.; Hodnett, B.; Maguire, A.; Rasmuson, Å.; Lawrence, S. Understanding The *p*-Toluenesulfonamide-Triphenylphosphine Oxide Crystal Chemistry: A New 1:1 Cocrystal And Ternary Phase Diagram. *Cryst. Growth Des.* **2011**, *12*, 869-875.

10. Lu, J.; Li, Y.; Wang, J.; Li, Z.; Rohani, S.; Ching, C. Pharmaceutical Cocrystals: A Comparison Of Sulfamerazine With Sulfamethazine. *J. Cryst. Growth* **2011**, *335*, 110-114.
11. Sangtani, E.; Sahu, S.; Thorat, S.; Gawade, R.; Jha, K.; Munshi, P.; Gonnade, R. Furosemide Cocrystals With Pyridines: An Interesting Case Of Color Cocrystal Polymorphism. *Cryst. Growth Des.* **2015**, *15*, 5858-5872.
12. Harriss, B.; Vella-Zarb, L.; Wilson, C.; Evans, I. Furosemide Cocrystals: Structures, Hydrogen Bonding, And Implications for Properties. *Cryst. Growth Des.* **2013**, *14*, 783-791.
13. Goud, N.; Babu, N.; Nangia, A. Sulfonamide−Pyridine-N-Oxide Cocrystals. *Cryst. Growth Des.* **2011**, *11*, 1930-1939.
14. Eccles, K. S.; Elcoate, C. J.; Maguire, A. R.; Lawrence, S. E. Cryst. Growth Des. **2011**, *11*, 4433−4439.
15. APEX2 v2009.3-0; Bruker AXS: Madison, WI, **2009**.
16. Sheldrick, G. M. Acta Crystallogr. **2008**, *A64*, 112−122.
17. Macrae, C. F.; Bruno, I. J.; Chisholm, J. A.; Edgington, P. R.; McCabe, P.; Pidock, E.; Rodriguez-Monge, L.; Taylor, R.; van de Streek, J.; Wood, P. A. J. Appl. Crystallogr. **2008**, *41*, 466−470.
18. CrystalExplorer (Version 3.1), S.K. Wolff, D.J. Grimwood, J.J. McKinnon, M.J. Turner, D. Jayatilaka, M.A. Spackman, University of Western Australia, **2012**.

Supplementary Information for Cocrystallization of Primary Aromatic Sulfonamides

PXRD comparison of sulfonamide cocrystals with that of the starting materials.	134
PXRD comparison of experimental line pattern with calculated profile from the X-ray crystal structure.	136
FT-IR spectra of sulfonamide cocrystals.	137
DSC of sulfonamide cocrystals.	138
ORTEP Diagram of sulfonamide cocrystals and starting materials.	140
^{1}H NMR of sulfonamide cocrystals.	141

PXRD comparison of sulfonamide cocrystals with the starting materials.

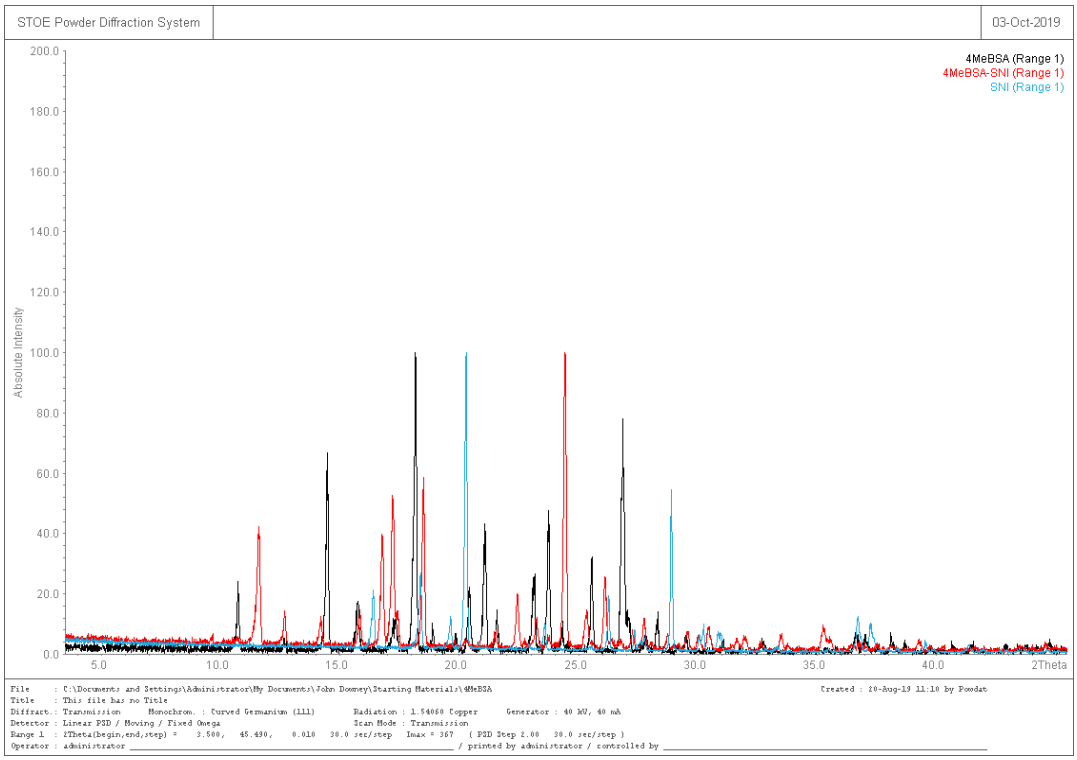


Figure S1: Overlay PXRD comparison of 4MeBSA-SNI (1:1) cocrystal.

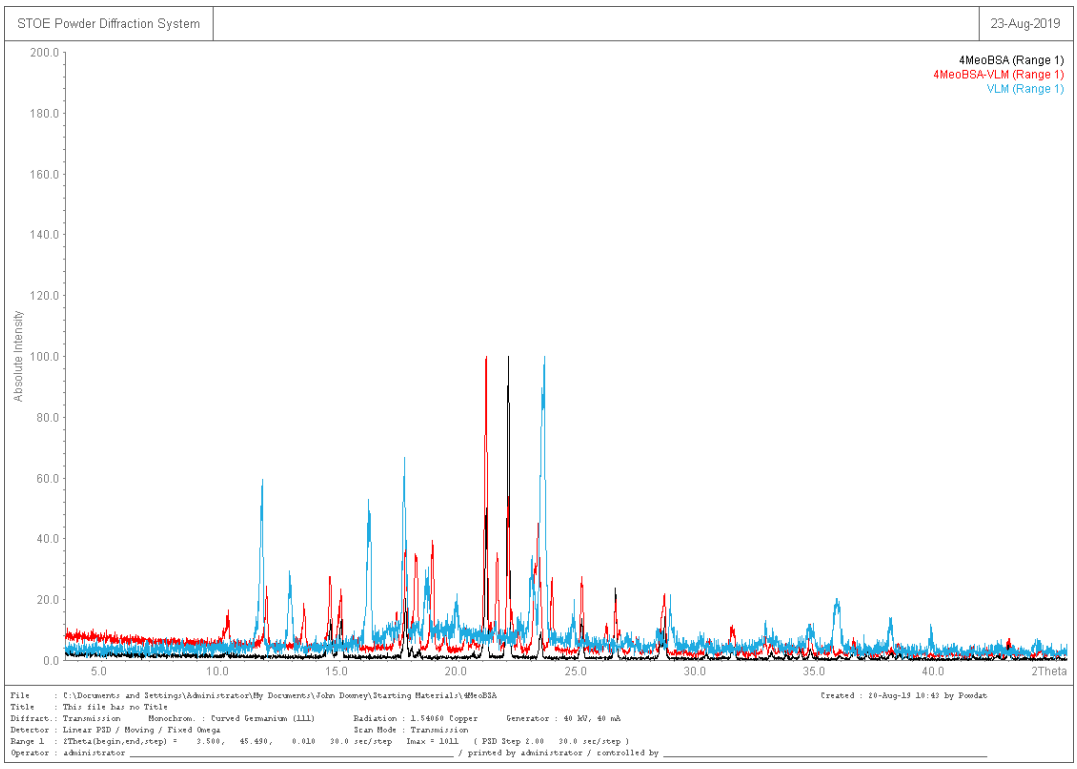


Figure S2: Overlay PXRD comparison of 4-OMeBSA—VLM cocrystal.

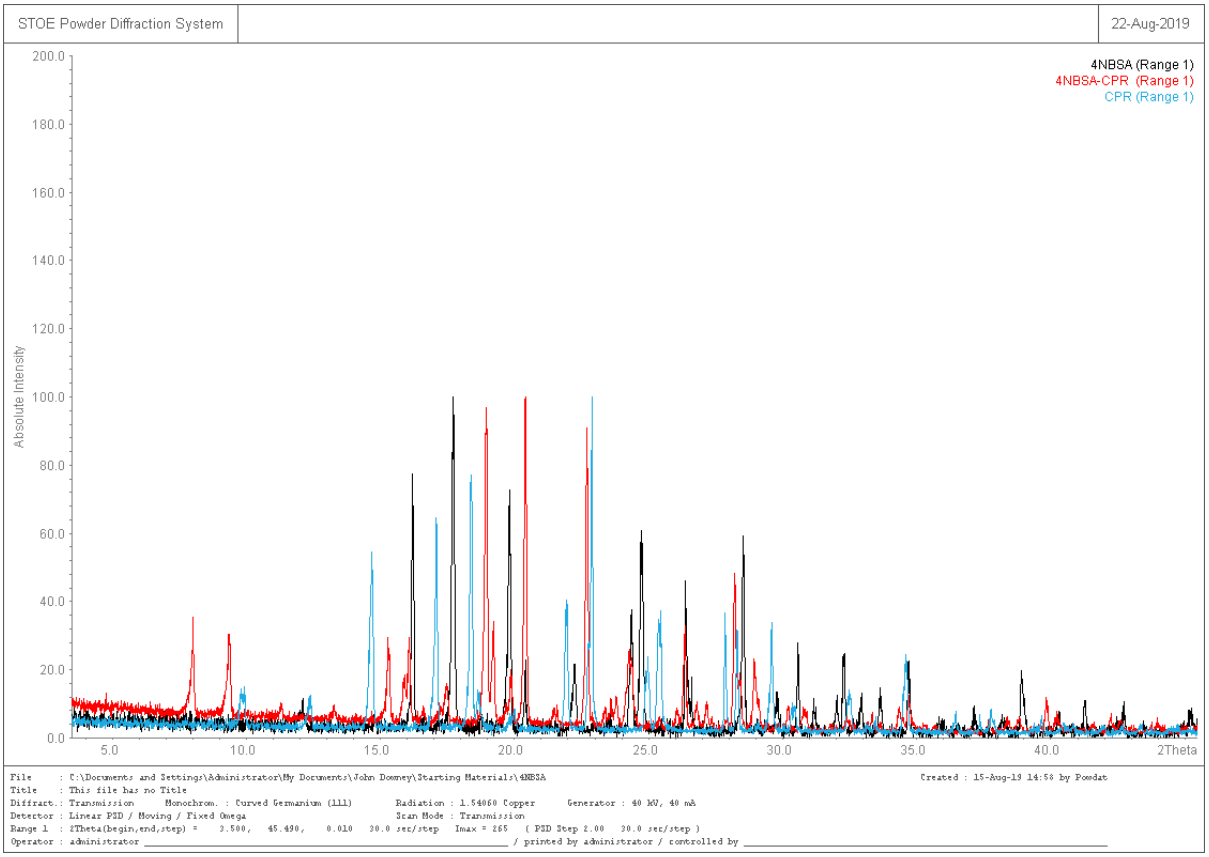


Figure S3: Overlay PXRD comparison of 4-NBSA-CPR cocrystal.

PXRD comparison of experimental line pattern with calculated profile from the X-ray crystal structure.

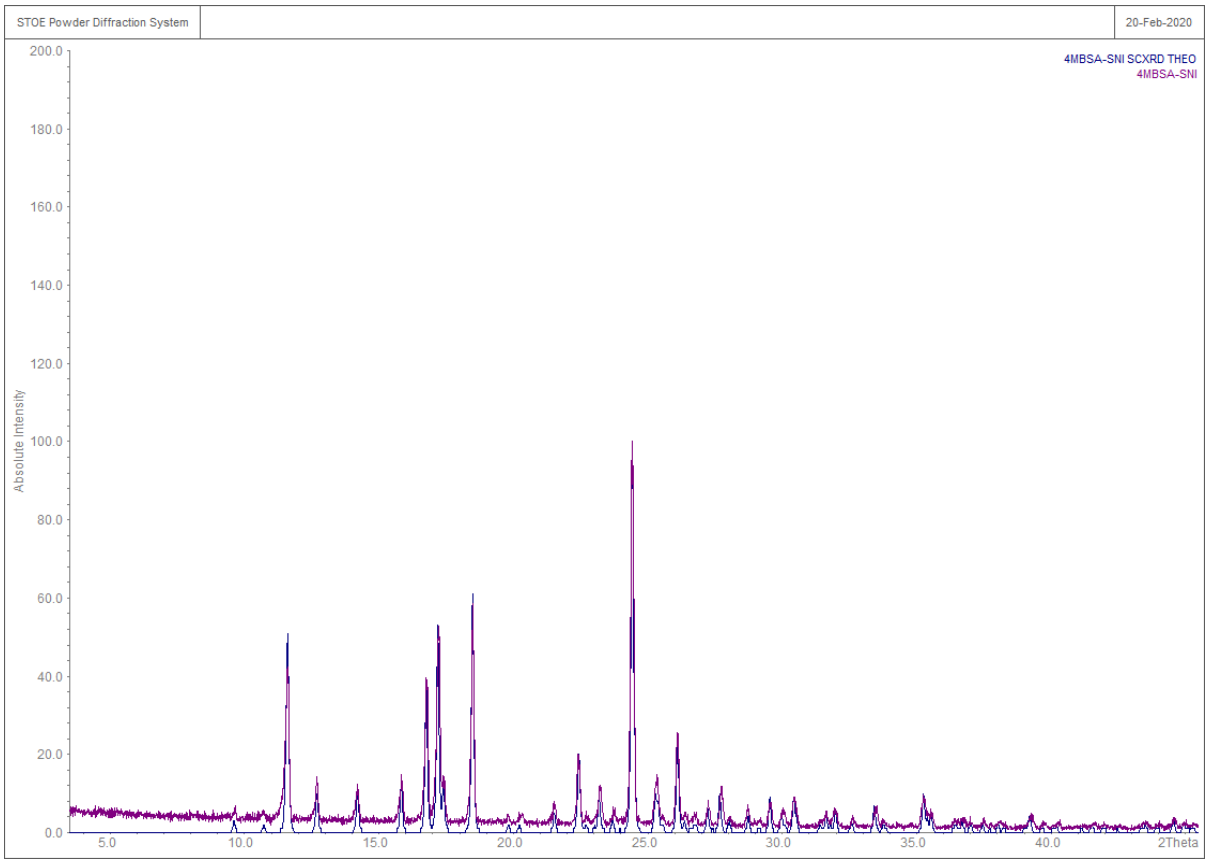


Figure S4: Overlay PXRD comparison of 4-MeBSA-SNI (1:1) cocrystal of powder pattern (purple) with the calculated pattern of the crystal structure (blue).

FT-IR spectra of sulfonamide cocrystals.

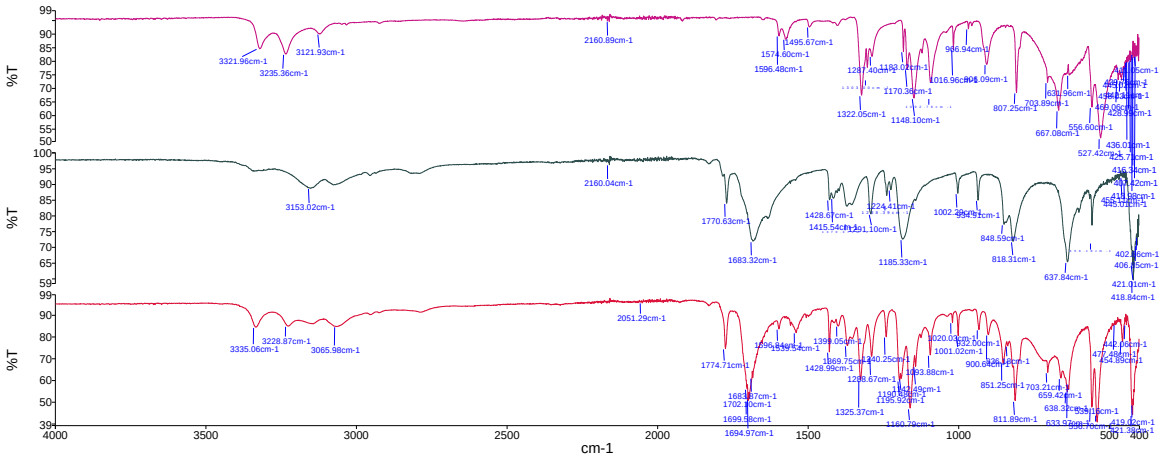


Figure S5: Stacked IR comparison of 4-MeBSA-SNI (1:1) cocrystal. (top – bottom, sulfonamide, succinimide, cocrystal).

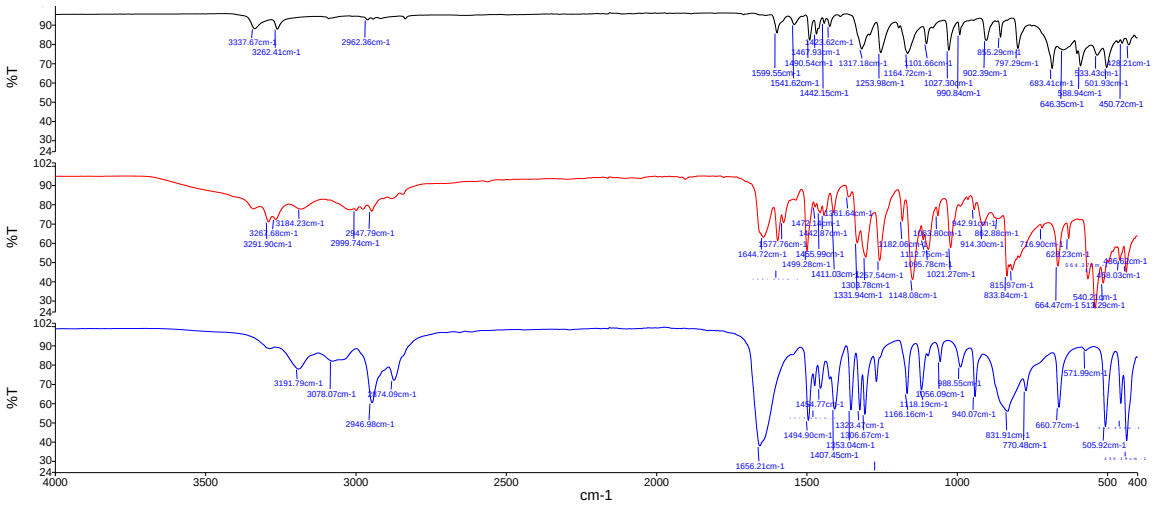


Figure S6: Stacked IR comparison of 4-OMeBSA-VLM cocrystal. (top – bottom, sulfonamide, cocrystal, valerolactam).

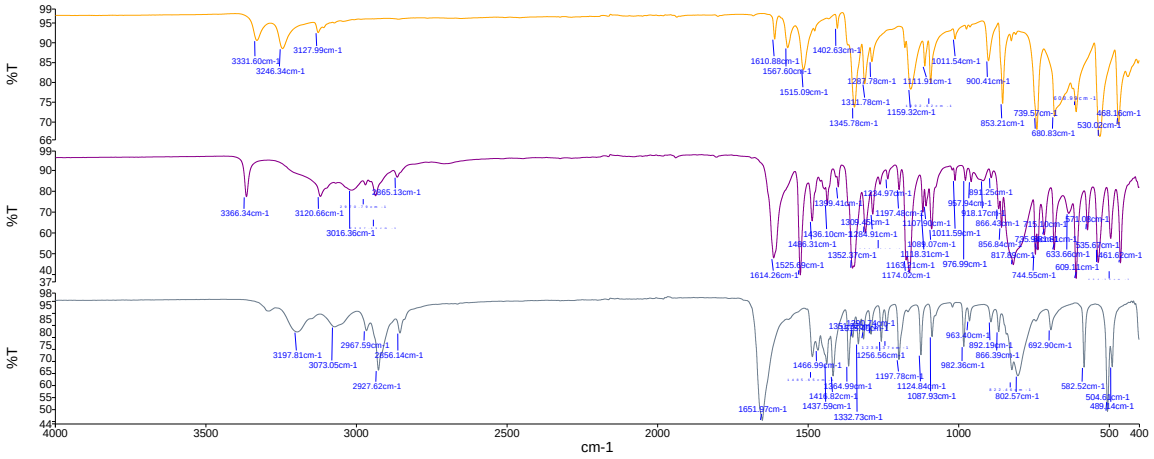


Figure S7: Stacked IR comparison of 4-NBSA-CPR cocrystal. (top – bottom, sulfonamide, cocrystal, caprolactam).

DSC of sulfonamide cocrystals.

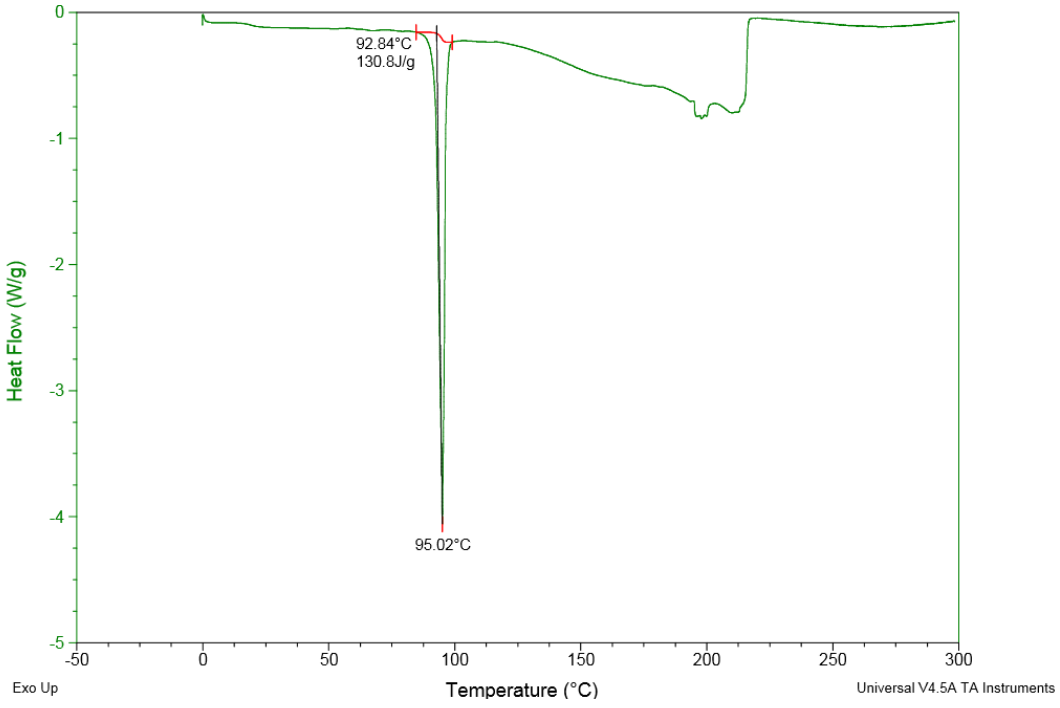


Figure S8: 4-MeBSA-SNI cocrystal.

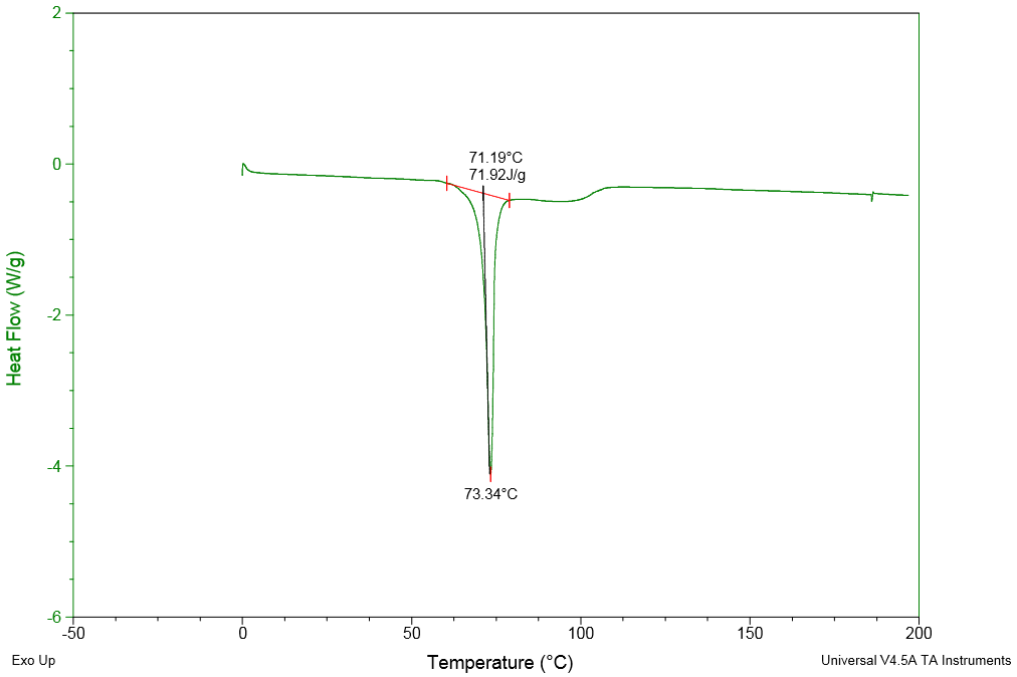


Figure S9: 4-OMeBSA–VLM cocrystal.

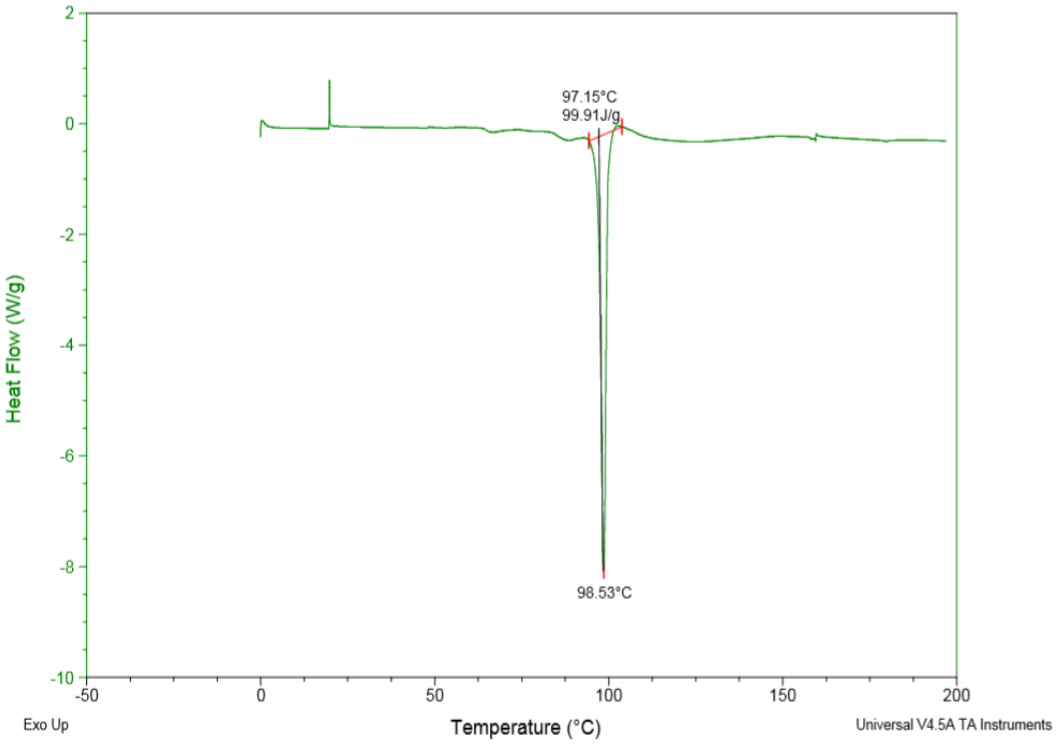


Figure S10: 4-NBSA-CPR cocrystal.

^{1}H NMR of Cocrystals.

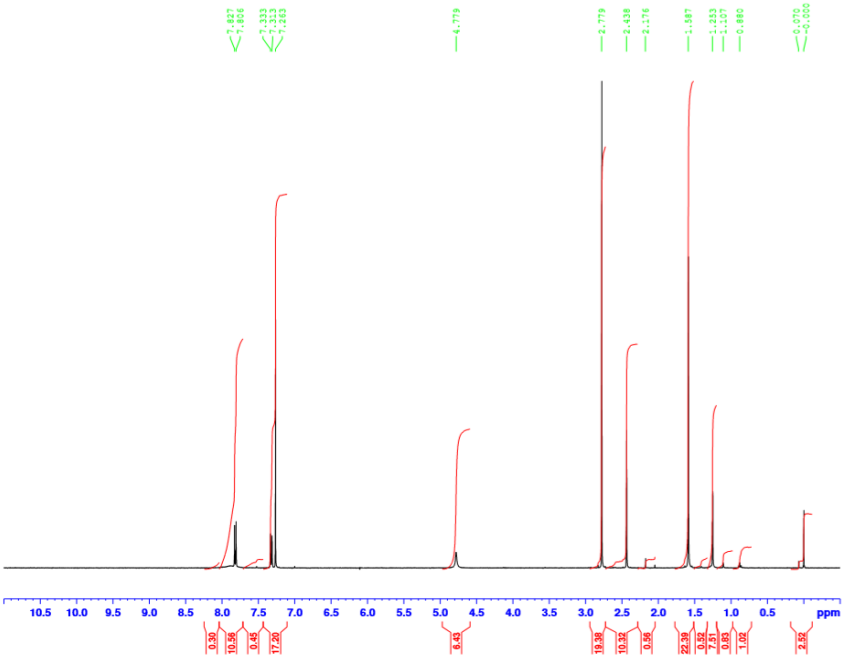


Figure S12: ^{1}H NMR of 4-MeBSA–SNI cocrystal

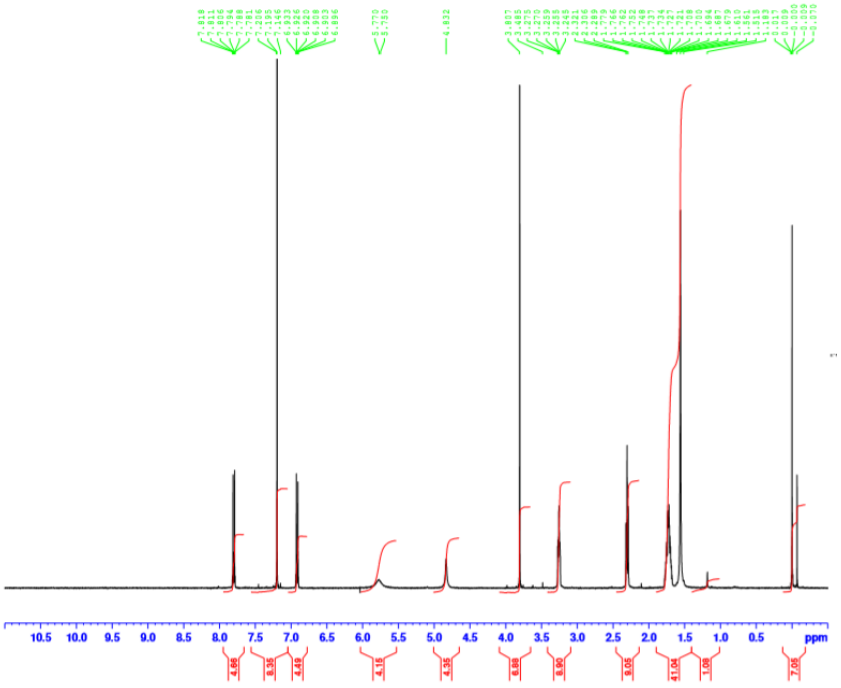


Figure S13: ^{1}H NMR of 4-OMeBSA–VLM cocrystal.

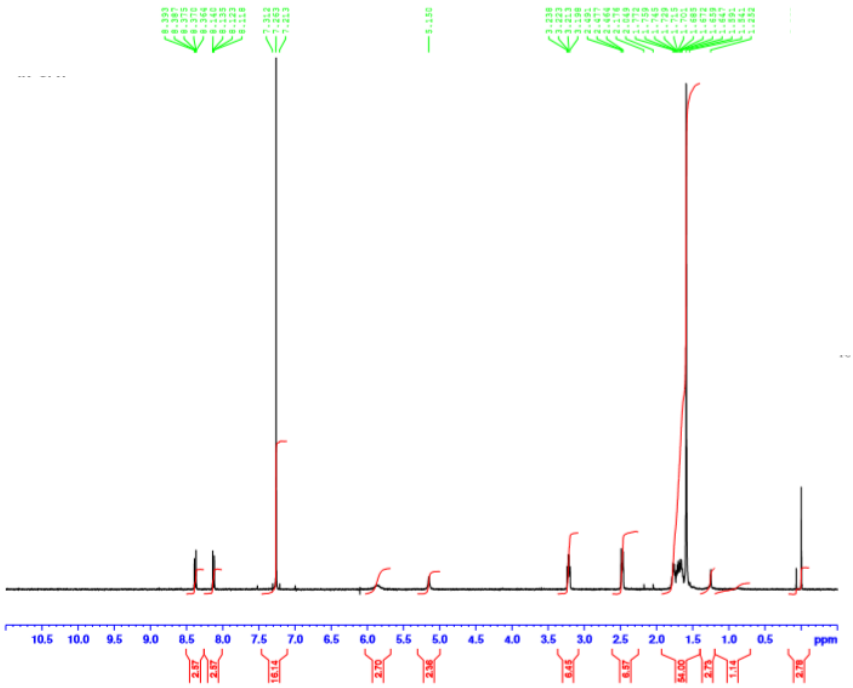


Figure S14: ^{1}H NMR of 4-NBSA-CPR (1:1) cocrystal.

ORTEP Diagram

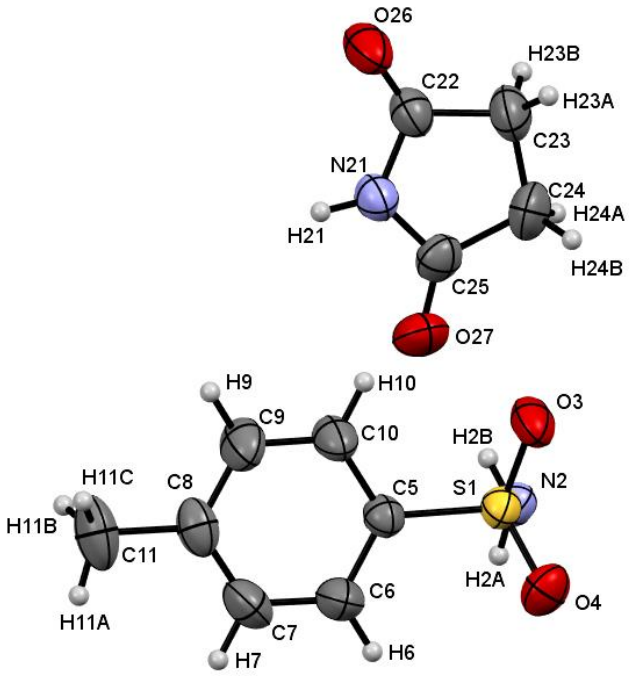


Figure S11: 4-MeBSA-SNI (1:1) cocrystal.

Chapter Four – Future Work

4. *Future Work*

Cocrystal projects often yield successful results and many varying avenues of research worth exploring. In this project, the focus was to critically assess the crystal landscape of the sulfonamides we were using and to synthesize and characterize novel cocrystals of our benzenesulfonamides with neutral, zwitterionic and ionic compounds. During this project I discovered some exciting questions I was not able to answer which warrant further investigation.

One of my discoveries was that the sulfonamides were preferring solvate formation in the presence of tartaric acid and nicotinic acid in ethanol solvent. When I was dissolving the starting materials in ethanol, I heated the solution to approximately 50 °C, capped the vial with a perforated lid and allowed it to cool to RT (the solution was sonicated if necessary). After a few days, the compounds crystallized and were removed from the mother liquor and stored on separate clock glasses. The crystals produced from slow evaporation require further analysis by IR and PXRD and SCXRD.

In addition to this I failed to cocrystallize the fluorobenzenesulfonamides as well as failing to cocrystallize any zwitterion or ionic cocrystals. Going forward I think it is essential to synthesise and characterise novel single crystals that contain either fluorobenzenesulfonamides or zwitterion coformers as there is a serious structural deficit in the CSD regarding these types of cocrystals. Ionic cocrystals have already been explored via *N*-Oxides in the Nangia group and are not as structurally relevant as the former compounds. As such I think it is essential to investigate sulfonamide-zwitterion cocrystals to further aid in the pharmaceutical development of sulfa-drugs.

I also discovered that some of my compounds were dissolving or melting during the milling process. This issue occurred predominantly with two highly hygroscopic materials, 4-

picoline-*N*-oxide and caprolactam. It was also observed with 2-imidazolidone and valerolactam, although less often. Further analysis is required. This avenue of research would have strong implications in the pharmaceutical eutectic field as sulfonamide eutectic systems could be explored as a new method of sulfa-drug development.

Lastly, is the complete characterization of the two novel benzenesulfonamide cocrystals outlined in chapter three by SCXRD.